Studies on the interaction of the cellular and the pathogenic isoforms of the prion protein in the presence of the lipid membrane

Inaugural-Dissertation

zur Erlangung des Doktorgrades
der Mathematisch-Naturwissenschaftlichen Fakultät
der Heinrich-Heine-Universität Düsseldorf

vorgelegt von

Agnieszka Salwierz
aus Kościerzyna, Polen

Düsseldorf, 2009

Angefertigt im	Institut für Physikalische Biologie Heinrich-Heine-Universität Düsseldorf
Abgabedatum	02. Juni 2009
Tag der mündlichen Prüfung	02. Juli 2009
Betreuer	Prof. Dr. D. Riesner
2. Gutachter	Prof. Dr. D. Willbold

Eidesstattliche Erklärung

Hiermit erkläre ich an Eides statt, dass ich diese Arbeit selbständig verfasst und keine anderen als die angegebenen Quellen und Hilfsmittel verwendet, sowie Zitate kenntlich gemacht habe.

Düsseldorf, 02.06.2009

Agnieszka Salwierz

Table of contents

Table of contents ..... **I**

Abbreviations

BSE	bovine spongiform encephalopathy
CBS	citrate-buffered saline
CHO-cells	Chinese hamster ovary cells
CHO-PrP^C	Chinese hamster ovary PrP^C
CJD	Creutzfeldt-Jakob-disease
DMPC	di-myristol-phosphatidylcholine
EDTA	ethylene diamine tetra acetic acid
GPI-anchor	glycosyl-phospatidyl-inositol-anchor
IMAC	immobilized metal-chelate affinity chromatography
kDa	kilodalton
MLV	multilamellar vesicle
NaPTA	sodium phosphotungstate
PK	proteinase K
PrP	prion protein
PrP^C	cellular prion protein
PrP^{Sc}	disease-associated form of PrP
PrP 27-30	PK-resistant fragment of PrP^{Sc}
recPrP (90-231)	recombinant PrP with the amino acid sequence of PrP 27-30
SDS	sodium-dodecyl-sulfate
SDS-PAGE	sodium-dodecyl-sulfate polyacrylamide gel electrophoresis
SHa	Syrian Gold hamster
SPR	surface plasmon resonance
SUV	small unilamellar vesicle
TIR	total internal reflection
TSE	transmissible spongiform encephalopathy

Table of figures

Introduction

Materials and methods

Results

1 Introduction

1.1 Transmissible spongiform encephalopathies

Transmissible spongiform encephalopathies (TSEs) are a group of rare and fatal neurodegenerative disorders that occur in animals and humans. According to its extraordinary infectious agent, the so called prion (cf. chapter 1.2.1), these diseases will shortly be denoted as prion diseases. Unlike other neurodegenerative disorders, prion diseases can be not only of genetic or sporadic, but also of transmissible etiology, that occurs by ingestion or inoculation of contaminated material. Most of the observed TSEs are scrapie in sheep, Bovine Spongiform Encephalopathy (BSE) in cattle and Creutzfeldt-Jakob disease (CJD) in humans (cf. Table 1-1).

Table 1-1 Overview und designation of prion diseases.

See chapter 1.2 for definition of the prion protein PrP and its gene *PRNP*.

Host	Disease	Abbreviation	Etiology
Human	Creutzfeldt-Jakob disease:		
	sporadic	sCJD	somatic mutation or spontaneous conversion of PrP^{C} to PrP^{Sc}
	iatrogenic	iCJD	infection *via* contaminated surgical devices
	familial	fCJD	mutation in *PRNP* gene
	new variant	vCJD	infection *via* bovine prions
	Gerstmann-Sträussler-Scheinker-syndrome	GSS	mutation in *PRNP* gene
	Fatal Familial Insomnia	FFI	mutation in *PRNP* gene
	Kuru	Kuru	infection *via* ritual cannibalism
Sheep	Scrapie	Scrapie	infection *via* genetically susceptible sheep
Cattle	Bovine spongiform encephalopathy	BSE	infection *via* contaminated meat and bone meal
Mule, deer, elk	Chronic wasting disease	CWD	not known but definitely infectious
Mink	Transmissible mink encephalopathy	TME	most probably infection *via* from down-cows

Primary symptoms of prion diseases in humans are typically ataxia and dementia and the disease leads to the certain death of the patient. However, it takes often a very long incubation period for those clinical manifestations to appear. Neuropathological investigations of the brains of affected animals and humans show characteristic spongiform degenerations in the grey matter of the brain caused by many vacuoles located extracellulary in the neuropil and intracellulary in the neuronal cell bodies. This severe vacuolization causes death of the neurons, which in turn correlates with unusual growth and proliferation of astrocytes and microglia (Masters *et al.* 1978). Other characteristic features of TSE-brains morphology are extracellular protein deposits, in form of amorphous aggregates, fibrillar structures or solid plaques (Ironside 1998).

1.1.1 Scrapie

The prototypic TSE disease is scrapie, a naturally occurring disease affecting sheep and goats. It has been identified in 1732 and so it is the historical TSE. The pathological description of scrapie-infected sheep brain followed in year 1898 (Cassirer 1898) and in 1936 Cuille could show its transmissibility demonstrating so that this disease is an infectious one (Cuille 1936). The following transmissions experiments to mice (Chandler 1961) and Syrian golden hamsters (Kimberlin *et al.* 1975) yielded excellent animal models, allowing scientists to intensify their research on that disease. The name scrapie is derived from one of the symptoms of the condition, wherein affected animals compulsively scrape off their fleece against rocks, trees or fences. The disease apparently causes an itching sensation in the animals. Other symptoms are lip-smacking, strange gait and convulsive collapse.

1.1.2 Bovine Spongiform Encephalopathy (BSE)

In the two past decades, the Bovine Spongiform Encephalopathy (BSE) epidemic in the United Kingdom has brought international attention to the TSE family of diseases. The first appearance of BSE cattle in UK in year 1986, which rapidly evolved into a major epidemic, was widely attributed to transmission of sheep scrapie to cattle *via* contaminated feed prepared from rendered carcasses (Wilesmith 1988). An alternative hypothesis states that epidemic BSE resulted from recycling of rare sporadic BSE cases, as cattle were also rendered to produce cattle feed. Whether or not BSE originated from sheep scrapie, it became clear that lowering the temperature during sterilization and discarding the lipid extraction step in the process of

producing meat and bone meal from animal carcasses allowed the BSE-agent to resist inactivation (Wells *et al.* 1991). More than 180,000 BSE cases have been confirmed in the UK. The peak was reached in year 1992 when almost 37,000 cases were recorded. The appearance in the UK in year 1995 of a novel human prion disease, variant Creutzfeldt-Jakob disease (vCJD), and the biochemical and histopathological evidence that it is caused by the same prion strain that causes BSE, has raised the possibility that a major epidemic of vCJD will occur as a result of dietary or other exposure to BSE prions (Cousens *et al.* 1997; Collinge 1999). Till now almost 200 cases of vCJD world wide have been recorded.

1.1.3 Creutzfeldt-Jakob disease (CJD)

The most common human prion disorder is the CJD. It can be divided into three etiological categories: sporadic, iatrogenic and familial. Sporadic CJD occurs in all countries with a random case distribution and an annual incidence of one per million. Iatrogenic CJD arises from accidental exposure to human prions through medical or surgical procedures. Such iatrogenic routes include the use of inadequately sterilized intracerebral electrodes, dura mater transplants, corneal grafting and use of human growth hormones. Epidemiological studies do not provide any evidence for an association between sheep scrapie and the occurrence of CJD in humans (Brown *et al.* 1987). Around 15% of human prion diseases are the familial ones and all cases to date have been associated with coding mutations in the prion protein gene (*PRNP*) of which 20 distinct types are recognized (Collinge 1997). A common PrP polymorphism at residue 129, where either methionine or valine can be encoded, is a key determinant of genetic susceptibility to iatrogenic and sporadic prion diseases, the large majority of which occurs in homozygous individuals (Collinge *et al.* 1991; Palmer *et al.* 1991; Windl *et al.* 1996).

Classic CJD is a rapidly progressive, multifocal dementia with onset usually occurring in the 45- to 75-year age group, with a peak of onset between 60 and 65 years. The clinical progression is typically within several months, developing akinetic mutism and death mostly in 8 – 12 months. Common features, present in approximately one third of the cases, include fatigue, insomnia, depression, weight loss, headaches, general malaise and ill-defined pain sensations. The vCJD has a clinical presentation in which behavioral and psychiatric disturbances occur predominantly. The most prominent feature is depression, but anxiety, withdrawal and behavioral changes are also frequent. Most patients develop a progressive cerebellar syndrome combined with gait and limb ataxia. Dementia usually develops later in the clinical course. The age of onset ranges from

16 to 51 years (mean: 29 years) and the clinical course is unusually prolonged for 9 – 35 months (mean: 14 months). All cases to date are homozygous for methionine at *PRNP* codon 129 (Collinge *et al.* 1996; Hill *et al.* 1999). vCJD can be diagnosed by detection of characteristic digestion patter of PrP and occurence of prions on tonsil biopsy (Hill *et al.* 1997). It is important that prions are only detectable in tonsil and other lymphoreticular tissues in vCJD and not other form of human prion diseases, indicating its distinctive pathogenesis.

1.2 Molecular basics and characteristics of prion protein

1.2.1 Identification of the infectious agent

The first hypothesis suggested that TSEs could be caused by a particular type of virus called a "slow-virus". This was based on the fact that first clinical symptoms of scrapie often occurred after a very long, symptomless time (Sigurdsson 1954). Ultrafiltration studies revealed that the infectious agent must be a very small one, although a virus has not been identified. Further experiments showed that ionizing radiation and exposure to ultraviolet light fails to inactivate the scrapie agent. Even very high dose compared to those required for inactivation of any viruses or other agents did not yield an effective inactivation (Alper *et al.* 1967). Prusiner, who extended systematically Alper's *et al.* experiments developed a protocol to purify the scrapie agent from experimentally infected hamsters. He showed that the infectivity of purified extract can be reduced with methods that denature proteins, but remains intact after using methods that modify or destroy nucleic acids (Prusiner *et al.* 1981; Prusiner *et al.* 1982). This led him to the conclusion that the scrapie agent is not a virus, but must be some novel type of infectious agent. He called it "prion" as a short form of "*pro*teinaceous *in*fectious particle" indicating that the main, if not the only component of prion is a protein (Prusiner 1982). The fact that prions, although composed solely of proteins, can undergo a replication process changed the basics of molecular biology, which stated that nucleic acid is the only possible information carrier needed for a replication.

It took another several years to finally purify and characterize this protein that has been called prion protein (PrP)(Bolton *et al.* 1982). Purification of PrP was followed by identification of the localization of PrP gene. Cloning the gene of this protein surprisingly resulted in finding a single copy gene of the host both in infected and uninfected animals (Chesebro *et al.* 1985; Oesch *et al.* 1985). The human PrP gene (*PRNP*) is located on chromosome 20 and was first sequenced in

1986 (Kretzschmar *et al.* 1986). PrP protein is mainly expressed in the central nervous system (CNS). However, it has been also found in other organs of the body. Pancreas and liver are here the only exceptions (Weissmann *et al.* 1993). Moreover, it has been shown that in the healthy organism the PrP gene is present in an active form that continuously expresses the PrP protein which does not cause the disease (Basler *et al.* 1986). This explains also the observation that in the course of disease all types of immunological response are missing. The fact that a chemically identical protein, expressed from the same gene sequence, was isolated from healthy as well as from infected animal led to the conclusion that PrP can adopt different forms. And so: in the healthy organism the cellular isoform – PrP^{C} is being found, while the infected organism contains an abnormal, harmful conformation designated PrP^{Sc} (for scrapie).

1.2.2 Structural characteristics of prion protein

The isolation of a chemically identical prion protein either from healthy or infected animals raised a discussion about the relation between PrP^{C} and PrP^{Sc} and their possible structural and functional differences. Electron microscopy studies showed that PrP^{C} forms monomeric or oligomeric bulky particles, while PrP^{Sc} is found in form of fibrillar structures (Riesner *et al.* 1996).

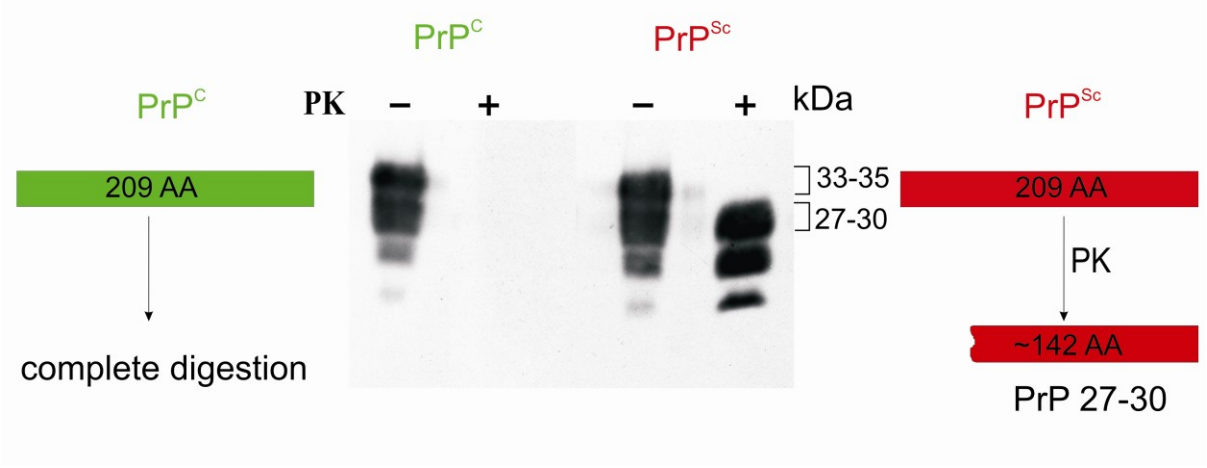

Figure 1.1 Proteinase K resistance

Digestion of the PrP^{C} and PrP^{Sc} samples with proteinase K (PK) was followed by a SDS-PAGE electrophoresis and Western blot. The clearly visible three bands disappeared completely after PK digestion of PrP^{C}. When PrP^{Sc} was subjected to digestion with PK, an N-terminally truncated form, designated PrP 27-30, appeared (Riesner 2002).

The strong tendency to aggregation correlates directly with PrP^{Sc}-specific resistance to digestion with proteinase K (PK). Natural prion protein, purified from healthy animals, shows in a denaturing gel a mixture of three forms – unglycosylated, mono- and diglycosylated with a size of 33 – 35 kDa. Digestion with PK leads to a complete loss of signal presenting a high sensitivity of PrP^{C} to such a treatment. The same experiment performed on a pure PrP^{Sc} isolate shows again presence of these three bands, However, shifted to lower M_r. This represents the N-terminally truncated form of PrP^{Sc} called, according to its molecular size, PrP 27-30 (cf. Figure 1.1). An interesting feature of this new, partially digested form is its intact infectivity (Riesner 2002).

Further biophysical studies showed that different sensitivity to PK-digestion was not the only feature that differentiated these two forms (Cohen *et al.* 1998; Ironside 1998; Riesner 2003). Fourier-transform infrared (FTIR) and circular dichroism (CD) studies showed that PrP^{C} contains about 40% α-helix and little β-sheet (~3%) (Pan *et al.* 1993). The insolubility of PrP^{Sc} prevented many biophysical studies, but it could be shown that disease-associated PrP^{Sc} fibrils consist mostly of β-sheet rich structures. Another difference was found when the solubility of these two proteins was compared. PrP^{C} was soluble in water after addition of mild detergents, whereas PrP^{Sc} formed large, insoluble aggregates (cf. Table 1-2). Moreover,, till now it was not possible to solubilize PrP^{Sc} aggregates without losing their infectivity, which would mean that this feature of PrP^{Sc} correlates strongly with the structure of the protein. It has been also shown that solubilized PrP 27-30 particles undergo a certain structural change: the high content of β-sheet decreased significantly while the α-helix content increased (Riesner *et al.* 1996). All these hints led to a hypothesis that the prions infectivity depends strongly on the secondary, tertiary and quaternary structure of the protein.

Table 1-2 Comparison of biophysical properties of PrP^{C} and PrP^{Sc}

Property	PrP^{C}	PrP^{Sc}
Infectivity	not infectious	infectious
PK-resistance	sensitive	partially resistant
Secondary structure	mainly α-helical	β-sheet-rich
Solubility	soluble (in mild detergents)	insoluble

First NMR analyses of PrP^{C} were carried out by Wüthrich's group in year 1996. The structure of the mouse PrP domain comprising residues 121-23, i.e. the C-terminus, (Riek *et al.* 1996) was

resolved and was followed by the structures of recombinant hamster (Liu *et al.* 1999) and the human PrP domain (Hosszu *et al.* 1999). These studies showed great similarities in the molecular structure. Together with studies on full-length PrP it was shown that PrP consist of an N-terminal region of about 100 amino acids which is unstructured in solution. The C-terminal fragment, also approximately 100 amino acids in length contains a short two-stranded antiparallel β-sheet and three extended α-helices. The twisted V-shaped arrangement of the second and the third helix, which are stabilized by a single disulfide bond, forms the scaffold onto which the short β-sheet and the first helix are anchored (cf. Figure 1.2 a).

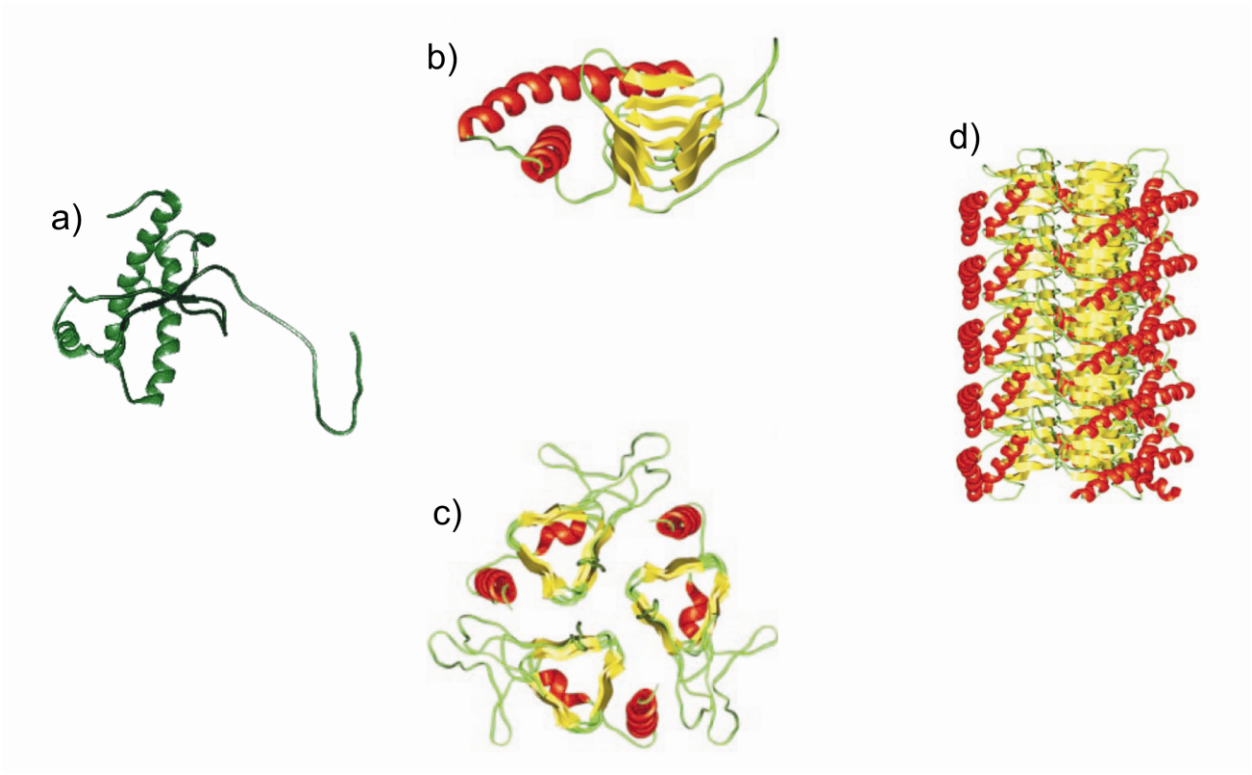

Figure 1.2 Structural comparison of PrP^{C} and PrP^{Sc}

a: NMR-structure of recombinant SHa PrP (90-231) (modified after Liu *et al*. 1999); **b:** model of PrP^{Sc} derived from electron microscopic 2D-crystals data (Wille *et al.* 2002);the N-terminus forms a β-helix with parallel sheets **c:** the trimeric subunit of PrP 27-30 built by arranging three monomers in a disc; **d:** a model for the PrP 27-30 fiber was constructed by assembling five trimeric discs (Govaerts *et al.* 2004).

The discovery that PrP 27-30 has an ability to form 2D-crystals under particular solubilization conditions led to studies with EM and model building. The results showed that parallel β-helix is the only known fold that provides the necessary β-structure content, parallel β-architecture and enough room to accommodate the α-helices that are expected at the C-terminus of the molecule

(cf Figure 1.2 b) (Wille *et al.* 2002). Further studies showed that the left-handed β-helices readily form trimers, providing a natural template for a trimeric model of PrP^{Sc}. Moreover,, this model may provide important clues to the fibrillar structure of mature PrP^{Sc} particles (cf. Figure 1.2 c/d) (Govaerts *et al.* 2004).

1.2.3 Biosynthesis and cellular trafficking of prion protein

The mammalian PrP gene encodes a protein of 254 amino acids (hamster) that contains several distinct domains, including an N-terminal signal peptide, a series of five proline- and glycine-rich octapeptide repeats, a highly conserved central hydrophobic segment, and a C-terminal hydrophobic region that acts as a signal for addition of a glycosyl-phosphatidylinositol (GPI) anchor (cf. Figure 1.3).

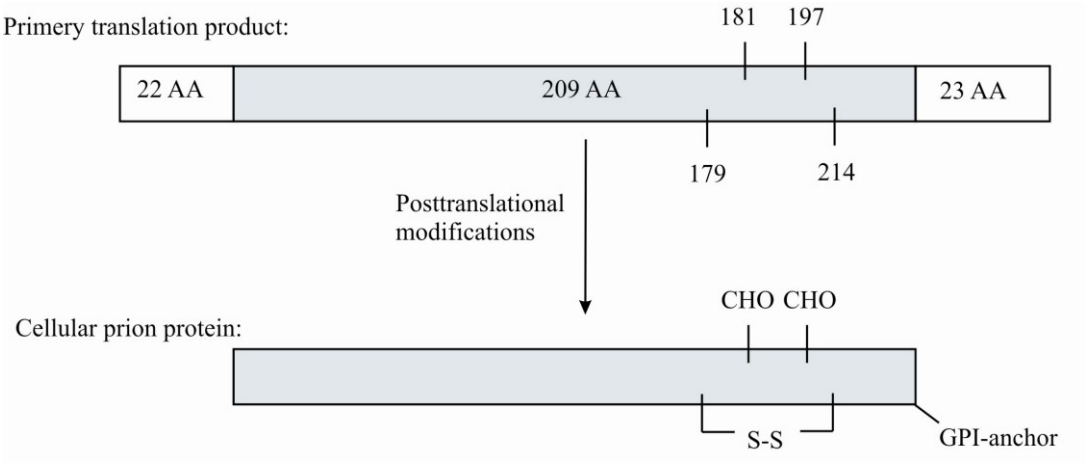

Figure 1.3 Biosynthesis of PrP^{C}

The primary translation product undergoes posttranslational modifications that lead to cleavage of two signal sequences, attachment of GPI-anchor, two N-linked oligosaccharides and formation of disulfide bond.

Like other membrane proteins, PrP^{C} is synthesized in the rough endoplasmic reticulum (ER) and transits the Golgi on its way to the cell surface. During its biosynthesis, PrP^{C} is subject to several kinds of posttranslational modifications. The first 22 amino acids encode a peptide that is cleaved off after directing the protein into ER. Next, two N-linked oligosaccharide chains are attached to asparagines residues 181 and 197, followed by formation of a disulfide bond between cystein residues 179 and 214. Peptide 232-253, located at the C-terminus is cleaved and GPI-

anchor is linked to amino acid 231. This takes place in the ER-lumen (Stahl *et al.* 1990). Moreover,, the two N-linked oligosaccharide chains added initially in the ER, which are of the high mannose-type, are subsequently modified in the Golgi to yield complex-type chains that contain sialic acid (cf. Figure 1.4) (Caughey *et al.* 1989). Finally, the fully modified protein is transported to the outer plasma membrane where it stays attached *via* the GPI-anchor. This anchor has a core structure common to other glycolipid-anchored proteins. It consist of an ethanolamine residue that is amide-bound to the C-terminal amino acid, three mannose residues, an unacetylated glucosamine residue and a phosphoinositol (PI) molecule that is embedded in the outer leaflet of the lipid bilayer. The GPI-anchor is unusual, because its core is modified by the addition of the sialic acid residues. Available evidence indicates that the oligosaccharide chains and GPI-anchors of PrP^{C} and PrP^{Sc} do not differ, although complete structures have been worked out only for PrP^{Sc} (Stahl *et al.* 1992).

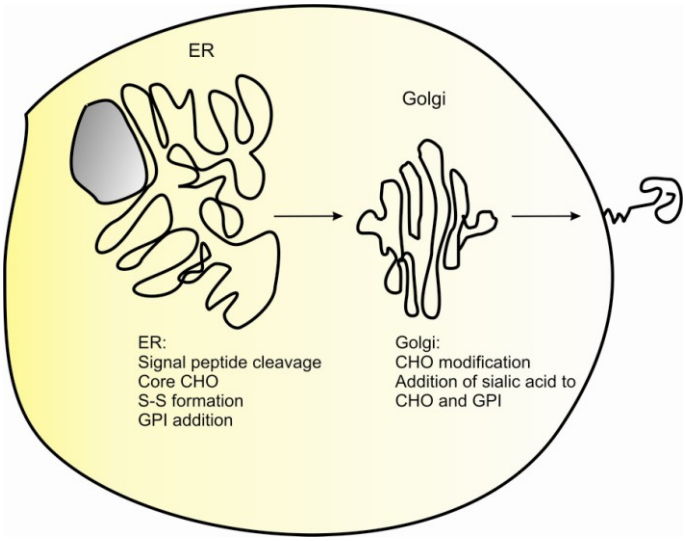

Figure 1.4 Steps in the biosynthesis of PrP^{C}

The biosynthesis and the main posttranslational modifications take place in the ER lumen. Final modifications take place in the Golgi from where the protein is directed to the cellular membrane.

1.2.4 Cellular localization of prion protein

Like all GPI-anchored proteins, PrP^{C} is directed to particular plasma sites – the so called rafts (Gorodinsky *et al.* 1995). Rafts represent membrane microdomains, wherein lipids of specific chemistry can associate with each other to form platforms that segregate membrane proteins. Rafts usually consist of cholesterol, sphingolipids and cerebrosides. Another feature that

identifies these microdomains is their insolubility after extraction with non-ionic detergent, such as Triton X-100. Therefore, they are also often designated as detergent-resistant membranes (DRMs) (Brown *et al.* 1997; Wang *et al.* 2000).

The precise localization of PrP^C remains still enigmatic. Till now, PrP^C has been found in the neurons and glia of the brain and spinal cord as well as in several peripheral tissues and leukocytes (Caughey *et al.* 1988; Bendheim *et al.* 1992; Dodelet *et al.* 1998). The *in situ* hybridization studies showed that the highest amount of PrP^C–mRNA was found in neurons (Kretzschmar *et al.* 1986) However,, the total amount of PrP^C compared to other central nervous system proteins was very low, reaching barely a level of 0.1 % (Turk *et al.* 1988). This makes the PrP^C purification attempts from healthy animal brains very hard with regard to the yield of the protein of interest (Pan *et al.* 1992; Pergami *et al.* 1996). Significantly higher yields can be achieved by using the *E.coli* expression system (Mehlhorn *et al.* 1996). However, a great disadvantage of this prokaryotic system is the lack of posttranslational modifications, i.e. N-linked oligosaccharides and GPI-anchor, in the expressed protein of interest.

The subcellular distribution of PrP^{Sc} is even more difficult to determine, primarily because this form of the protein displays poor immunoreactivity, unless treated with denaturing agents that have a damaging effect on cell morphology. As a result of prion conversion, triggered either by prion infection, or by mutations on the *PRNP* gene, or other unknown reasons, a misfolded PrP^{Sc} is generated, progressively accumulated and deposited as amyloid plaques in the brain. In general, a range of studies indicate that it has a wide distribution in particular at the plasma membrane, in the late endosomal and lysosomal compartments (Caughey *et al.* 1991; Jeffrey *et al.* 1992; Arnold *et al.* 1995). The purification attempts of PrP^{Sc} are, as in the case of PrP^C, also very challenging. The first protocols to purify and characterize the scrapie prions were developed by the Prusiner's group. Their protocol for the agent from hamster brains resulted in preparations enriched for the prion rods, PrP 27-30, between 100- and 1000-fold with respect to protein. The protocol includes successive extraction and precipitation steps, combined with proteinase K digestion in the presence of sarkosyl and sedimentation through a discontinuous sucrose gradient (Prusiner *et al.* 1982). Another method for purification of PrP^{Sc} is a selective precipitation of prions by sodium phosphotungstate (NaPTA). This substance at neutral pH and in the presence of Mg^{2+} forms complexes with oligomers and polymers of infectious PrP^{Sc} and PrP 27-30, but not with PrP^C. The resultant dense aggregates are collected by low-speed centrifugation and the pellet should contain about 99% of the prions and less than 1% of other proteins (Safar *et al.*

1998). One should keep in mind that the purified or partially purified prions are not always reproducible in their consistency and stability and experiments should be done shortly after purification to avoid potential changes in the properties of the samples.

1.2.5 Subcellular sites of PrP^{Sc} formation

There is surprisingly little information available about how extracellular PrP^{Sc} is taken up by cells during the initial stage of infection. If this uptake were to occur *via* an endocytic mechanism, PrP^{Sc} could interact with PrP^{C} on the plasma membrane or in the endosome and key events in the conversion process could take place at these locations. There are several pieces of evidence suggesting that the endocytic pathway is involved in the generation of new PrP^{Sc} particles. This idea is consistent with the localization of at least some PrP^{Sc} molecules in endosomes and lysosomes. Treatment of cells with PI-specific phospholipase C (PI-PLC), a bacterial enzyme which cleaves off the diacylglycerol portion of the GPI-anchor, inhibited the production of PrP^{Sc}, presumably by removal of the PrP^{C} as PrP^{Sc}-precursor from the cell surface (Caughey *et al.* 1991; Borchelt *et al.* 1992). Consistent with these last results, generation of new PrP^{Sc} was also inhibited by treatment of cells with fungal metabolite brefeldin A, which blocks surface delivery of membrane and secretory proteins (Taraboulos *et al.* 1992). However,, these results do not distinguish between the plasma membrane and endosomes as the relevant sites for PrP^{Sc} production.

Recent experimental observations suggest that an interaction of the prion protein with rafts may play an important role in conversion of PrP^{C} into PrP^{Sc}. With a help of floatation assay it was shown that in N2a- and ScN2a-cells, cell lines sensitive to prion infection, both isoforms of PrP were associated with the DRMs fraction (Vey *et al.* 1996; Naslavsky *et al.* 1997). Furthermore, small amounts of lipids like galactosylceramide and sphingomyelin were found as components of natural prions prepared from infected animal brains (Klein *et al.* 1998). As mentioned before these lipids participate, amongst others, in the composition of rafts microdomains. In addition, pharmacological depletion of cellular cholesterol, which is known to disrupt rafts, also inhibited PrP^{Sc} formation (Taraboulos *et al.* 1995). Furthermore, it was shown, that the conversion of PrP^{C} to PrP^{Sc} took place only when PrP^{C} was attached *via* its GPI-anchor to the membrane. Transmembrane PrP^{C} did not take part in the conversion process (Kaneko *et al.* 1997). These findings confirm the hypothesis that the interaction of PrP^{C} and possibly PrP^{Sc} with the membrane could play an important role in the conversion of PrP^{C} into PrP^{Sc}. The main issue is

how rafts could control the formation of PrP^{Sc}. Although the exact mechanisms are unknown, one could propose following different models. First, rafts could be involved in targeting PrP^{C} to the specific compartment, like outer cell surface, endosome or lysosomes, in which PrP^{Sc} transformation could occur. Second, rafts might contain machinery that is indispensible for PrP^{Sc} formation, such as proteins that facilitate its conversion. Third, rafts could provide a favorable environment for PrP^{Sc} conversion by facilitating close encounters between the PrP^{C} as substrate and PrP^{Sc} as seed, by concentrating these molecules within specific domains of the plasma membrane or aligning them in a way that promotes their interaction.

1.3 Normal cellular function of PrP^{C}

The precise cellular function of PrP^{C} remains still unknown. PrP is a highly conserved protein with highest levels of expression seen in the central nervous system, in particular in association with synaptic membranes. PrP is also widely expressed in the cells of the immune system (Dodelet *et al.* 1998). Based on that information one could speculate that PrP^{C} plays an essential role in the development and live of the host organism. Surprisingly, mice lacking PrP as a result of gene knockout ($PrP^{0/0}$-mice) showed normal development and only slight changes in their phenotype (Bueler *et al.* 1992). These mice were shown to have only minor disturbances in the circadian rhythm and sleep (Tobler *et al.* 1996). The fact that $PrP^{0/0}$ mice were completely resistant to prion disease following an inoculation and did not replicate prions shows that PrP^{C} is is necessary for PrP^{Sc} to replicate (Bueler *et al.* 1993).

A number of lines of evidence argue that PrP^{C} may be a metalloprotein *in vivo*. It has been shown that PrP^{C} binds copper with much higher affinity when compared to other ions like zinc, manganese or nickel (Brown *et al.* 2000; Jackson *et al.* 2001). In the human prion protein two types of high-affinity binding sites for metals have been characterized, consistent with affinities seen with authentic metal binding proteins. One of them is in the N-terminal octapeptide-repeat segment where four histidine residues are responsible for the binding. The other site is around histidines 96 and 111, a region of molecule known to be important for prion propagation (cf. Figure 1.5) (Jackson *et al.* 2001). The fact that $PrP^{0/0}$ mice showed almost 50 % decreased levels of copper in their synaptosomal fractions strengthens the hypothesis that PrP^{C} could play an important role in maintaining a balanced homeostasis of copper. Also, an observation that copper rapidly and reversibly stimulates endocytosis of PrP^{C} from the cell surface could suggest a

physiologically relevant role as a recycling receptor for uptake of copper ions form the extracellular milieu (Pauly *et al.* 1998).

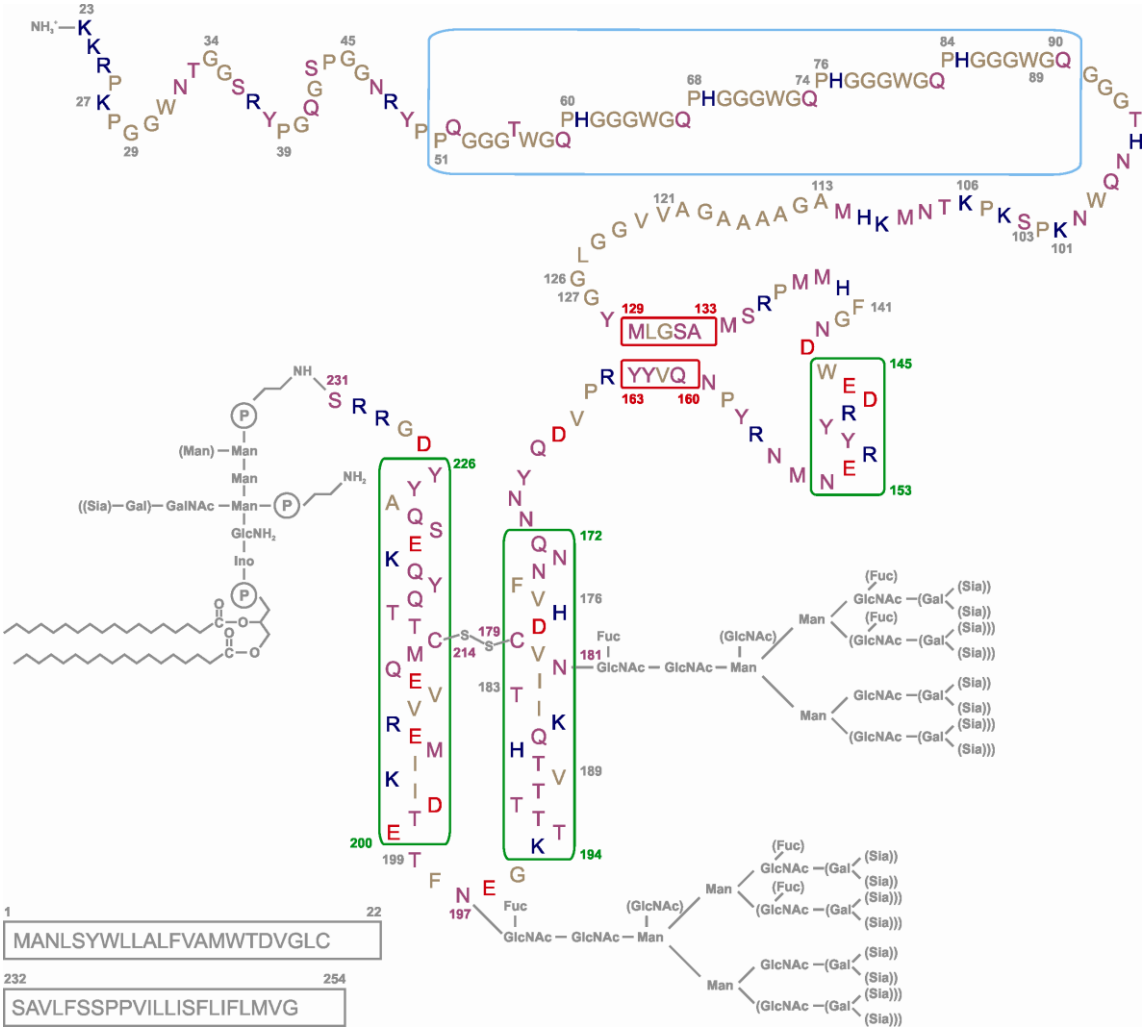

Figure 1.5 Schematic picture of the cellular prion protein from Syrian hamster

Amino acids (aa) 1-22 and 232-254 code for the signal sequences responsible for the transport to the ER-lumen and attachment of the GPI-anchor (lower left). Hexarepeats are located at aa 34-50 and octarepeats at aa 51-90. This segment is also responsible for the binding of copper ions. The three α-helices are located at aa 145-153, aa 172-194 and aa 200-226. Short β-sheet strands are located at aa 129-133 and aa 160-163. Two N-linked oligosaccharides are attached to N181 and N197 and the GPI-anchor to S231. The disulfide-bridge forms between C179 and C214.

Red = negatively charged aa; blue = positively charged aa; violet = neutral hydrophilic aa; brown = hydrophobic aa (all at pH 7.0).

1.4 *in vitro* conversion systems

The "protein-only" hypothesis, introduced by Prusiner, states that a simple protein is main, if not the only component of the infectious agent, and that it is able to replicate itself (Prusiner 1998). The finding that PrP exists in two isoforms expanded this hypothesis to an assumption that the replication mechanism of PrP^{Sc} depends on the PrP^{C} to PrP^{Sc} conversion (Prusiner *et al.* 1990). An ultimate proof for the "protein-only" hypothesis would be to create an *in vitro* system in which the not infectious PrP molecules undergo a conformational transition not only manifested in gaining structural features characteristic for PrP^{Sc} but also showing infectivity. This was finally done by Legname and colleagues, who showed that in highly denaturing conditions recombinant mouse prion protein recMoPrP(89-230) could be polymerized into amyloid fibrils showing a subset of β-sheet rich structures (Legname *et al.* 2004). To differentiate between natural prions and *in vitro* produced ones, the latter were denoted as synthetic prions. When the recombinant fibrils were inoculated into transgenic mice (Tg), also expressing the truncated form of PrP, animals developed neurologic dysfunction. However, the incubation times compared to natural prions were significantly prolonged showing a very low infectivity rate of the synthetic prions. A second passage of Tg mice brain extracts inoculated into wild-type mice, expressing full length PrP^{C}, resulted in almost normal incubation times. This fact points out the importance of GPI-anchor and N-glycosylations, because the prions replicated after the second passage in wild type mice carried all posttranslational modifications.

Another *in vitro* conversion system showed that among many detergents sodium dodecyl sulfate (SDS) in low concentrations (≥ 0.2%) effectively induced transition from recombinant hamster prion protein recHaPrP(90-231) to PrP^{Sc}-like particle. This state was well characterized in terms of the size, PK resistance, increase in β-sheet content and ability to form fibril structures (Post *et al.* 1998; Leffers *et al.* 2005). The SDS has been chosen not only for its denaturing ability, but mostly for its membrane-like character which can well mimic cell membrane environment. In the so-called "SDS- *in vitro* conversion system" concentration of 0.2 % SDS induced a monomeric, partially denaturated α-helical structure (cf. Figure 1.6) (Jansen *et al.* 2001). In ~0.06 % SDS, a α-helical dimer was present as a thermodynamically stable state, which was then converted in a cooperative manner in ~0.04 % SDS to a β-sheet-rich oligomeric PrP^{Sc}-like structure. Further decrease in SDS concentration (≤0.02 %) led to large, insoluble, β-sheeted aggregates, which remained stable after the SDS has been washed out.

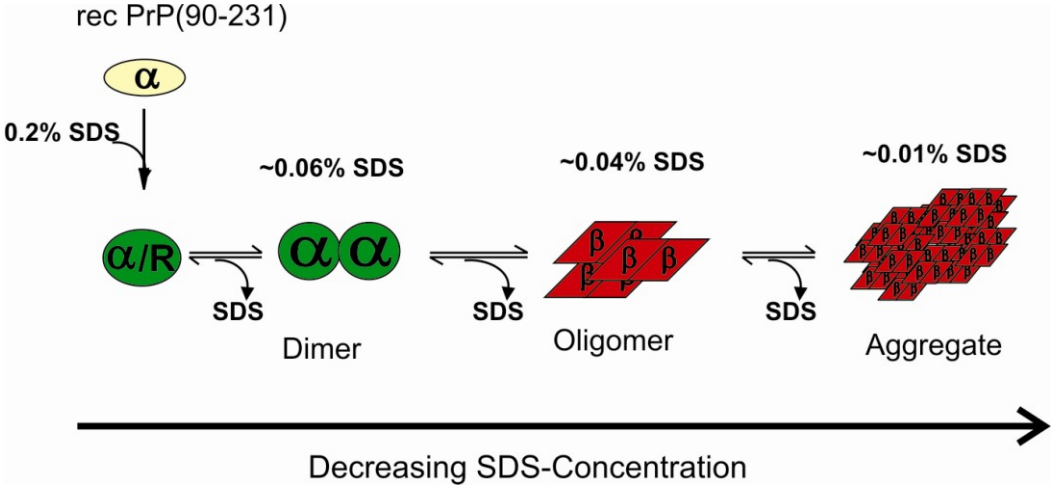

Figure 1.6 SDS *in vitro* conversion system

Decrease of SDS concentration induced the transition process from a mainly α-helical monomer to a β-sheet rich aggregates. The occurring intermediates, i.e. α-helical dimer and β-sheet rich oligomer, have been identified and well described (Jansen *et al.* 2001).

1.5 Prion replication hypotheses

Based on the described structures or structure models of PrP (cf. chapter 1.2.2) and on the data derived from *in vitro* conversion systems (cf. chapter 1.4), one could hypothesize about possible ways for prions to replicate themselves. The so called prion replication models should thus take in account all biological and structural features of both PrP^{C} and PrP^{Sc}. Furthermore, they should also have the ability to explain all known etiologies of prion diseases, namely the sporadic, genetic and transmissible one.

A very general and simple model assumes the direct or indirect contact between membrane-bound PrP^{C} and invading PrP^{Sc}. As an effect of that interaction a conformational transition of PrP^{C} is induced leading to formation of new PrP^{Sc} molecules. This would be the simplest model for the transmissible, i.e. infectious etiology. The model should also explain the sporadic cases of CJD with a spontaneous conversion of PrP^{C} to PrP^{Sc}, occurring with a coincidence of only 1 per 1,000,000 inhabitants per year. In the genetic case a decreased thermodynamic stability of PrP^{C} structure, as a consequence of mutations in *PRNP* gene, would lead to a higher rate of conversion and start of the prion replication. For the transmissible mode, namely the PrP^{Sc}-induced case of conversion, a couple of different models exist describing the process with more details. A so called heterodimer-model suggests a linear autocatalytic type of reaction (Cohen *et*

al. 1994). According to that model, PrP^{C} exists in equilibrium with a second structure, designated as PrP^{*}. It is an intermediate in the PrP^{Sc} formation pathway with slightly destabilized structure. It has the ability to act with an invading PrP^{Sc} particle forming so a heterodimer complex. The formation of the heterodimer is a critical step in the transition process. When successfully formed, PrP^{Sc} induces structural transition of PrP^{*} leading to a PrP^{Sc} homodimer. Next, this homodimer has to undergo a dissociation setting free new PrP^{Sc} particles which then in turn initiate a new replication cycle (cf. Figure 1.7). This model describes an autocatalytic reaction which leads to an exponential increase of the amount of PrP^{Sc} particles. Regarding the equilibrium between the PrP^{C} and PrP^{Sc} the latter state has to be the favored one, since otherwise there would be no driving force for the catalytic turnover.

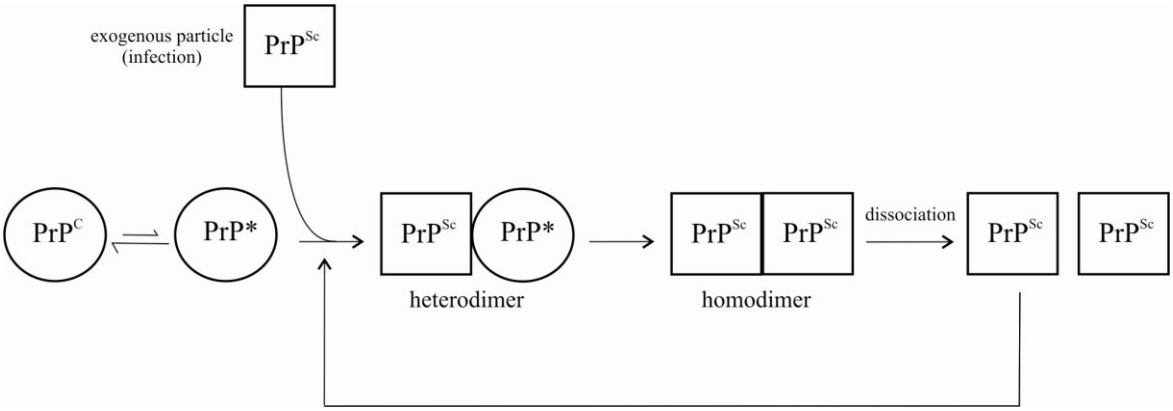

Figure 1.7 The heterodimer-model of prion replication

The conversion of PrP^{C} to PrP^{Sc} occurs after formation of a complex between exogenously added PrP^{Sc} particle and an intermediate molecule, designated as PrP^{*}. This leads to formation of a homodimer, which then in turn, after dissociation can initiate a new replication cycle (Cohen *et al.* 1994).

Thermodynamic calculations by Eigen (Eigen 1996) showed some defects of the heterodimer-model. The fact that spontaneous transformation occurs so rarely and shows very long incubation times led to the assumption that this process has to be extremely slow, otherwise PrP^{Sc} would grow spontaneously even without infection. Therefore, to induce such a slow process in the heterodimer complex one had to assume a catalytic acceleration of 10^{15}. This However, is rather unrealistic, considering the known enzymatic processes in nature. Eigen's calculations provided a scientific basis for a new model, the so called cooperative Prusiner-model. It acts as an extension of the heterodimer-model and states that several molecules of PrP^{Sc} have to cooperate to transform one molecule of PrP^{C}. PrP^{Sc} in this model is again thermodynamically favoured.

Every new molecule of PrP^{Sc} that binds to a primary heterodimer complex leads to a faster change in the conformation of the PrP^{C} which increases the affinity for binding more new molecules.

Lansbury proposed another mechanism of prion replication in which fibril formation and generation of infectivity are closely related (cf. Figure 1.8) (Rochet *et al.* 2000).

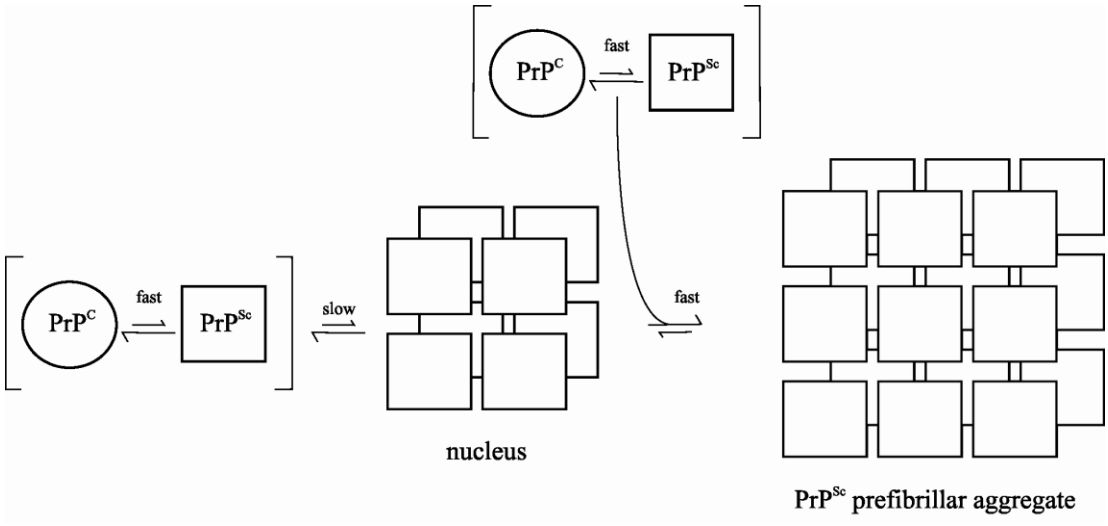

Figure 1.8 Seeded nucleation model

According to this model a formation or exogenous addition of a seed in form of PrP^{Sc} aggregate is necessary to start the replication process.

This nucleation-dependent model follows the principle of linear crystallization where the equilibrium between PrP^{C} and PrP^{Sc} is on the side of PrP^{C} molecule. Therefore, little amounts of PrP^{Sc} present in the system do not posses any pathogenic properties. Pathogenicity occurs only when a nucleation seed in form of PrP^{Sc} aggregate is formed or exogenously added, for example during the infection. Hence, the kinetic barrier to the conversion of PrP^{C} to PrP^{Sc} would be nucleation rather than a conformational conversion. Once a critical size barrier of PrP^{Sc}-oligomer has been passed following processes of PrP^{C} binding and conversion to new PrP^{Sc} particles can proceed much faster leading to amyloid and fibril formation.

All the models, described till now, have one common feature, namely the silent assumption that PrP conversion takes place in the solution. However,, as shown in chapter 1.2.5, PrP^{C} is found in a membrane-anchored state on the cell surface, and one might hypothesize that this location is the site of prion conversion or replication. Moreover,, the data collected with the help of *in vitro*

conversion systems showed that the presence of SDS with its membrane-like properties might influence the structure of PrP drastically (cf. chapter 1.4). All these observations led us to assumption that a membrane environment plays an important role in the prion conversion process. The experiments of Elfrink allowed quantitative studies on the equilibrium of PrP^C between the "free in solution" and "anchored to the membrane" states (Elfrink *et al.* 2007). The so called two-phase model describes a pre-equilibrium between membrane-bound PrP^C and free PrP^C in solution with a very low concentration of PrP^C in solution, i.e. in the range of 10^{-9} M. When the membrane is close to saturation, this concentration could be 10^{-8} M or even higher. In the case of a less occupied membrane, the concentration of PrP^C free in solution could be 10^{-10} M or lower. As shown in the Figure 1.9, the main point of the two-phase model is the instability of PrP^C in solution. It can either return to the membrane-bound state or undergo a spontaneous transition to amorphous or fibrillar aggregates in the aqueous phase.

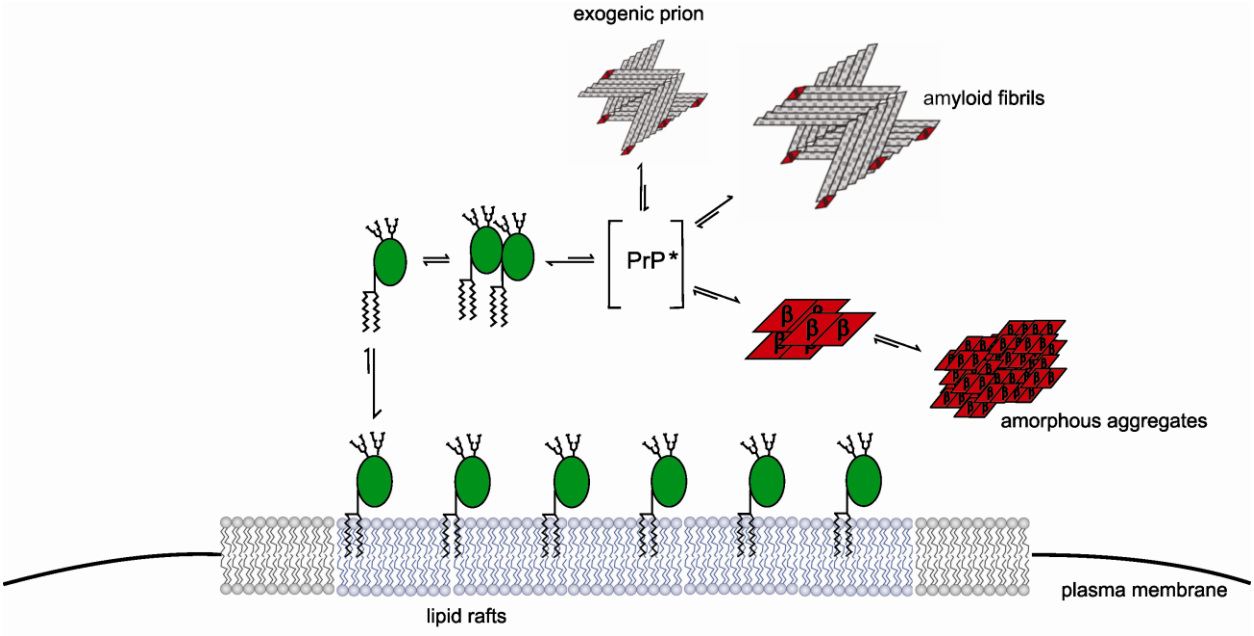

Figure 1.9 Two-phase model of PrP conversion

Schematic illustration of different intermediate states involved in PrP conversion (Elfrink *et al.* 2007).

However, this spontaneous transition would occur only with a marginal probability, and in that sense the free PrP^C could be compared to the slightly destabilized PrP^* form discussed earlier as an intermediate of conversion.

In summary, the "PrP^C in solution" state is possibly present only in low concentrations and the higher populated state is the "membrane-anchored" state. It appears most plausible that the invading prion particle meets the membrane-anchored PrP^C. Both processes nucleation and growth might also occur on the surface of the membrane.

1.6 Aims of the thesis

The two-phase model of concentration of membrane-bound PrP^C and low concentration of PrP^C in solution opened a new concept for further experimental analysis. It was just an obvious consequence to study as next step the onset of the disease. This could be done by introducing infectious prion particles as third component. The Biacore system, which was used for previous analysis would still be the method of choice when applied to this project. It not only allows one studying solely protein interactions but also due to the continuous flow of a sample in solution over a surface, a perfect simulation of events taking place in the nature at the membrane is possible. Having in mind all the information gathered till now about possible sites for PrP^{Sc} formation (cf. chapter 1.2.5) following scenarios are plausible and also possible to observe experimentally with the help of the membrane-PrP^C system in the Biacore device:

(1) The incoming infectious PrP^{Sc} particle interacts with the one or a few of the PrP^C molecules in solution, thereby shifting the equilibrium of PrP^C from the membrane into the solution. This sudden change of the environment surrounding the PrP^C particle could lead to a conformational change. As a consequence, the conversion of PrP^C to a new PrP^{Sc} particle would take place, which would be attached to the original, exogenous PrP^{Sc} as it is observed for the prion protein fibril elongation (cf. Figure 1.10 a).

(2) The invading, exogenous PrP^{Sc} particle interacts with the membrane-bound PrP^C. As the site of this interaction the rafts domains would be of particular interest, since infectious PrP^{Sc} also possess the GPI-anchor that would direct it to these specific microdomains. By reaching the outer membrane and binding to PrP^C a conversion process could be induced launching the formation of new PrP^{Sc} particles (cf. Figure 1.10 b).

Therefore, the main aim of this project was to study the mode of the interaction between membrane-anchored PrP^C and invading PrP^{Sc} and to find hints for a possible membrane-dependent conversion mechanism.

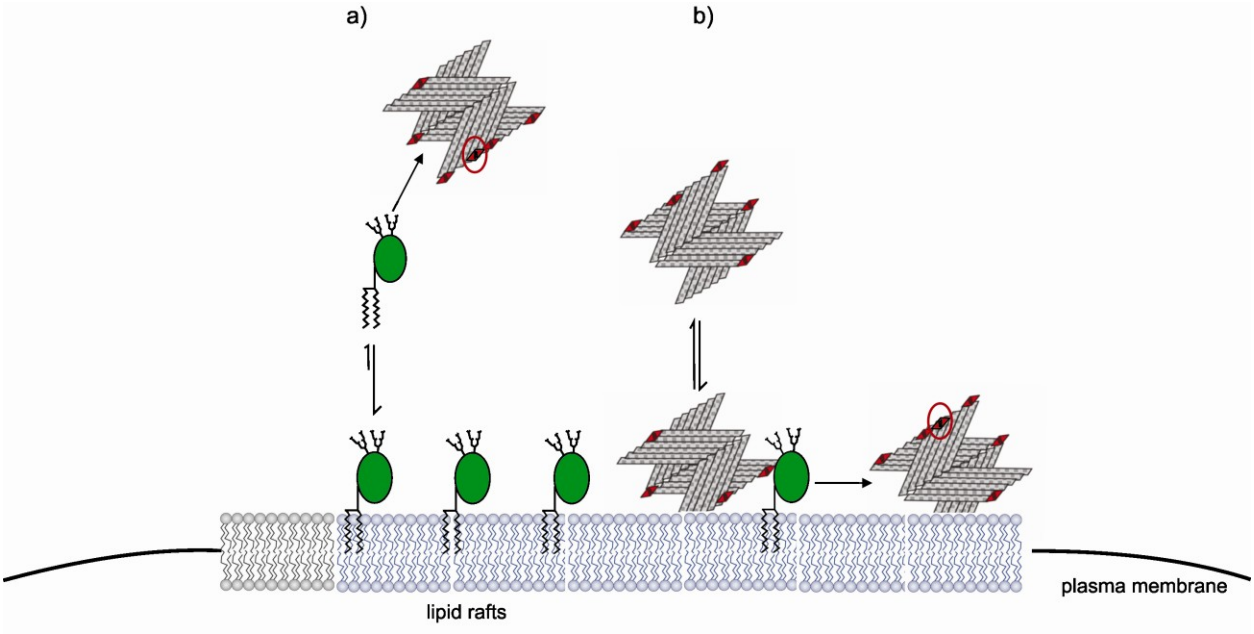

Figure 1.10 Aims of the thesis

In order to study the character of the PrP^{C} - PrP^{Sc} interaction and the possible membrane-dependent conversion process one has to utilize a system that contains all three components: the lipid membrane, the anchored PrP^{C} and the invading, exogenous PrP^{Sc}. Following effects could be then observed: PrP^{Sc} pulls out the membrane-anchored PrP^{C} and the conversion process takes place in the close proximity of the outer cell membrane (**a**), or invading PrP^{Sc} particles interact with PrP^{C} at the cellular membrane inducing so the conversion process (**b**). Red subunits of PrP^{Sc} represent sites of nucleation and newly formed PrP^{Sc} molecules (encircled).

2 Materials and Methods

2.1 Chemicals

If not stated otherwise, chemicals were of the highest purity grade available and obtained from regular commercial suppliers. For preparation of buffers and other dilutions a high-purity Milli-Q-Water was being used, designated as H_2O_{deion}.

2.2 Solutions and buffers

NaPi (Sodium Phosphate buffer)

100 mM Disodiumhydrogenphosphate (Na_2HPO_4) and

100 mM Sodiumdihydrogenphosphate (NaH_2PO_4)

were mixed to achieve the desired pH-value. If not stated otherwise the buffer was used at a final concentration of 10 mM at pH 7.2.

CBS (Citrate-buffered Saline)

10 mM Sodium citrate/Citrate acid pH 6.0

137 mM Sodium Chloride

TBS-T (Tris-buffered Saline, Tween)

10 mM Tris/HCl pH 8.0

150 mM NaCl

0.01 % Tween 20

Acrylamide stock solution

30 % Acrylamide (600 g)

0.8 % N, N'-bisacrylamide

a.d. 2 l H_2O_{deion}

The solution was stirred for at least 30 minutes after addition of amberlite MB3 (ionic exchanger), filtered and stored at 4°C.

2.3 Lipids

All lipids, obtained from Avanti Polar Lipids, Inc., were diluted in chloroform and stored at - 20°C. The concentrations of the lipids stock solutions differed from 10 to 25 mg/ml. Following natural lipids were used to create lipid mixtures:

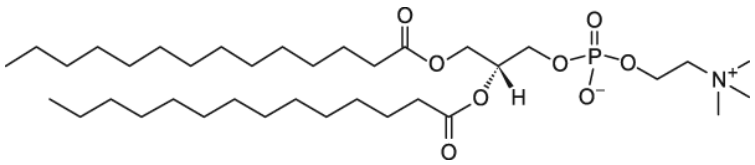

Di-Myristol-Phosphatidylcholine (DMPC)

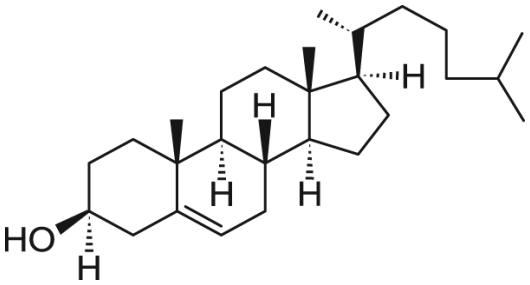

Cholesterol

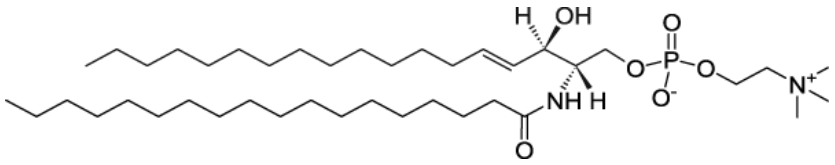

Brain sphingomyelin

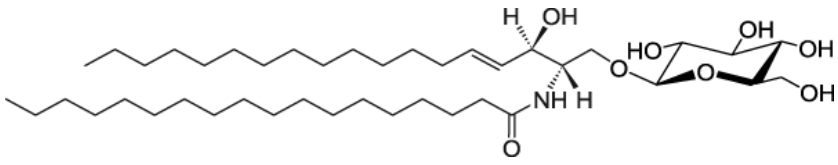

Brain cerebroside

2.3.1 Raft-like lipid composition

The exact composition of natural raft microdomains is still unknown. Therefore different protocols for preparation of raft-like model membranes can be found in the literature. However, they all have one thing in common, namely a high concentration of sphingomyelin and cholesterol. Sphingolipid-cholesterol-rich liposomes (SCRLs) containing DMPC, sphingomyelin, cerebroside and cholesterol in a 2:1:1:2 molar ratios were used (Schroeder *et al.* 1994).

2.4 Chinese hamster ovary (CHO) - cell culture

The transfected Chinese hamster ovary (CHO)-cell line was obtained as a kind gift from the Stanley B. Prusiner laboratory (UCSF, San Francisco, USA). All cell culture experiments were conducted under the Microflow Biological Safety Cabinet (Nunc GmbH). Cell suspension cultures in Bioreactor Flasks (Bellco Glass Inc.) were placed in a CO_2-Incubator (Nunc GmbH) at 2 % CO_2, 37°C and stirring speed of 75 rpm. In order to count the number of living cells, the cell suspension was being diluted 1:1 with a Trypan blue solution (Life-Technologies). Trypan blue is a vital stain used to selectively color dead cells. Since cells are very selective in the compounds that pass through their membrane, in a viable cell, Trypan blue is not being absorbed. It traverses However,, the membranes in dead cells, showing them in a distinctive blue color under a microscope. Since live cells are excluded from staining, this method is also described as a dye exclusion method. The Trypan blue-cell suspension solution was placed in a hemocytometer under a microscope and the live cells were counted. The cell concentration was then calculated using following formula:

$$N = \frac{n \cdot x}{y} \cdot 10^4 \ (cells/ml)$$

n = number of the counted live cells

x = dilution factor

y = number of the counted quadrants

N = cell concentration

2.4.1 Selection and amplification systems

CHO-cells growing in culture require glutamine for their proper growth and survival. Glutamine can either be obtained from the medium or synthesized by the cells from glutamate and ammonia in a catalysis reaction, by the enzyme called glutamine synthetase (GS):

Glutamate + ATP + NH_4^+ ⟶ Glutamine + ADP

CHO-cells grown in a medium that is glutamine free do not survive, unless they are able to produce sufficient amounts of GS. The selection mechanism is following: transfecting the cells with a vector that codes for the GS gene along with the PrP^C-gene, leads to survival of cells. CHO-cells, However,, contain an endogenous GS. Hence, specific gene expression can be achieved by plating the CHO-cells in a medium that contains methionine sulfoximine (MSX), an inhibitor of GS (Sanders *et al.* 1984). Only those cells that incorporated the vector and express GS at levels sufficiently high to overcome the MSX block will survive. The expression levels of endogenous GS are so low that cell without the vector do not survive. Expression of the PrP^C gene can be amplified by growing the cells in successively higher concentrations of MSX (Blochberger *et al.* 1997).

2.4.2 CHO-cells culture medium

CHO-cells suspension culture was grown in a special CHO-S-SFM II medium (Gibco Life Technologies) that contained 4.5 g/l glucose, 2.4 g/l sodium hydrogen carbonate, 15 mM HEPES and was glutamine free. Additionally following substances were added to 500 ml of the medium before each use:

MEM non essential amino acids (NEAA)	100x	5 ml
Sodium pyruvate	100x	5 ml
Penicillin/Streptomycin solution	100x	5 ml
Fungizone	100x	5 ml
Insulin-Transferrine-Selenium S Supplement	100x	5 ml
Nucleotide solution	50x	10 ml
Glutamate- and Aspartate-solution (G+A)	100x	5 ml
Methionine sulfoximine (MSX)	100 mM	250 µl

Composition of the used solutions:

50x nucleotide solution (100 ml)	35 mg Adenosine
	35 mg Guanosine
	35 mg Cytidine
	35 mg Uridine
	12 mg Thymidine

100x G+A solution (100 ml)	600 mg Glutamate
	600 mg Aspartate
100 mM MSX in PBS (10 ml)	180 mg MSX

2.5 Purification of CHO-PrP^C

CHO-cells suspension cultures were prior to each purification procedure centrifuged using the Allegra X-15R centrifuge (Beckman Coulter) at speed of 250 x *g* (S x 4750A rotor). Cell pellets were stored at - 20°C. The main purification takes place by two affinity-chromatographies: an immobilized metal chelate affinity chromatography (IMAC) using the intrinsic property of PrP^C to bind copper ions (cf. chapter 2.5.2) and an immune-affinity chromatography employing anti-PrP antibody scFvW226 (cf. chapter 2.5.3). All chromatographic steps were performed on a chromatography system (Äcta Prime, GE Healtcare) at 4°C (Elfrink *et al.* 2004).

2.5.1 Solubilization of CHO-PrP^C

The lysis step during the preparation of CHO-cells not only destroys the cell membrane to release the proteins, but also solubilizes the membrane-anchored natural PrP^C. This was done by diluting 4 x 10^9 pelleted cells in 100 ml solubilization buffer. Next the sample was swung for 1 h, at 4°C. The solubilization buffer contains both mild detergents (DOC and NP40) and protease inhibitors. Next the sample was centrifuged at 10,000 x *g* (S x 4750 A rotor) to divide the insoluble cell debris from the soluble PrP^C that remains in the supernatant.

Solubilization buffer

10 mM	NaPi, pH 7.5	2 mM	PMSF
0.5 mM	$MgCl_2$	1 mM	EDTA
1 µM	Pepstatine	0.5 %	Desoxycholate (DOC)
1 µM	Leupeptine	0.5 %	NP40

2.5.2 Copper immobilized metal-chelate affinity chromatography (Cu^{2+}-IMAC)

For IMAC, a Chelating Sepharose Fast Flow column (GE Healthcare) with a volume of 60 ml was used. Copper was loaded onto the column directly before each use. After the equilibration with 1 mM imidazole the sample, also adjusted to 1 mM imidazole, was loaded onto the column using a flow rate of 2.5 ml/min. In order to release weakly bound proteins the concentration of imidazole was increased stepwise to 10 and 15 mM, respectively. Elution of PrP^C took place at very stringent conditions of 150 mM imidazole. To prevent PrP^C aggregation every solution contained 0.15 % Zwittergent 3-12 (Zw 3-12). During the last step the column was regenerated by removing copper with the chelator ethylene diamine tetra acetic acid (EDTA).

2.5.3 Immunopurification

Purified single chain fragment W226 (scFvW226) antibody was covalently attached to NHS-activated Sepharose 4 Fast Flow (GE Healthcare). N-hydroxysuccinimide (NHS) coupling forms a chemically stable amide bond with ligands containing primary amino groups. 20 ml of antibody solution in PBS at a concentration of 0.3 mg/ml were loaded onto centricons with a pore size of 20 kDa (Vivaspin 2, Vivascience Sartorius Group) and centrifuged at 4,000 x *g* (S x 4750 A rotor). The resulting sample had a volume of 0.22 ml and protein concentration of 27 mg/ml as measured with the help of spectrophotometer (V-630 Spectrophotometer, Jasco). The ligand was then dissolved in the coupling buffer – 50 mM HCO_3/0.1 mM EDTA to a final volume of 2 ml and mixed with 1 ml washed NHS-activated Sepharose 4 Fast Flow beads. After the coupling reaction was completed (overnight at 4°C) the medium was blocked and washed with a method that alternates two different buffers with low and high pH, respectively. The column was washed 5 times with 2 ml of 20 mM Tris, pH 8 and 2 ml of 50 mM Glycine, pH 2.5 buffers. Finally, the resulting scFvW226-column with 2 ml end volume was equilibrated with TBSTE and used for immunopurification step. To obtain high binding capacities the flow rate during the sample load was set to 0.5 ml/min. After removing unbound protein elution took place by decreasing pH to 2.8 in order to abolish antibody antigen interaction. In contrast to the other solutions used during both chromatographies the elution buffer did not contain Zw 3-12. The resulting sample was pooled and ovalbumin at a final concentration of 1 mg/ml, alternatively 2 mg/ml was added to prevent the PrP^C aggregation.

2.5.4 Concentrating step

The purified sample was loaded onto centricons with a pore size of 5 kDa (Amicon Ultra Centrifugal Filter Devices, Millipore) in order to concentrate the protein. The sample was centrifuged at 4,000 x *g* (S x 4750 A rotor). Furthermore, an extensive washing during the concentrating step enabled a change of buffer to 1 x citrate-buffered saline (CBS) pH 6. Purified PrP^C was then fractionated and stored at - 80°C until use. However, addition of ovalbumin made an exact determination of PrP^C concentration not possible.

2.6 Preparation of CHO-PrP^C aggregates

One of the methods to accelerate prion protein aggregation is change of the solution pH. This was done according to the protocols developed previously (Salwierz 2004). CHO-PrP^C diluted in 1 mM NaAc, pH 4.2 was mixed with 10 mM NaPi buffer at pH 7.2 in a volume ration of 1:0.85. The samples with protein concentrations of 50 ng/µl and 10 ng/µl were incubated over night at room temperature. Finally a dilution with CBS buffer to concentrations of 5 ng/µl and 1 ng/µl, respectively took place. The aggregation efficiency was tested using the differential ultracentrifugation method (cf. chapter 2.11) and the binding ability of so prepared aggregates was measured with the help of the Biacore device (cf. chapter 2.17).

2.7 Selective precipitation of PrP^{Sc}

Safar and colleagues found out that at neutral pH in the presence of Mg^{2+} a substance called sodium phosphotungstate (NaPTA) forms complexes with oligomers and polymers of infectious PrP^{Sc} and PrP 27-30 but not with PrP^C (Safar *et al.* 1998). This observation was used for a selective precipitation of PrP^{Sc} from hamster brain homogenates. 5 % hamster brain homogenate (weight/volume) containing 2 % sarkosyl was mixed with stock solution containing 4 % NaPTA and 170 mM $MgCl_2$, pH 7.4, to obtain a final concentration of 0.25 % NaPTA. The sample was then incubated overnight at 37°C on a shacking platform and centrifuged at 14,000 x *g* for 30 min (TLA 45 rotor, Optima TL Ultracentrifuge, Beckman). The pellet was then washed three times with PBS buffer containing 250 mM EDTA/0.1 % sarkosyl, 250 mM EDTA, and 50 mM EDTA, respectively and additional two times with CBS buffer. Each washing procedure was separated from the following one with a 30 min centrifugation step. Finally the pellet,

corresponding to $2.5 \cdot 10^{-2}$ g BE (brain equivalent), was resuspended in 600 µl CBS buffer, sonicated three times for 3-4 sec and fractionated in 120 µl samples (corresponding to $5 \cdot 10^{-3}$ g BE) that were directly used for the SPR measurement. In order to test the efficiency after each precipitation experiment a SDS-PAGE followed by Western Blot analysis was performed. Both pellet samples from scrapie-infected and healthy controls were used and the amount, purity and specificity of the precipitated material were analyzed. This was done by comparing the samples after proteinase K (PK) digestion. The precipitated pellet was fractioned into samples, each in a duplicate. The first sample from the duplicate remained intact, while to the second one PK at final concentration of 50 ng/µl or 10 ng/µl, for the limited PK digestion protocol, was added. The incubation of the samples at 37°C took place for 1 h or 30 min, respectively and followed by SDS-PAGE analysis.

2.8 Preparation of prion rods

PrP 27-30 from brains of scrapie-infected Syrian hamsters was provided by Stanley B. Prusiner laboratory (UCSF, San Francisco, USA). As the last step of the purification protocol (Prusiner *et al.* 1983) the sucrose gradient fractions were diluted with H_2O_{deion} in order to obtain sucrose concentration less than 20 %. Next, the samples were loaded onto centrifugation tubes (38 ml Beckman Tubes, Thick Wall) and centrifuged (SW-28 swing-out rotor) for 20 h, 100,000 x *g* spin at temperature of 4°C (Optima L-80XP Ultracentrifuge, Beckman Coulter). The supernatants were discarded and the pellets were washed twice with 100 µl of H_2O_{deion}, pooled and centrifuged again (TLA-45 rotor) for 1 h, 100,000 x *g* spin at 4°C (Optima TL Ultracentrifuge, Beckman). Finally, the pellet was diluted in 750 µl of CBS buffer and sonicated twice (30 sec, 200 W, Sonicator 3000, Misonix). This procedure leads to optimal dilution of the pellet and disruption of possible protein aggregates. Afterwards sample was fractionated and stored at - 80°C.

2.8.1 Lipid extraction

For this procedure a ready pellet after second 100,000 x *g* spin (cf. chapter 2.8) was diluted in 100 µl of n-Butanol and incubated for 15 min at room temperature. Afterwards it was centrifuged for 2 min at 14,000 rpm (table centrifuge, EBA 12). The supernatant was the discarded and the lipid extraction of the pellet was repeated two more times. Since n-Butanol

damages the tube wall, the sample was transferred to a new tube before each centrifugation step. Finally, the pellet was dried out, diluted in 750 µl of CBS buffer and sonicated twice (30 sec, 200 W, Sonicator 3000, Misonix). Afterwards samples were fractionated and stored at - 80°C.

2.9 Preparation of insulin fibrils

Insulin is a small hormone consisting of two polypeptide chains – A (21 residues) and B (30 residues), linked by two inter-chain disulfide bridges. When heating of the insulin sample at high temperature and low pH is followed by quick freezing it, a series of structural changes occur that result in formation of fibrillar structures (Brange *et al.* 1997). Here, a temperature-induced fibril formation was conducted by heating the insulin sample (10 mg/ml) to 92°C for 10 min and then rapidly freezing it in liquid nitrogen. These freeze-thaw cycles were repeated 7 times, but the heating time in the last 6 cycles was reduced to 3 min. This procedure led to unfolding of the native protein resulting in formation of amorphous aggregates and mature fibrils. After the 7^{th} cycle insulin sample was diluted in CBS buffer to a final concentration of 1 mg/ml and stored at 4°C.

2.10 Preparation of small unilamellar vesicles (SUVs)

Hydration of thin, dried lipid films leads to creation of lipid vesicles. This occurs when dry lipid bilayers stacked onto each other swell and become fluid. The hydrated lipid films are released from the surface and create spontaneously large multilamellar vesicles (MLVs) with an "onion-like" structure. In order to create small unilamellar vesicles (SUVs) a high-shear sonication has to be applied (cf. Figure 2.1).

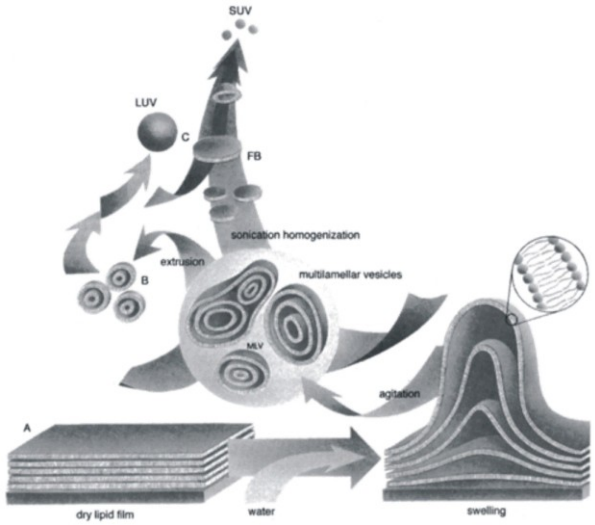

Figure 2.1 Preparation of lipid vesicles

Hydration of dry lipid films leads to creation of MLVs. Due to sonication process a reduction of the vesicle size takes place and SUVs can be obtained (Figure from Avanti Polar Lipids, Inc.).

2.10.1 Vesicles manufacture

Raft-like lipid mixture (cf. chapter 2.3.1) was transferred to a cone-shaped glass vial. Since all lipids were previously diluted in chloroform only glass vials and glass micro-pipettes could be used. Lipids were then dried under a stream of nitrogen and evacuated for 15 h. To keep the membranes fluidic, all subsequent procedures were carried out at 37°C. Dried lipids were hydrated to a concentration of 200 µg/ml in 1 x CBS for 1 h. This led to the formation of MLVs. After sonication (Labsonic® U, B. Braun Biotech International) using a microtip probe at low settings (40 V) for 30 min, SUVs could be formed (Benes *et al.* 2004). The solution was filtered through a 0.45 µm filter (Whatman) to remove any tip-generated debris. Vesicles were used within 1 h to avoid formation of MLVs by relaxation.

2.11 Differential ultracentrifugation

The solubility of the prion protein under given conditions was determined according to the standards of Hjelmeland and Chrambach (Hjelmeland *et al.* 1984), defining that particles that remain in the supernatant after a 100,000 x *g* spin for 1 h (TLA 45 rotor, Optima TL Ultracentrifuge, Beckman) are regarded as soluble, representing the PrP^{C}–like form, whereas the particles remaining in pellet are insoluble and indicate the PrP^{Sc}-like form of the prion protein.

After centrifugation supernatants were diluted and pellets were resuspended in sample buffer. Next a SDS-PAGE, followed by semi-dry blot was carried out in order to determine the relative amounts of protein in supernatant and pellet (cf. chapter 2.15).

2.12 Protein gel electrophoresis (SDS-PAGE)

Sodium-dodecyl-sulfate polyacrylamide gel electrophoresis (SDS-PAGE) is a technique widely used to separate proteins according to their molecular size. Protein gel electrophoresis was carried out in a Hoefer SE 600 chamber by GE Healthcare according to the protocol of Laemmli (Laemmli 1970) different sizes of glass plates were used: 18 cm x 16 cm and 18 cm x 24.5 cm (wide x height). First a 12 % resolving gel was being prepared. This gel can be effectively used for separating proteins with size between 14 and 66 kDa. Next, a 3 % stacking gel was cast over the ready resolving gel. Analyzed samples were incubated with sample buffer, for 10 miutes, at 100°C. The gel electrophoresis process took place in 1x Laemmli buffer in the presence of 0.1 % SDS for 30 min at 180 V followed by approximately 180 min at 300 V or until the bands had reached the desired position in the gel. To determine the molecular weight both the Spectra™ Multicolor Broad Range Protein Ladder and the PageRuler™ Plus Prestained Protein Ladder protein markers from Fermentas, Life Science were used.

Following buffers and gels were used:

10 x gel electrophoresis buffer (10x Laemmli buffer)

1.9 M	Glycine (288 g)
0.25 M	Tris/HCl (60 g), pH 8.3

Resolving gel (12 %)

380 mM	Tris/HCl pH 8.8
12 %	Acrylamide/Bisacrylamide (30:0.8)
0.1 %	SDS
0.1 %	TEMED (N,N,N´,N´-tetramethyl-ethane-1,2-diamine)
0.1 %	APS (Ammonium Peroxydisulfate)

Stacking gel (3 %)

124 mM	Tris/HCl pH 6.8
3 %	Acrylamide/Bisacrylamide (30:0.8)
0.1 %	SDS
0.1 %	TEMED
0.1 %	APS

Sample buffer

70 mM	Tris/HCl pH 6.8
5 %	2-β-Mercaptoethanol
2 %	SDS
5 %	Glycerol
0.05 %	Bromphenolblue

2.13 Silver staining of protein gels

With the help of the silver staining method developed by Heukeshoven (Heukeshoven 1985) detection of 50 ng of protein band is possible. The staining of protein gels after SDS-PAGE was performed as followed: 20 min fixation with 50 % ethanol/10 % acetic acid, 10 min wash with 10 % ethanol/5 % acetic acid, 20 sec incubation with 0.05 % sodium carbonate/0.15 % potassium ferrocyanide/0.3 % sodium thiosulfate, wash with H_2O_{deion}, incubation with 0.012 M silver nitrate, wash with H_2O_{deion}, development with 3 % sodium carbonate/0.02 % formaldehyde and reaction stop with 1 % acetic acid.

2.14 Dot blot

In a dot blot procedure the protein is directly applied to a polyvinylfluoride- (PVDF-) membrane (Millipore GmbH) using a weak vacuum. The device, used in this method, allows processing of 96 samples at the same time (S & S Minifold I). The PVDF-membrane was first activated with ethanol and then shortly equilibrated in H_2O_{deion} ,along with a sheet of Whatman paper. Next the device was assembled by placing the Whatman paper on top of the lower chamber, followed by the PVDF-membrane and the 96-well cover. After the device was prepared, 200 µl of H_2O_{deion} was applied to the slots followed by samples of different volume. The transfer of protein to the

PVDF-membrane took place under a weak vacuum. Detection of the protein was carried out using the monoclonal antibody 3F4 (UCSF, San Francisco, USA). The 3F4 antibody recognizes only denatured protein, therefore membrane was incubated for five min in 1 % KOH and then briefly washed in TBS-T prior to the immunologic reaction (cf. chapter 2.16).

2.15 Semi-dry blot

With a help of this technique a transfer of proteins from SDS-PAGE to a PVDF-membrane can be achieved. After gel electrophoresis the polyacrylamide gel is briefly incubated in 1x gel electrophoresis buffer (cf. chapter 2.12) without SDS along with 6 sheets of Whatman paper and the PVDF-membrane that was moistened with ethanol. Then the SU20-SDB (Sigma Aldrich) or the EBU-6000 (C.B.S. Scientific Co) device was assembled in a following manner: anode, three sheets of Whatman paper, PVDF-membrane, polyacrylamide gel, three sheets of Whatman paper, cathode. Transfer was carried out for 45 - 60 min at 0.8 mA/cm². Next the membrane was removed and the protein was detected using an immunologic reaction.

2.16 Immunologic protein detection

As mentioned above, the immunologic detection of PrP was carried out using the PrP-specific primary antibody 3F4 (Kascsak *et al.* 1987). PVDF-membranes with bound proteins after semi-dry blot treatment were incubated in TBS-T, pH 8.0 containing 5 % milk powder (Oxoid Skim Milk Powder) for 1 - 2 h at room temperature (optional: overnight at 4°C). This allows blocking unspecific protein binding sites on the PVDF-membrane. Next, the membrane was briefly washed in TBS-T, pH 8.0 and then incubated with the primary antibody 3F4 (1:10,000 in TBS-T, pH 8.0). This procedure took place for 1 - 2 h at room temperature or optional, overnight at 4 °C. Then, the membrane was washed twice in TBS-T, pH 8.0 for 10 minutes. Next, an incubation with the secondary antibody GaM-PO (goat-anti-mouse-IgG-antibody labeled with horseradish-peroxidase; Jackson ImmunoResearch Laboratories, Inc.) at a dilution of 1:5,000 in TBS-T, pH 8.0 for 1 - 2 h at room temperature took place. Afterwards antibody that did not bind to 3F4 was washed out in three steps using TBS-T, pH 8.0. Immunological detection was carried out using a chemoluminescence reaction in a following mechanism: the detection reagent contains luminol, which is oxidized by the peroxidase coupled to the secondary antibody. This reaction releases energy in the form of light. The membrane was incubated with the detection reagent kit

SuperSignal® West Pico Chemoluminescent Substrate (Pierce) for five minutes. The emission of light lasts for approximately one hour. In order to make the protein visible, the membrane was exposed to x-ray film (Hyperfilm, Amersham Pharmacia Biotech) for approximately 15 - 30 sec and then developed using a Curix 60 table-top processor (Agfa).

2.17 Kinetic analysis of molecular interactions

The kinetic analysis of CHO-PrP^C with PrP 27-30 in the presence of lipid membranes was performed with the help of Biacore 1000 device (GE Healtcare). Biacore technology is a label-free technology for monitoring biomolecular interaction as they occur. The detection principle relies on surface plasmon resonance (SPR), an electron charge density wave phenomenon that arises at the surface of metallic film when light is reflected at the film under specific conditions. In Biacore system, SPR is used to monitor interactions occurring in a biospecific surface on a metal layer by measuring changes in the solute concentration at the surface as a result of the interactions (Raether 1977; Welford 1991).

2.17.1 Total internal reflection and evanescent field

In order to describe SPR it is helpful to start with the phenomenon of total internal reflection (TIR) which occurs at an interface between non-absorbing media. When a light beam propagating in a medium of higher refractive index meets an interface at a medium of lower refractive index at an angle of incidence above a critical angle, the light is totally reflected at the interface and propagates back into the high refractive index medium. Although the fully reflected beam does not lose any net energy across the TIR interface, the light beam leaks an electrical field intensity called an evanescent field wave into the low refractive index medium (cf. Figure 2.2). The amplitude if this evanescent field wave decreases exponentially with the distance from the interface, decaying over a distance of about one light wavelength from the surface. If the TIR-interface is coated with a layer of a suitable conducting material, such as a metal, the p-polarized component of the evanescent field wave may penetrate the metal layer and excite electromagnetic surface plasmon waves propagating within the conductor surface that is in contact with the low refractive index medium (cf. Figure 2.3 a). For a non-magnetic metal like gold, this surface plasmon wave will also be p-polarized and, due to its electromagnetic and surface propagating nature, will create an enhanced evanescent wave. A resonant absorption of

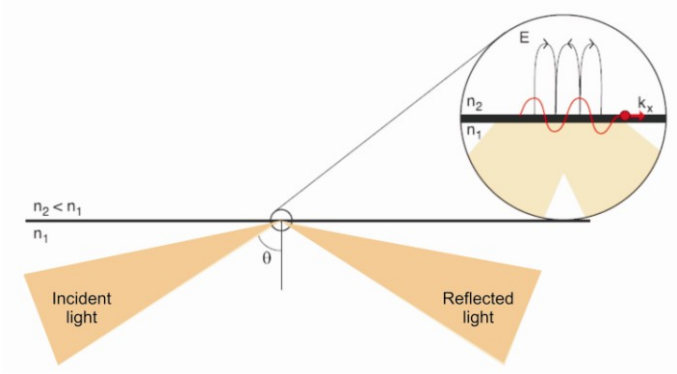

Figure 2.2 TIR for non-absorbing media

Light propagating in a medium of refractive index n_1 undergoing a total internal reflection at the interface with the medium of a lower refractive index n_2. The evanescent field, E, is a non-transverse wave having components in all spatial orientations, decreasing in field intensity with penetration into the medium of n_2. Θ is the angle of incidence (Figure from Biacore Technology Note, GE Healthcare).

energy via the evanescent wave field causes a characteristic drop in the reflected light intensity. For a given wavelength of incident light, SPR is seen as a dip in the intensity of reflected p-polarized light at a specific angle of incidence (cf. Figure 2.3 b).

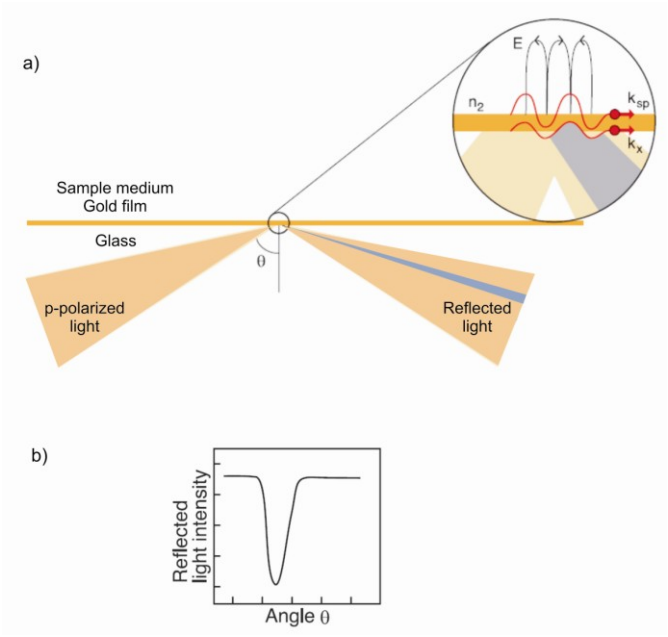

Figure 2.3 Evanescent field

SPR is excited by p-polarized totally internally reflected light at a glass/metal film interface. In Biacore systems which use a sensor chip, this interface takes a form of an exchangeable gold-coated glass slide (**a**). SPR is observed as dip in the reflected light intensity at a specific angle of reflection (**b**) (Figure from Biacore Technology Note, GE Healthcare).

2.17.2 Surface plasmon

In physics, a plasmon is a quanta of plasma oscillation. For a plasmon excitation by a photon to take place the energy and momentum of these "quantum-particles" must both be conserved during the photon "transformation" into a plasmon. This requirement is met when the wave vector for the photon and plasmon are equal in magnitude and direction for the same frequency of the waves. The direction of the wave vector is the direction of the wave propagation while its magnitude depends on the refractive indices of the media that the electromagnetic field wave interacts with along its propagation path.

2.17.3 Biacore set-up

In Biacore systems which use a sensor chips, monochromatic light is focused on a wedge-shaped beam on the TIR interface and the angle of minimum reflectance intensity is determined using two-dimensional detector array. The low refractive index medium is the surface coating of the sensor chip and the "surrounding" sample solution (cf. Figure 2.4 a).

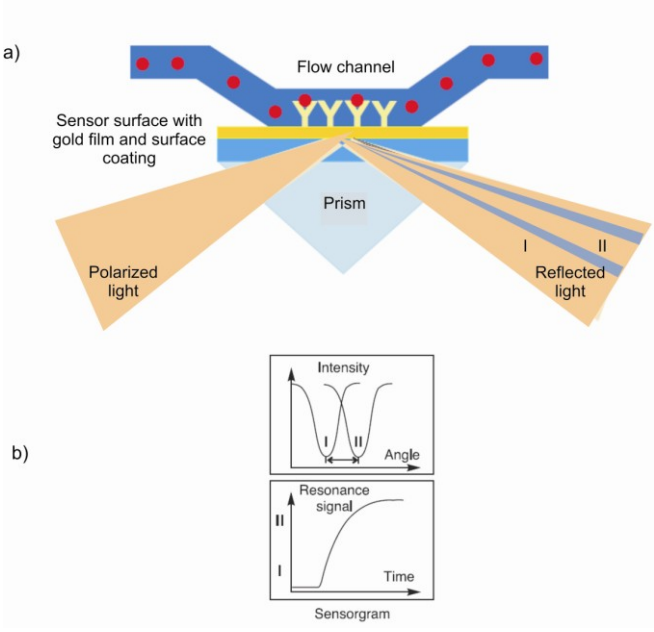

Figure 2.4 Biacore set-up

In Biacore systems the incident polarized light is focused into a wedge-shaped beam. An increased sample concentration in the surface coating of the sensor chip causes a corresponding increase in refractive index which alters the angle of incidence required to create the SPR phenomenon (**a**). This SPR angle is monitored as a change in the detector position for the reflected intensity dip (from I to II). By monitoring the SPR-angle as a function of time the kinetic events in the surface are displayed in a sensorgram (**b**) (Figure from Biacore Technology Note, GE Healthcare).

Biomolecular interactions occurring at the sensor surface change the solute concentration and thus the refractive index within the evanescent wave penetration range. The angle of incidence required to create the SPR phenomenon – the SPR angle, is therefore altered and it is this change which is measured as a response signal (cf. Figure 2.4 b). Essentially, biomolecular interactions measured by SPR are changes in mass in the aqueous layer close to the sensor chip surface. When molecules in the test solution bind to a target molecule the mass increases, when they dissociate the mass falls. This simple principle forms the basics of the sensorgram – a continuous, real-time monitoring of the association and dissociation of the interacting molecules. The sensorgram provides quantitative information on specificity of binding, active concentration of molecule in a sample, kinetics and affinity.

2.17.4 Sensor chip L1

The Biacore sensor chip is one of the most important parts of the SPR technology. Quantitative measurements of the binding interaction between one or more molecules are dependent on the immobilization of a target molecule to the sensor chip surface. Binding partners to the target can be captured from a complex mixture as they pass over the chip. Interaction between proteins, nucleic acids, lipids, carbohydrates and even whole cells can be studied.

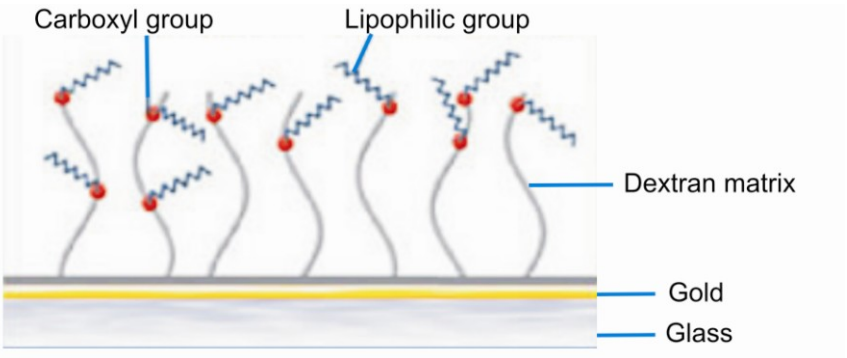

Figure 2.5 L1 chip composition

A dextran matrix with lipophilic groups is bound to the gold layer allowing immobilization of lipid vesicles and creation of membrane-like lipid bilayers.

The sensor chip consists of a glass surface, coated with a thin layer of gold. This forms a basis for a range of specialized surfaced designed to optimize the binding of a variety of molecules. In

this study a L1 sensor chip was used. Matrix of this chip consists of lipophilic groups that are covalently attached to carboxymethylated dextran, making the surface suitable for direct attachment of lipid membranes such as liposomes (cf. Figure 2.5). After such attachment the lipid bilayer structure is retained, making studies of interactions in a membrane-like environment possible.

3 Results

Natural PrP^C presented at the outer cellular membrane is the key player in the pathogenesis of prion diseases. Its attachment to special membrane microdomains, the so called rafts, occurs *via* proteins own GPI-anchor. The onset of prion disease requires involvement of infectious PrP^{Sc}. It is hypothesized that the cellular membrane could act as a site for the first contact between host PrP^C and invading PrP^{Sc}. Moreover, most of the data on the influence of cellular membrane on PrP conversion process, come from trials with recombinant PrP. They, however, cannot be seen as very reliable since the hydrophobic mode of PrP^C-membrane interaction is not granted. This was the main aspect that led to development of a new *in vitro* system, that in order to guarantee a high biological relevance was composed of following components:

(1) lipid bilayer as a mimic for the cellular membrane
(2) membrane-bound PrP^C
(3) invading, infectious PrP^{Sc}

In this part, I am going to present the steps that led to development of this novel *in vitro* system and the results that could be obtained with the help of it.

3.1 Purification of CHO-PrP^C

The purification method for PrP^C was based on an earlier developed protocol (Elfrink *et al.* 2004). Its main advantage was the use of Chinese hamster ovary cell culture (CHO), that produces, as an eukaryotic system, posttranslationally modified prion proteins possessing the GPI-anchor and two N-linked oligosaccharide chains. The protocol utilized two affinity chromatography steps, namely metal chelate and antibody affinity. It was completed with a concentrating step of the small amounts of purified protein and with a buffer exchange (cf. Figure 3.1). The details of this method are described in chapter 2.5.

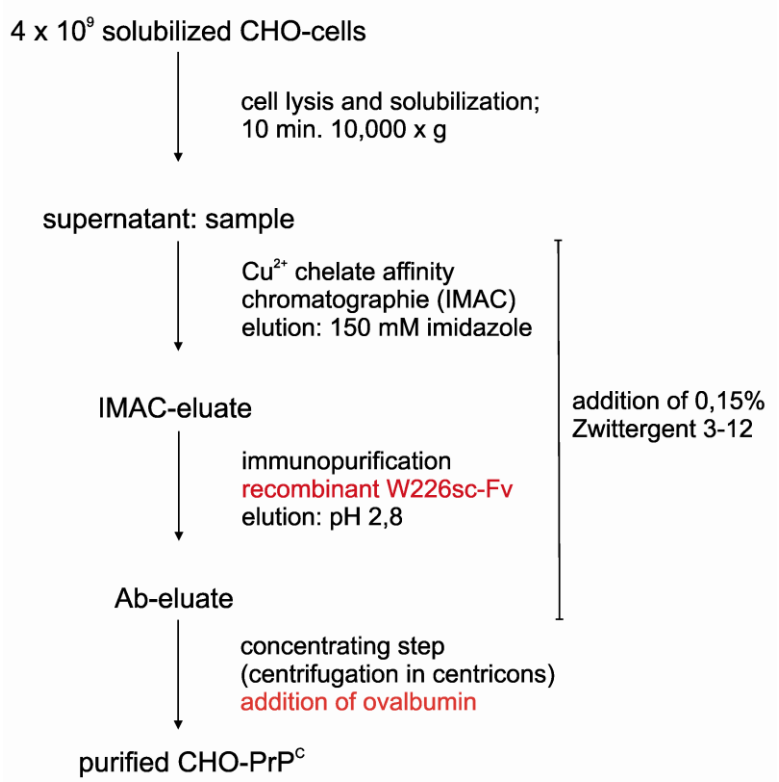

Figure 3.1 Purification of CHO-PrP^C

According to the protocol of Elfrink, the purification of CHO-PrP^C involved cell lysis and solubilization, two affinity chromatography steps, elution in presence of Zw 3-12 to prevent aggregation of the protein and concentrating the sample (Elfrink *et al.* 2004). All optimization steps undertaken in this work are shown in red.

3.1.1 Optimization steps

The original protocol utilized 3F4 antibody for immunopurification. However, the lack of suitable material and purity problems of the CHO-PrP^C forced me to search for an alternative antibody. As a kind gift of Carsten Korth's laboratory (Department Neurology, Heinrich-Heine-University, Düsseldorf, Germany) a purified single chain fragment W226 (scFvW226) antibody was obtained. A scFv antibody is a fusion product of the variable regions of the heavy and the light chains of immunoglobulins that are linked together *via* a short linker composed of four glycine and one serine residues. This chimeric molecule retains its specificity of the original immunoglobulin, despite removal of the constant regions and the introduction of the linker peptide. scFvW226 is a mainly monomeric antibody that recognizes the helix 1 of PrP (Muller-Schiffmann *et al.* 2009). It possesses a Myc- and His-tag and has a size of 33 kDa. Purified scFvW226 was covalently attached to NHS-activated Sepharose 4 Fast Flow (cf. chapter 2.5.3) and the resulting column was used for CHO-PrP^C purification. Figure 3.2 shows an analysis of

the coupling efficiency performed using SDS-PAGE and silver staining (cf. chapter 2.12 and 2.13). Lane 1 shows 3 µg of the starting material – scFvW226 diluted in the coupling buffer – that was used for incubation with NHS-Sepharose beads. Lanes 2-15 show flow-through samples collected during the coupling and washing procedure. The comparison of the lane 1 with following lanes shows that only minor amounts of unbound antibody could be found in the flow-through samples (lanes 2B, 3B, 7 and 13) proving that almost 100 % of the used antibody was successfully coupled to the beads.

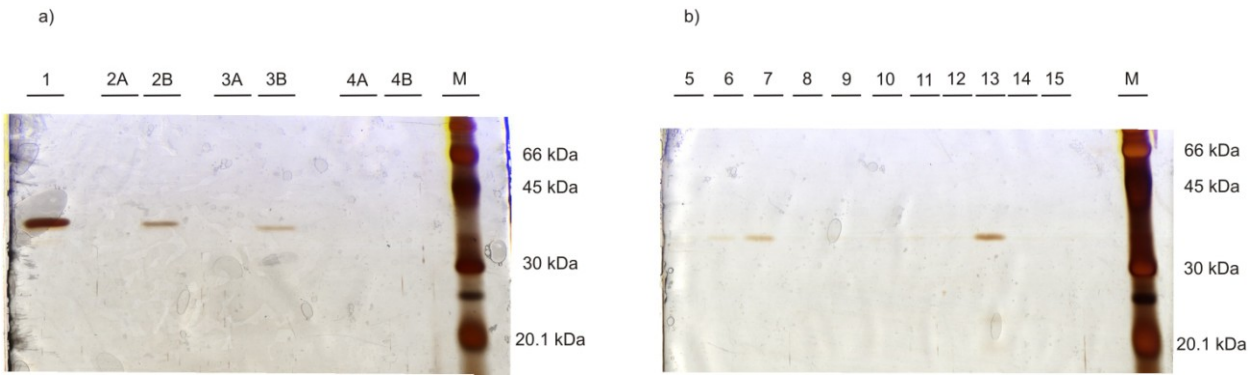

Figure 3.2 Analysis of the scFvW226 coupling efficiency

Silver staining analysis (**a** and **b**): **Lane 1**: scFvW226 solution as a starting material (relative volume ratio: 1x). **Lanes 2A-2B**: incubation flow-through (1x and 10x, respectively). **Lanes 3A-3B**: TBS/EDTA wash flow-through (1x and 10x, respectively). **Lanes 4A-4B**: water wash flow-through (1x and 10x, respectively). **Lanes 5-15**: Tris, pH 8 and Gly, pH 2.5 washes flow-through (99x). **M**: molecular size marker.

3.1.2 Immobilized metal chelate affinity chromatography (IMAC)

The property of PrP^C that was used as a basis for this type of chromatography is its ability to bind copper (cf. chapter 1.3). Therefore as a chromatographic matrix Cu^{2+}-IMAC with two free Cu^{2+} coordination sites was used. The column was loaded with Cu^{2+} solution (cf. chapter 2.5.2). A typical chromatogram of the Cu^{2+}-IMAC is shown in the Figure 3.3 a. The solubilized sample was loaded onto the column and the flow-through was collected. It contained proteins that did not bind to copper-immobilized column. The column was washed twice with 10 mM and 15 mM imidazole, respectively. Since imidazole competitively bound copper, all proteins with a weaker affinity to Cu^{2+} were washed out. By increasing the concentration of imidazole, the wash effect was strengthened. Finally elution was induced by 150 mM imidazole. Analysis with SDS-PAGE showed that not all CHO-PrP^C was able to bind to so prepared column, since it was found in the

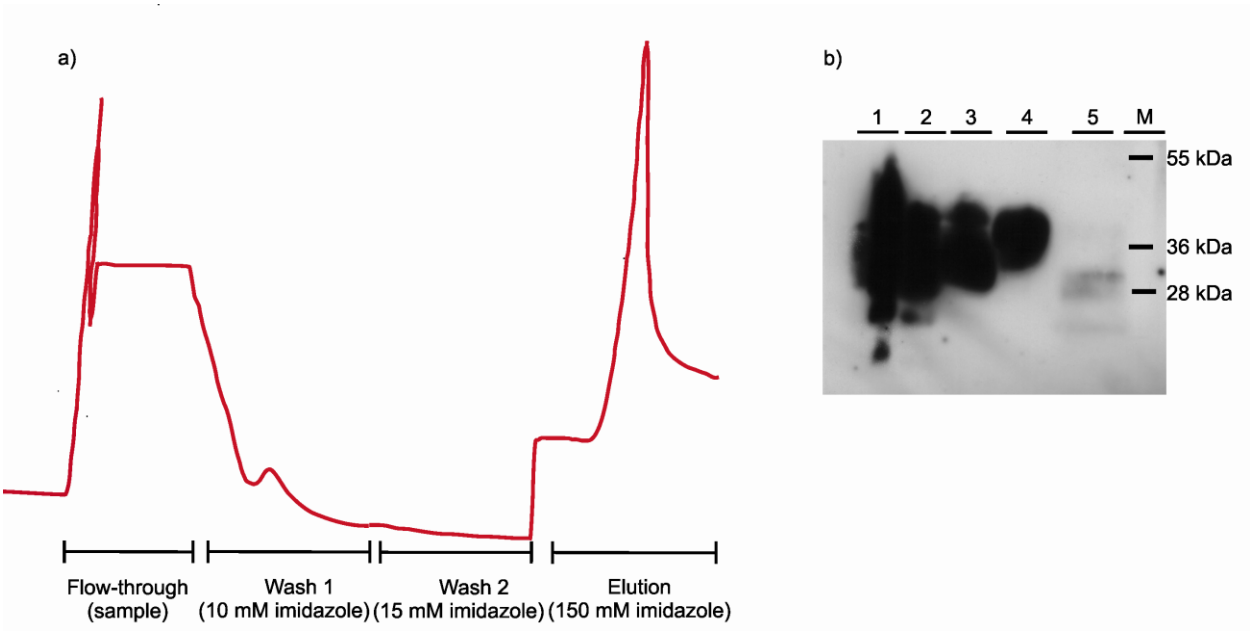

Figure 3.3 Cu^{2+}-IMAC characteristics

A relative absorption measured at the wavelength of 280 nm was recorded during the course of chromatography measurement. During the elution the sensitivity of the recorder device was increased two times (**a**).

Western blot analysis of the relative amounts of CHO-PrP^C in the fractions collected during IMAC (**b**): **Lane 1**: solubilized sample as a starting material (relative volume ratio: 1x). **Lane 2**: flow-through (1x). **Lane 3**: wash step 1 (1x). **Lane 4**: wash step 2 (1x). **Lane 5**: IMAC-eluate (4x). **M**: molecular size marker.

flow-through (cf. lane 2; Figure 3.3 b). Also during the first wash step some amounts of CHO-PrP^C were eluted (lane 3). However, the second wash step showed no more CHO-PrP^C arguing that the rest stayed strongly bound to the copper column. Lane 5 shows eluted CHO-PrP^C as a final product of this affinity chromatography. This fraction was then used for immunopurification.

3.1.3 Immunopurification

For immunopurification the scFvW226 column was used (cf. chapter 2.5.3). The IMAC-eluate was loaded onto the column as shown in the Figure 3.4 a. A wash step with buffer at pH 7 took place. By decreasing the pH to 2.8 the antibody-protein binding could be abolished and elution of the CHO-PrP^C occurred. After the purified protein was concentrated by using centricons with a pore size of 5 kDa (cf. chapter 2.5.4) its solubility and purity were tested. This was done with the help of differential ultracentrifugation (cf. chapter 2.11) and silver staining method of protein

gels. With the new column a highly purified CHO-PrP^C was obtained (cf. Figure 3.4 c), however, its solubility was unsatisfactory. This could be explained by the fact that due to the use of this new, high affinity recombinant antibody the efficiency of immunopurification step increased immensely, i.e. the presence of other proteins which might have increased solubility was removed. The low solubility typical for a membrane-bound protein led to a rapid aggregation in solution. I was able to eliminate this undesirable effect by adding a known protein stabilizer, namely ovalbumin, to the purified CHO-PrP^C at final concentration of 1mg/ml (cf. Figure 3.4 d). With the help of this method almost a half of the purified protein was retained in the soluble fraction and since ovalbumin did not show any membrane-specific binding (cf. chapter 3.3) the CHO-PrP^C with ovalbumin was used in all following experiments.

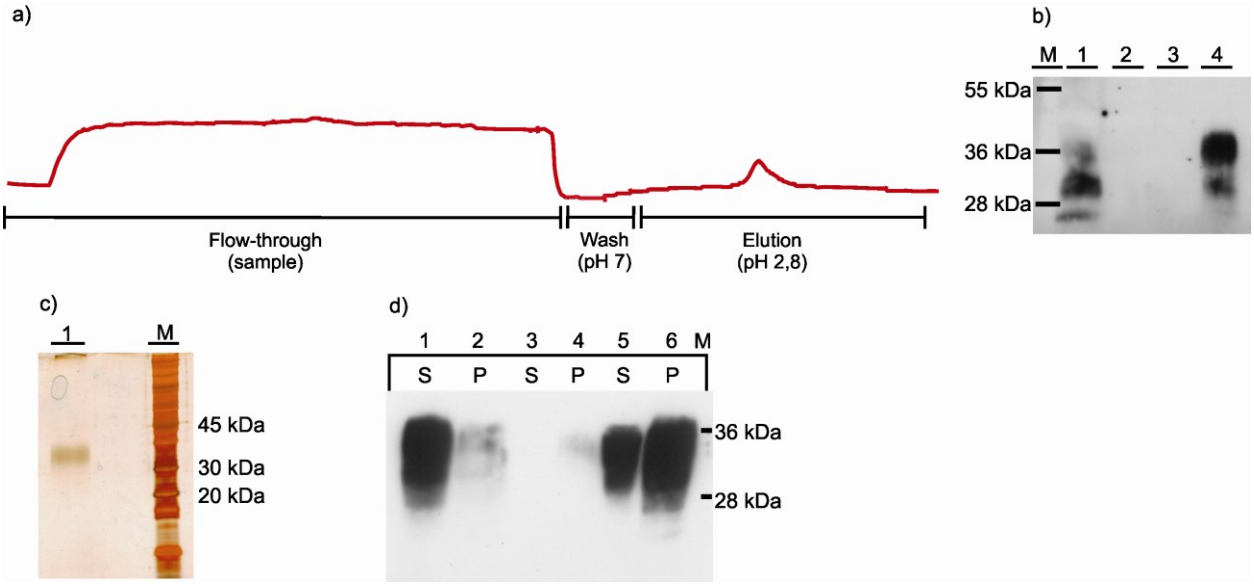

Figure 3.4 Immunopurification characteristics

A relative absorption measured at the wavelength of 280 nm was recorded during the course of chromatography measurement. During the elution the sensitivity of the recorder device was increased three times (**a**).

Western blot analysis of the relative amounts of CHO-PrP^C in the fractions collected during immunopurification (**b**): **M**: molecular size marker. **Lane 1**: IMAC-eluate as a starting material (relative volume ratio: 1x). **Lane 2**: flow-through (1x). **Lane 3**: wash step (1x). **Lane 4**: purified CHO-PrP^C (5.8x).

Silver staining analysis of the purity of CHO-PrP^C (**c**): **Lane 1**: 10 µl of purified CHO-PrP^C loaded onto gel directly after elution. **M**: molecular size marker.

Western blot analysis of the solubility of purified CHO-PrP^C tested with help of differential ultracentrifugation (**d**): **Lane 1-2**: supernatant (S) and pellet (P) of sample collected directly from the column. **Lane 3-4**: supernatant (S) and pellet (P) of sample after concentrating with CBS buffer. **Lane 5-6**: supernatant (S) and pellet (P) of sample after concentrating with ovalbumin. **M**: molecular size marker.

3.2 Formation of a lipid bilayer

In order to mimic the natural membrane environment of PrP^C, a composition of lipids that are present in raft domains was chosen. As described in chapter 2.10 a solution of small unilamellar vesicles (SUVs) was prepared and used for the Biacore measurement. Surface plasmon resonance technique, established in the Biacore device, allowed us both: studying the binding of biomolecules to different surfaces and observation of differences in progression of the binding (cf. chapter 2.17). In this work the Biacore 1000 device was used. It is equipped with four separate flow cells (cf. Figure 3.5 a), flow cell volume of 0.06 µl (cf. Figure 3.5 b) and has a maximum injection volume of 300 µl. The continuous flow of the sample passed through the flow cell guarantees a constant concentration of the protein of interest at all time points and allows real-time measurement of occurring interactions.

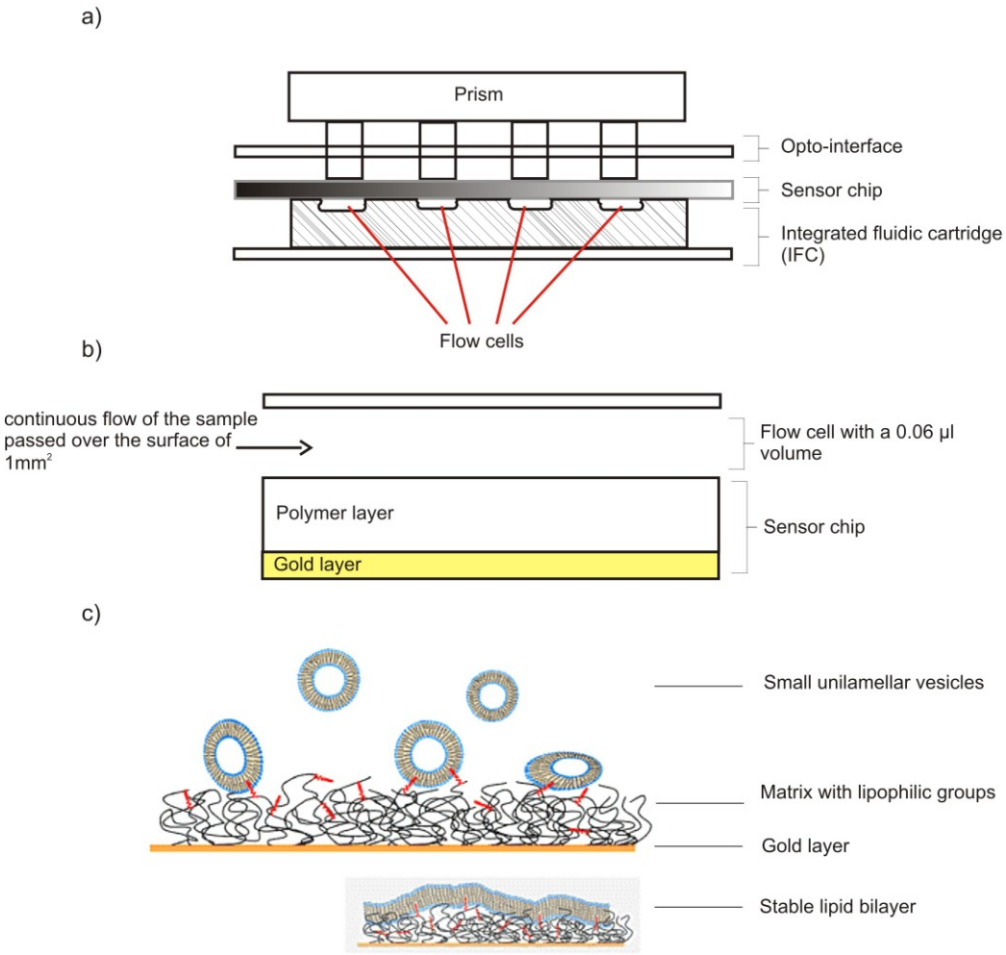

Figure 3.5 Scheme of the flow cells set up and formation of a bilayer

Four separate flow cells are formed by pressing the integrated fluidic cartridge (IFC) against the chip surface (**a**). The sample is passed over the surface of the chip in a continuous flow modus. The flow cell has a volume of 0.06 µl and forms with the chip a contact surface of 1 mm^2 (**b**). The L1 chip allows formation of a stable lipid bilayer structure by breaking down lipid vesicles (**c**).

In order to observe the interaction between membrane-anchored PrP^C and its potential partners first a stable lipid surface had to be formed. This was done using the Biacore standard protocol developed for the L1 chip. Its matrix consists of lipophilic groups that are covalently attached to modified dextran, making the surface suitable for direct attachment of SUVs. The obtained lipid bilayer structures were stable and could be used for further experiments (cf. Figure 3.5 c). During all measurements the temperature was set to 37° in order to keep the lipid layer in the fluid phase.

Figure 3.6 shows a typical sensorgram that was recorded during bilayer formation. The Biacore system not only allows studying kinetics of biomolecular binding, but also gives information about mass deposition on the chip surface during the measurement. The recorded signal is presented in form of resonance units (RU) whereas 1 RU equals a mass of 1 pg of the molecule bound to the surface of 1 mm^2. First the chip surface was cleaned with an injection of 20 mM CHAPS. This mild detergent removed all possible impurities from the system. Next, solution of rafts-like SUVs in CBS buffer was injected and passed over the chip surface for app. 40 min. The continuous mode of the injection allowed formation of a bilayer which was characterized by two features: a fast ascending signal and a slow saturation phase. The first effect shows a high affinity the vesicles to the modified dextran surface. The second effect, namely the following

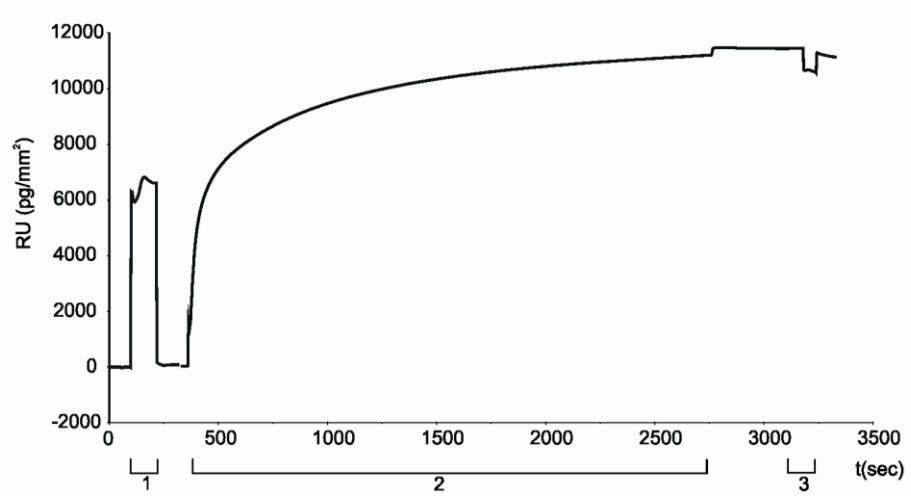

Figure 3.6 Formation of a lipid bilayer

SPR measurement: In order to cleanse the chip surface 100 µl of 20 mM CHAPS were injected at the flow rate of 50 µl/min. (**1**). As next, 300 µl of SUVs solution in CBS buffer were injected at the flow rate of 10 µl/min and formation of bilayer was observed (**2**). Finally, an injection of 10 mM NaOH at the flow rate of 50 µl/min was performed removing all intact or unbound vesicles (**3**).

association and the very slow dissociation are characteristic for the high stability of the bilayer formed from lipid vesicles. Finally, an injection of 10 mM NaOH took place. With this step all intact vesicles and multilamellar structures were removed leaving a stable lipid bilayer.

3.3 Saturation of the lipid bilayer with CHO-PrP^C

Once the bilayer was formed saturation with CHO-PrP^C could be studied. As it was already described (Elfrink *et al.* 2007) a single injection of CHO-PrP^C resulted in a fast association phase, during which the binding of protein to the bilayer occurred. After introduction of pure buffer a slow dissociation phase was observed (cf. Figure 3.7 dashed line). The binding was demonstrated to be GPI-anchor mediated and so mimicked well the natural PrP^C anchoring. The same results were obtained by using the purified PrP^C stabilized with ovalbumin (cf. Figure 3.7 solid line).

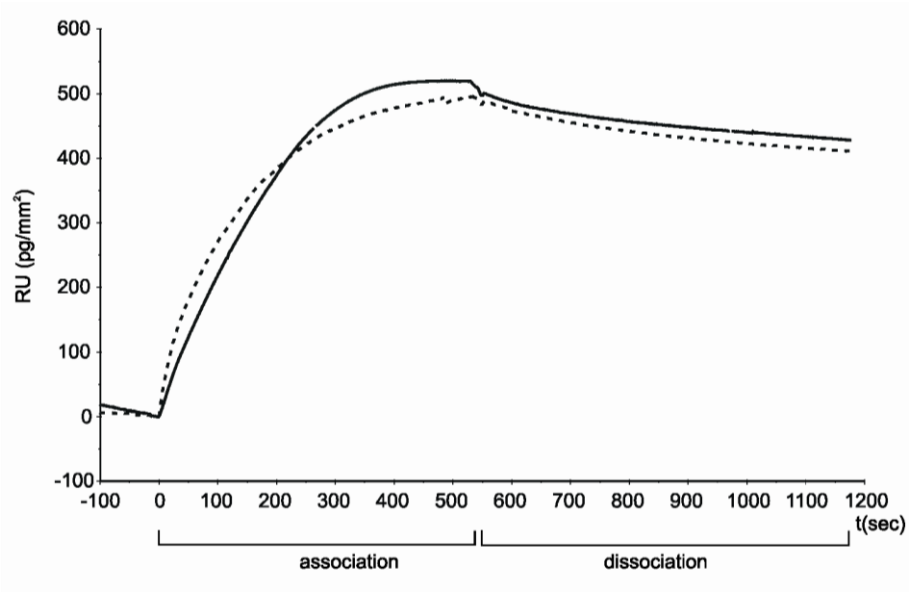

Figure 3.7 CHO-PrP^C binding to rafts-like lipid bilayer

SPR measurement: Pure CHO-PrP^C was diluted in CBS buffer to a final concentration of 4 ng/µl and a sample of 90 µl was passed over the bilayer at a flow rate of 10 µl/min (association phase). This was followed by a CBS buffer wash observed for another 600 s (dissociation phase). The binding of PrP^C purified according to a previous protocol (cf. chapter 3.1; dashed line) was compared with the binding of CHO-PrP^C purified with addition of ovalbumin (solid line). No great differences in the binding characteristics were observed when measurements of the protein purified according to two slightly different protocols were compared.

It showed a high affinity of the CHO-PrP^C to the lipid bilayer and a good stability of the bound protein. Since no essential differences in the binding of PrP^C purified with the two slightly different protocols were observed, the CHO-PrP^C with ovalbumin was used in all following experiments and is denoted as CHO-PrP^C.

To test if ovalbumin, present in the CHO-PrP^C solution, showed affinity to the raft-like bilayer different concentrations of only this protein were passed over the lipid membrane. Injection of pure ovalbumin diluted in 1 mM NaAc resulted in a strong and stable binding to the bilayer. However, the use of CBS buffer (with 137 mM NaCl) diminished this effect completely (data not shown). This clearly shows that binding of ovalbumin to raft-like bilayer occurred only *via* unspecific, electrostatic type of interaction that could be successfully blocked by usage of salt containing, i.e. physiological buffer. Therefore in all following experiments the salt-rich CBS buffer was used.

Furthermore, the experiments of Elfrink showed that a complete saturation of the raft-like lipid bilayer with CHO-PrP^C was only possible when multiple injections were performed. This was also observed when CHO-PrP^C with ovalbumin was used. As shown in the next sensorgram repetitive injection of CHO-PrP^C at a constant concentration led to a fast signal increase and an elevated level of the final binding plateau (cf. Figure 3.8 a).

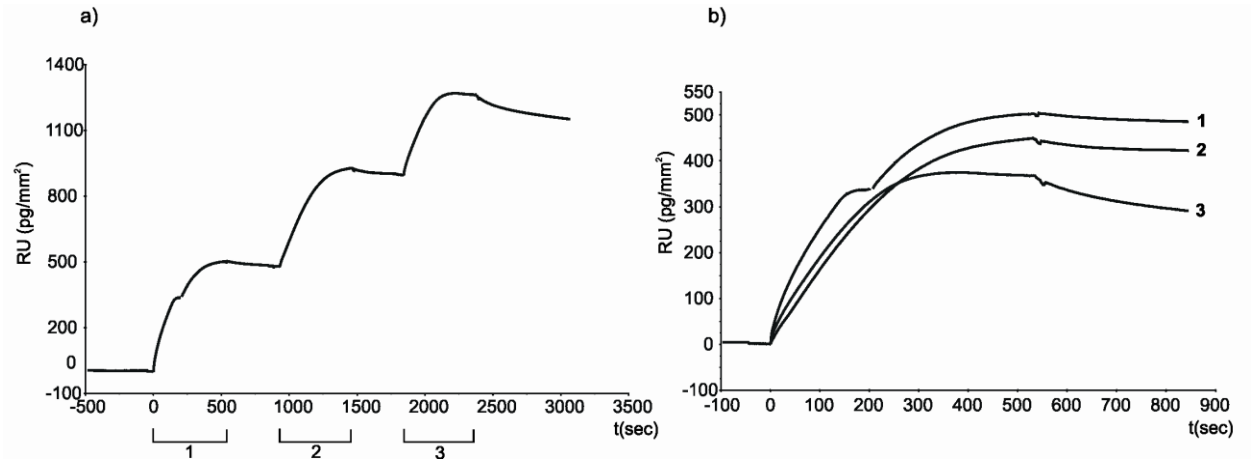

Figure 3.8 Saturation of bilayer with multiple injections method

SPR measurement: CHO-PrP^C was diluted in CBS buffer and injected repetitively at a flow rate of 10 µl/min. Three injections intercepted by short dissociation phase of 420 sec led to a signal increase of app. 1,000 RU (**a**). To better observe the saturation effect, the three measured binding curves were cut, overlaid and aligned to "0". The curves 1, 2 and 3 show the first, second and third injection, respectively (**b**).

However, a precise observation of the single binding curves showed that with each repetitive injection both the association rate and the amount of protein bound to the membrane decreased, reaching the saturation level. This was observed after superimposing the single curves and aligning them to the "0" value (cf. Figure 3.8 b). Since for the further experiments a saturated lipid bilayer was needed, the method of multiple injections was chosen and app. 1,000 RU – 1,500 RU (pg/mm^2) were bound for each following measurement.

3.4 Interaction of aggregated proteins with membrane-anchored PrP^C

As already described in chapter 1.2.4, native PrP^C is being brought to the outer cellular membrane where it stays attached *via* the GPI-anchor. Like all other GPI-anchored proteins PrP^C can only be found in special membrane microdomains, called rafts. These domains are characterized by an increased content of sphingolipids, cholesterol and cerebrosides. Studies using planar lipid bilayer mimicking raft domains and purified, natural PrP^C showed essential dependence of the membrane binding of PrP^C on the presence of GPI-anchor (Elfrink *et al.* 2007).

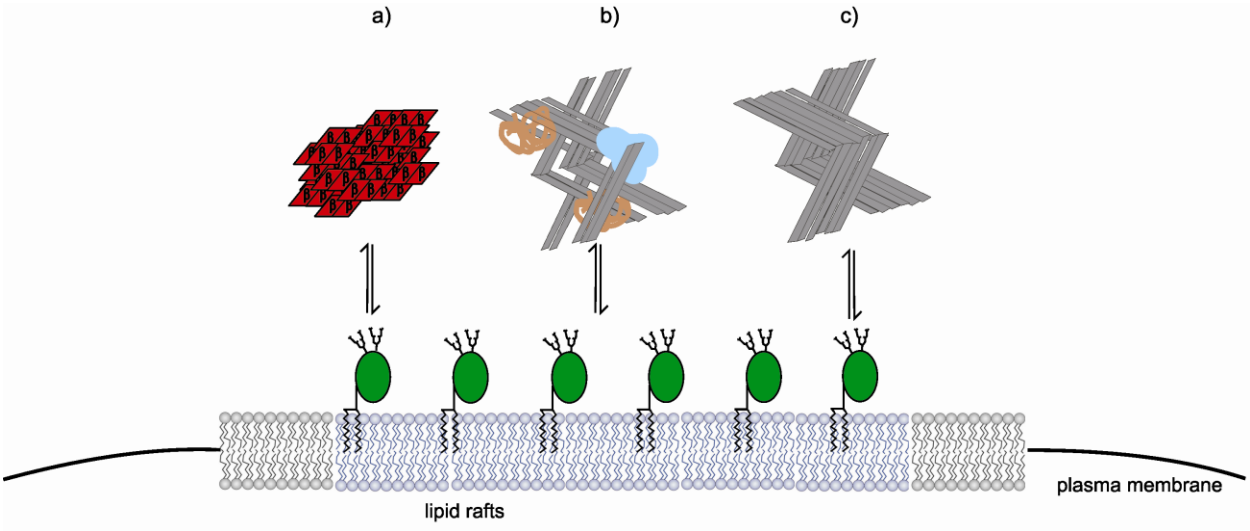

Figure 3.9 Scheme of the experimental set up

In order to test the interaction and possible conversion processes between membrane-anchored PrP^C and incoming PrP^{Sc} different types of protein aggregates were used. The interactions with non-infectious prion protein aggregates (**a**), partially purified PrP^{Sc} (**b**) and pure prion rods (**c**) were studied.

The main step in the pathogenesis of prion diseases is the interaction of incoming PrP^{Sc} with PrP^{C}. However, the exact site of this interaction and of consequential conversion is still not known. There are some hints pointing out the importance of the membrane-attachment in the conversion process (cf. chapter 1.2.5). Therefore in my work I developed a biologically relevant *in vitro* system that contained all components: lipid membrane, anchored PrP^{C} and exogenously introduced PrP^{Sc} (cf. Figure 3.9). With its help the interaction and possible conversion of membrane-attached natural PrP^{C} with third components in form of non-infectious PrP aggregates, partially purified PrP^{Sc} and with prion rods was studied.

3.4.1 Interaction studies with non-infectious aggregates

The binding and interaction properties of non-infectious prion protein aggregates were studied in order to test both the biochemical system (cf. Figure 3.9) and the Biacore device for use of protein aggregates.

Amorphous prion protein aggregates can be produced with different methods. As an example, only one of the applied methods is described. It was based on the pH change using the known characteristic of prion protein, namely its solubility at pH 4 and insolubility at pH 7. Different concentrations of CHO-PrP^{C} aggregates were prepared according to the protocol described in chapter 2.6. Figure 3.10 presents a dot blot showing the results of solubility analysis performed using the differential ultracentrifugation method (cf. chapter 2.11). According to it, all prion protein particles found in the supernatant fraction, after a 100,000 x *g* spin, are regarded as soluble. The pellet fraction represents in this case the aggregated state of the prion protein.

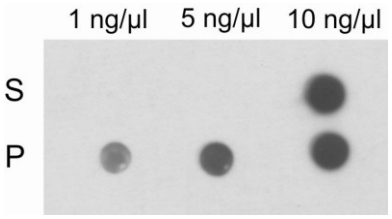

Figure 3.10 Aggregation of CHO-PrP^{C}

Dot blot analysis after differential ultracentrifugation: Solubility analysis performed after overnight incubation of CHO-PrP^{C} at pH 7. Samples with final protein concentrations of 1 ng/µl and 5 ng/µl showed signal in the pellet fraction only (P) representing the aggregated form, whereas a concentration of 10 ng/µl showed partial aggregation with signals appearing in both supernatant (S) and pellet (P) fractions.

These results clearly showed that overnight incubation of CHO-PrP^C with buffer at pH 7 led to a complete aggregation of the protein at concentrations of 1 ng/µl and 5 ng/µl, while the sample set to a concentration of 10 ng/µl showed only partial aggregation effect. Therefore in the following experiments samples with CHO-PrP^C amorphous aggregates at 1 ng/µl and 5 ng/µl were used.

After amorphous aggregates were successfully formed the next step was to test their binding ability to the lipid membrane without and with PrP^C layer. This was done with the help of SPR method. The aggregated samples were first passed over the lipid bilayer. Figure 3.11 shows a typical sensorgram measured with the 5 ng/µl aggregated sample, which was characterized by a slow, but continuously ascending curve that finally reached the level of 380 RU (pg/mm^2). The used aggregates stayed stably bound at the lipid bilayer, which was shown during the course of the dissociation phase. However, a comparison between binding strengths of soluble and aggregated CHO-PrP^C showed that the latter bound weaker, since for soluble PrP^C at a concentration of 1ng/µl an average signal increase of 500 RU (pg/mm^2) was achieved (cf. Figure 3.7).

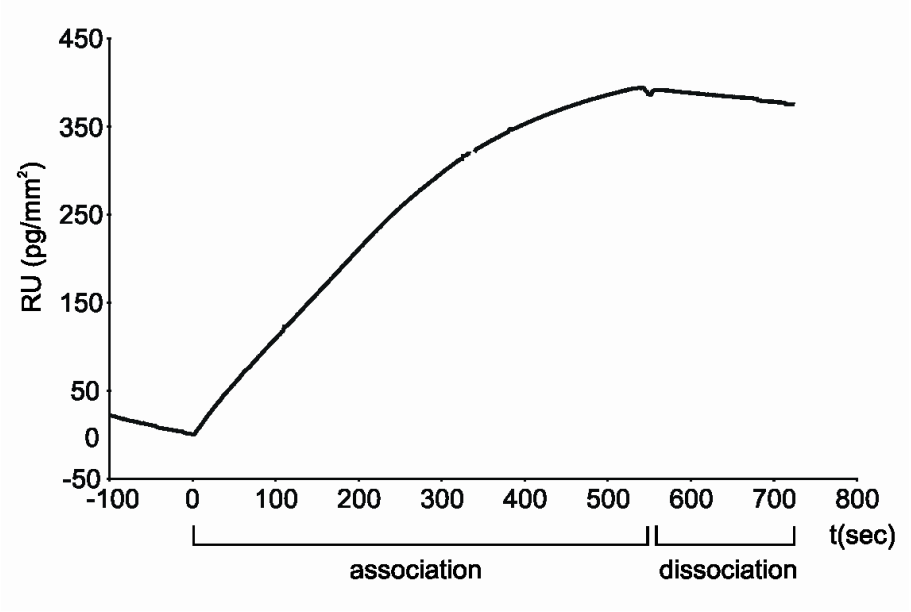

Figure 3.11 Binding of CHO-PrP^C aggregates to lipid bilayer

SPR measurement: A 90 µl sample of CHO-PrP^C aggregates of final concentration of 5 ng/µl was passed over the previously formed lipid bilayer at a flow rate of 10 µl/min. The 540 sec lasting association phase was followed by a short dissociation phase (240 sec). A signal increase of 380 RU (pg/mm^2) was observed.

Nevertheless, such an effect of aggregated protein stably bound to the lipid bilayer was reproducible when different concentrations or differently prepared aggregates were used or when multiple injection mode was applied (data not shown). This can be explained by the fact that just like the soluble PrP^C, the aggregates also posses GPI-anchors that induced a stable bilayer-binding.

After the interaction between aggregated prion protein and raft-like lipid bilayer was observed, the experimental setup was extended and the binding ability of aggregates to anchored, soluble PrP^C was tested. In this particular experiment a level of 3,000 RU (pg/mm^2) was achieved when immobilizing the soluble CHO-PrP^C (data not shown). After the bilayer saturation was finished the aggregated sample at a concentration of 5 ng/µl was passed through the flow cell and the interaction between the two prion protein forms was observed. Surprisingly, during this experiment almost no binding of aggregates was detected and the association phase showed an extremely unstable course (cf. Figure 3.12). As shown in the sensorgram a slight signal increase occurred during the first 400 sec of the association phase which then abruptly dropped down in a very turbulent way.

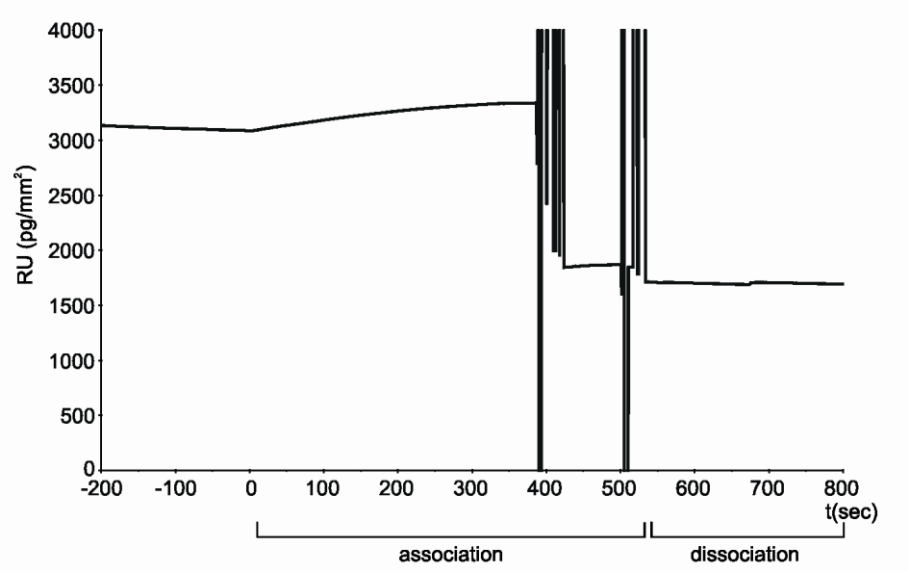

Figure 3.12 Binding of CHO-PrP^C aggregates to membrane-anchored PrP^C

SPR measurement: At first saturation of lipid bilayer took place as described in chapter 3.3. As a result 3,000 RU (pg/mm^2) of soluble CHO-PrP^C were immobilized. Next, a 90 µl sample of CHO-PrP^C aggregates of a final concentration of 5 ng/µl was passed over lipid-protein bilayer at a flow rate of 10 µl/min. During the association phase, at time point of 400 sec, a sudden signal decrease took place resulting in washing of almost a half of the previously immobilized soluble CHO-PrP^C. The following dissociation phase was characterized by a stable signal measured for the next 260 sec.

This sudden signal decrease to a level of app. 1,500 RU resulted in loosing almost the half of the previously immobilized CHO-PrP^C. This disrupting interaction between aggregated and soluble prion protein was also observed when differently prepared or different concentrations of the amorphous aggregates were used (data not shown). These data fitted hypothesis, which states that the invading PrP^{Sc}, represented in this experiment by amorphous PrP^C aggregates, pulls the anchored PrP^C out of the membrane. However, these effects had to be studied in detail and in order to better mimic the start of the infection *in vivo*, infectious aggregates were used as next.

3.4.2 Interaction studies with infectious protein aggregates

One of the methods to obtain infectious PrP^{Sc} aggregates is selective precipitation of PrP^{Sc} from infected animal brains. Use of the sodium phosphotungstate (NaPTA), a polyoxometalate, at neutral pH and in the presence of Mg^{2+} leads to formation of NaPTA complexes with infectious PrP^{Sc} oligomers or polymers (Safar *et al.* 1998). As described in the chapter 2.7, 5 % hamster brain homogenate from scrapie-infected animals and healthy controls, was used as a starting material. After the precipitation aliquots of different volumes were formed from the resulting pellet, corresponding to $2.5 \cdot 10^{-2}$ g BE (brain equivalent). Each sample was prepared in duplicate to analyze the effect of proteinase K (PK) digestion. Partial resistance to digestion with this enzyme is one of the features that differentiate between PrP^{Sc} and PrP^C (cf. chapter 1.2.2).

In order to first determine the prion protein quantity in the starting material, $2.2 \cdot 10^{-3}$ g BE of brain homogenate were analyzed by Western blot. This was performed before the precipitation procedure started. The results demonstrated that brain homogenate from scrapie-infected animal (lane 1A) showed significantly higher amounts of prion protein when compared with the non-infected control (lane 2A; cf. Figure 3.13 a). To analyze the content of PrP^{Sc} in these samples, their duplicates were digested with PK and analyzed in the gel. It was found, in accordance with the literature, that after digestion large amounts of resistant, N-terminally truncated PrP^{Sc} were present in the scrapie-infected brain homogenate (lane 1B), while the negative sample underwent a full digestion (lane 2B). This showed that the protein signal found in the sample from healthy control brain homogenate before PK digestion correlated directly with soluble, monomeric PrP^C. With the method of NaPTA-precipitation infectious prion protein aggregates should be selectively precipitated, however, as shown in this figure small amounts of PrP^C were also detected.

The same analysis, demonstrating the quantity of PrP^{Sc}, was performed with samples that underwent the NaPTA-precipitation. The resulting pellet was diluted in 600 µl CBS buffer, and $6.25 \cdot 10^{-3}$ g BE, $3.75 \cdot 10^{-3}$ g BE and $1.87 \cdot 10^{-3}$ g BE were analyzed either after PK digestion or prior to it (cf. Figure 3.13 b). As already observed, significantly higher amounts of prion protein were detected in the scrapie-infected samples (lanes 3A, 4A, and 5A) when compared with the healthy controls (lanes 6A, 7A and 8A). Also the PK digestion showed similar results as before, demonstrating large amounts of PK-resistant PrP^{Sc} (lanes 3B, 4B, 5B) and a complete digestion of the PrP^{C} in the non-infected samples (lanes 6B, 7B and 8B).

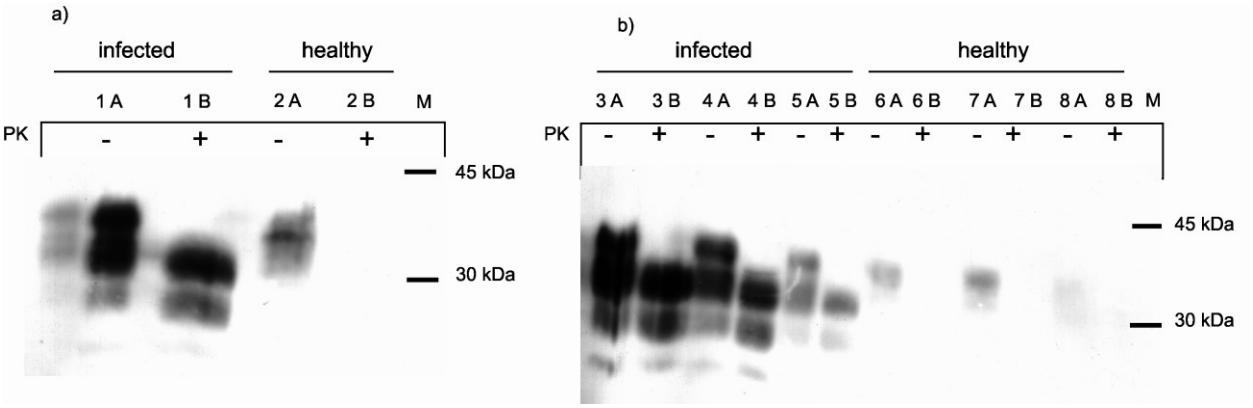

Figure 3.13 Efficiency analysis of the selective precipitation of PrP^{Sc}

Samples with and without PK-digestion are compared. PK digestion was performed as described in chapter 2.7. Western blot analysis was performed after denaturing gel electrophoresis.

Starting material (**a**): **Lane 1A**: $2.2 \cdot 10^{-3}$ g BE (brain equivalent) of scrapie-infected hamster brain homogenate. **Lane 1B**: $2.2 \cdot 10^{-3}$ g BE of scrapie-infected hamster brain homogenate after PK digestion. **Lane 2A**: $2.2 \cdot 10^{-3}$ g BE of healthy hamster brain homogenate. **Lane 2B**: $2.2 \cdot 10^{-3}$ g BE of healthy hamster brain homogenate after PK digestion. **M**: molecular size marker.

Precipitated pellet (**b**): **Lanes 3A, 4A, 5A**: $6.25 \cdot 10^{-3}$ g BE, $3.75 \cdot 10^{-3}$ g BE and $1.87 \cdot 10^{-3}$ g BE, respectively, of scrapie infected pellet. **Lanes 3B, 4B, 5B**: $6.25 \cdot 10^{-3}$ g BE, $3.75 \cdot 10^{-3}$ g BE and $1.87 \cdot 10^{-3}$ g BE, respectively, of scrapie infected pellet after PK digestion. **Lanes 6A, 7A, 8A**: $6.25 \cdot 10^{-3}$ g BE, $3.75 \cdot 10^{-3}$ g BE and $1.87 \cdot 10^{-3}$ g BE, respectively, of non-infected pellet. **Lanes 6B, 7B, 8B**: $6.25 \cdot 10^{-3}$ g BE, $3.75 \cdot 10^{-3}$ g BE and $1.87 \cdot 10^{-3}$ g BE, respectively, of non-infected pellet after PK digestion. **M**: molecular size marker.

The NaPTA-precipitated PrP^{Sc} aggregates were tested for binding to membrane-anchored PrP^{C} using the Biacore device. The same procedure was chosen as for the non-infectious aggregates (cf. chapter 3.4.1). Figure 3.14 demonstrates typical results of these experiments showing PrP^{Sc} aggregates binding to raft-like lipid bilayer (dashed line) in comparison with the binding of the

same aggregates to CHO-PrP^C saturated bilayer (solid line). To better compare the binding extents both curves were superimposed and aligned to the "0" value. The courses of the association and dissociation phases in these measurements were similar, however, the presence of soluble PrP^C anchored at the lipid bilayer clearly strengthened the binding of PrP^{Sc} aggregates.

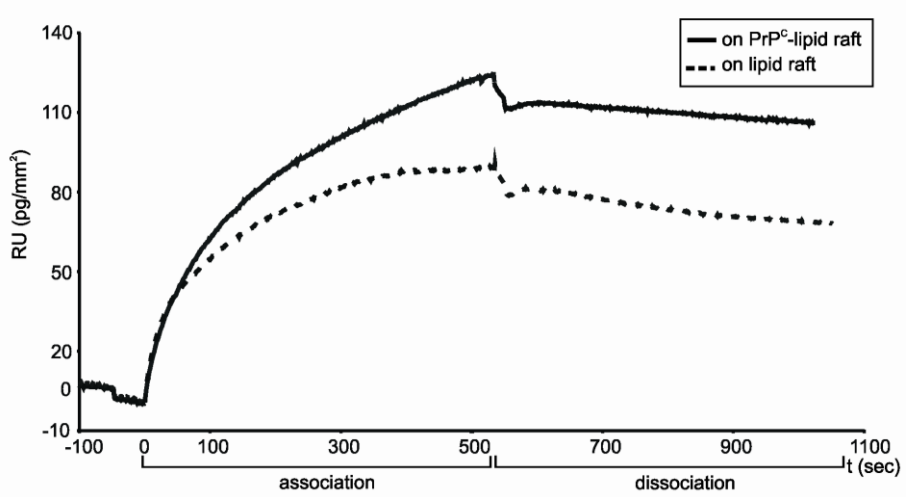

Figure 3.14 Analysis of the full length PrP^{Sc} binding

SPR measurement: $7.5 \cdot 10^{-3}$ g BE (brain equivalent) of PrP^{Sc} precipitated from scrapie hamster brain homogenates were injected over raft-like lipid bilayer (dashed line) and over CHO-PrP^C saturated bilayer (solid line) at the flow rate of 10 µl/min. After an association phase of 540 sec, dissociation was observed for additional 600 sec at the flow rate of 1 µl/min.

This tendency for PrP^{Sc} aggregates to bind stronger to the PrP^C saturated lipid bilayer than to rafts alone was observed in every following measurement. However, the differences were only slight and could not be regarded as significant. Moreover, control experiments using the NaPTA-precipitate from healthy hamster brain homogenate also demonstrated binding characteristics, which were even stronger than the obtained for PrP^{Sc} aggregates (cf. Figure 3.15). It was also found that the precipitated control sample bound quite similarly to both raft-like lipids alone and to CHO-PrP^C covered lipid bilayer, demonstrating no specificity for any of these layers. According to the precipitation method, described above, only minor amounts of PrP^C could be precipitated together with the PrP^{Sc} complexes. However, these results clearly showed that the NaPTA precipitation method not only yielded PrP^{Sc} aggregates, but also other proteins or substances, which bind to rafts and PrP^C-rafts as detected by a very sensitive system like Biacore. It should be emphasized, however, that as a tendency it was seen, that PrP^C on the raft-

like bilayer increased the binding of PrP^{Sc}, whereas it diminished binding of the NaPTA-precipitate from healthy controls.

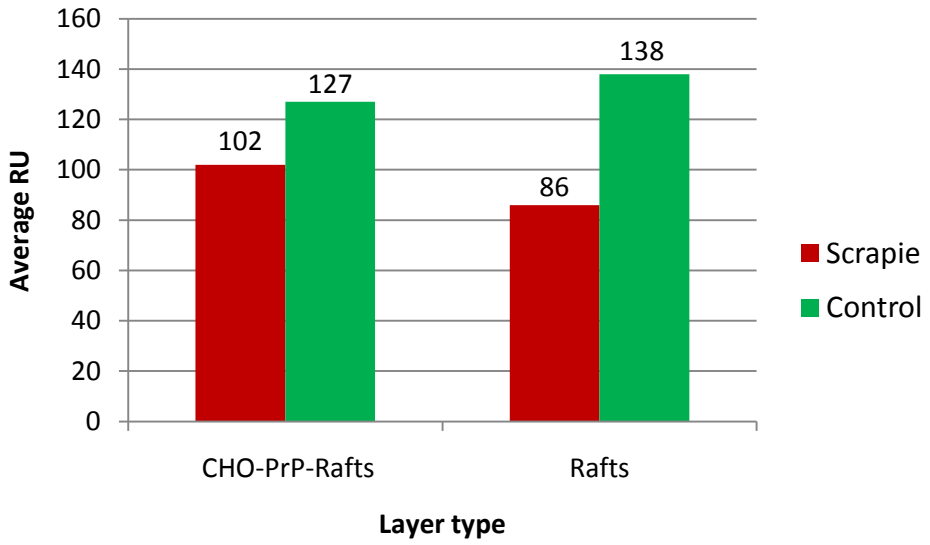

Figure 3.15 Binding of partially purified PrP^{Sc} and NaPTA-precipitate from non-infected animals

Binding of NaPTA-precipitate from scrapie-infected hamster brain homogenate (red) was compared with precipitate from healthy hamster brain homogenate (green). Binding to CHO-PrP^{C} saturated rafts was compared to rafts only, as control. Data are the average of four and five independent experiments, performed in a duplicate, for the scrapie and control samples, respectively.

One might argue that the NaPTA-precipitate from healthy hamster brain contained too many proteins, membranes etc., which showed an unspecific interaction with the membrane and PrP^{C}. To solve problem of sample impurity and the unspecific binding an optimization step was undertaken and the so called limited PK-digestion method was chosen. In comparison to a standard procedure this new protocol utilized lower concentration of PK and shorter incubation times (cf. chapter 2.7). This approach should not only lead to a formation of truncated PrP^{Sc} particles, the so called prion rods, but also eliminate all other proteins that were eventually trapped in the complexes with NaPTA. Application of this new protocol led to results that indeed showed the presence of truncated PrP^{Sc} and elimination of other proteins in the control sample (data not shown). However, the PK that was left in the samples after the precipitation and digestion procedures, even after proper inactivation, showed strong interaction with the bilayer and the CHO-PrP^{C}. This is demonstrated in the Figure 3.16, where exact the same extent of

binding was observed for the control sample when measured at both types of layers. Since silver stained protein gel after SDS-PAGE procedure showed that only PK was left in these samples (data not shown), one could conclude that the observed binding was PK-specific. Therefore, the fact, that scrapie samples contained both the PrP^{Sc} and the PK made the proper evaluation of the observed data not possible. One could not distinguish between the binding of PrP^{Sc} truncated aggregates and proteinase K. The possibility that PK in the sample has not been completely inactivated and destroyed PrP^{C} layer could be ruled out. Protein gel analysis demonstrated that addition of CHO-PrP^{C} to an inactivated PrP^{Sc} sample left the PrP^{C} intact (data not shown). Therefore, a highly pure and well-defined material in form of purified PrP 27-30 was needed.

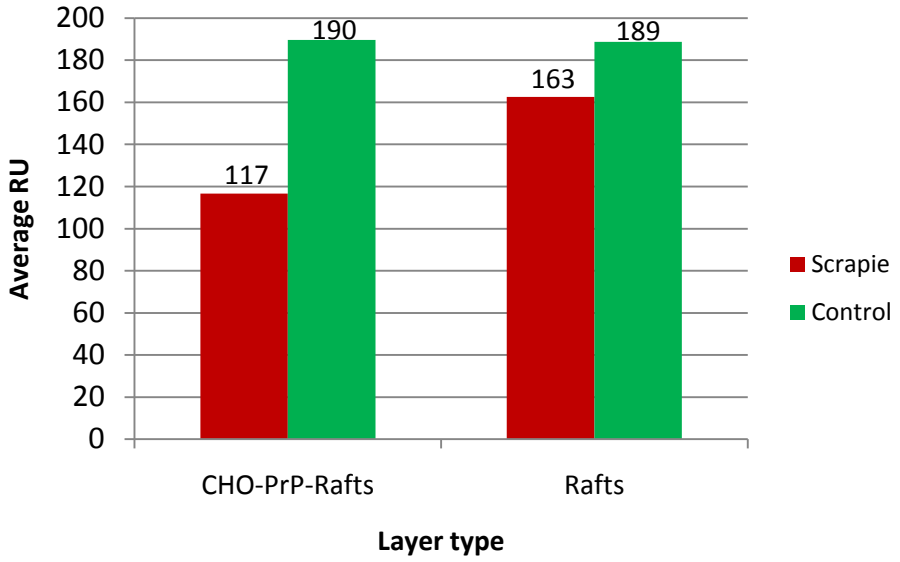

Figure 3.16 Comparison of the binding extent of the truncated PrP^{Sc}

Binding extent of the precipitate from scrapie-infected hamster brain homogenate after limited PK-digestion (red) was compared with the corresponding precipitate from healthy hamster brain homogenate (green). Binding to CHO-PrP^{C} saturated rafts was compared to rafts only, as control. Data are the average of four independent experiments, performed in a duplicate.

3.4.3 Interaction studies with prion rods

PrP 27-30 was received as a kind gift from Stanley B. Prusiner laboratory (UCSF, San Francisco, USA). The samples were delivered in form of sucrose fractions obtained from a large scale purification of prions from scrapie-infected hamster brains (Prusiner *et al.* 1983). A final purification of these fractions was necessary. It included additional centrifugation and washing

steps (cf. chapter 2.8). At first the fraction number four was prepared and measured with the PrP^C –membrane system, as described above. The total amount of protein contained in this fraction equaled 19 µg (0.5 µg/ml). The pellet was diluted in 0.75 ml of CBS buffer leading to a final concentration of the purified prion rods of 25 ng/µl. That corresponds to 760 nM concentration of the monomeric PrP^C. Before each SPR measurement an aliquot with 60 µl volume was diluted with 60 µl of CBS buffer, sonicated for 15 sec at 165 W and 90 µl of the sample were injected directly into the Biacore at flow rate of 10 µl/min. If not stated otherwise, this procedure was chosen for all following measurements. The results of this experiment are shown in the next figure: binding of purified PrP 27-30 was measured again on both the CHO-PrP^C saturated lipid bilayer and lipid rafts only (cf. Figure 3.17). For a better comparison the recorded curves were superimposed and aligned to the "0" value. It was observed that PrP 27-30 bound significantly stronger to the anchored CHO-PrP^C (solid line) when compared with raft-like lipid bilayer (dashed line). Single injection of prion rods passed over the PrP^C layer led to a binding level of 600 RU (pg/mm^2), whereas at the raft-like only lipid bilayer a signal increase of 240 RU (pg/mm^2) was detected.

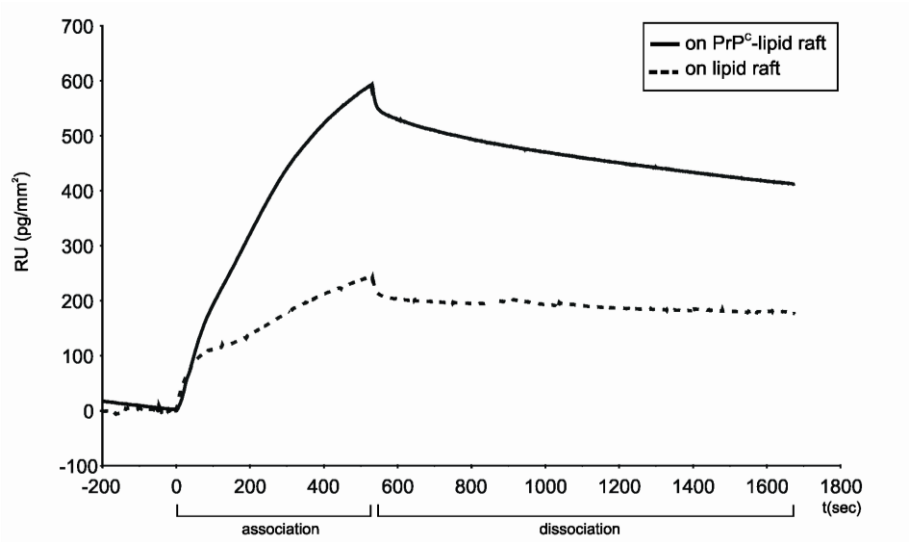

Figure 3.17 Analysis of the PrP 27-30 binding

SPR measurement: 90 µl samples of highly purified PrP 27-30 were injected at concentration of 12.5ng/µl over raft-like lipid bilayer (dashed line) and a CHO-PrP^C saturated bilayer (solid line) at the flow rate of 10 µl/min. After an association phase of 540 sec, dissociation was observed for additional 1100 sec.

Furthermore, also the shape of the curves recorded during the association phase clearly differed. While the prion rods sample measured on the PrP^C layer showed a quite steep, but constantly increasing binding course, the curve recorded over raft-only bilayer showed in the first 100 sec a fast signal increase that was then followed by a slower binding course. These differences observed in both the extent of binding and the character of the association course led to assumption that different mechanisms had to be responsible for the interaction of PrP 27-30 with the both types of layers.

In order to study these differences in more detail following measurements were performed using slower flow rate, namely 5 µl/min. By decreasing the flow rate and keeping the injected volume unchaged the interaction time during the association phase was increased raising the binding potential of the injected components. As it was already observed, also results of this experiment showed that there was a significant difference in the binding strength of the PrP 27-30 to CHO-PrP^C saturated lipid bilayer when compared with the raft-only control (cf. Figure 3.18). By decreasing the flow rate an even greater signal increase of the sample applied to the PrP^C layer

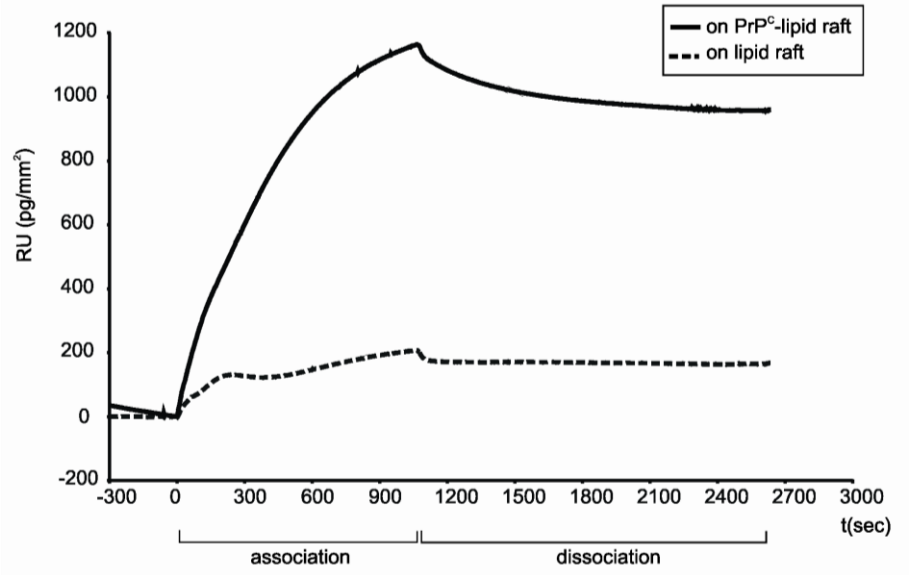

Figure 3.18 Flow rate effect on the extent of binding of PrP 27-30

SPR measurement: Samples containing 90 µl of highly purified PrP 27-30 were injected at concentration of 12.5ng/µl over raft-like lipid bilayer (dashed line) and a CHO-PrP^C saturated bilayer (solid line) at the flow rate of 5 µl/min. After an association phase of 1080 sec, the dissociation phase was observed for additional 1500 sec at the flow rate of 5 µl/min. During the association phase five flow-through samples were collected. During the dissociation phase another two fractions each with 50 µl volume were collected.

(solid line) could be achieved, reaching a level of almost 1200 RU (pg/mm^2), which is twice as much when compared to the previous measurement performed at flow rate of 10 µl/min. Surprisingly, this flow rate effect could only be observed for the PrP^C layer. The prion rods sample passed over the raft-like lipid bilayer (dashed line) reached exact the same binding level as previously, namely 200 RU (pg/mm^2). Moreover, the characteristic transient decrease detected previously was also recorded here, but now, due to the slower flow rate a more detailed analysis was possible: the interaction of prion rods with raft-like lipid bilayer is characterized by a fast binding step, then a weak signal drop followed by a final signal increase that However, is slower as at the beginning. The time point, at which the peak for the first fast binding step was achieved, was recorded at 200 sec. This value corresponds to a 1/5th of the association phase time and this ratio correlates well with the results obtained previously.

Also for a more detailled analysis this SPR measurement was complemented with a SDS-PAGE analysis of the flow-through fractions collected during the association and dissociation phases.The fractions during the association phase were collected by placing a tube at the waste outlet of the Biacore device. The tubes were changed after each 10 µl of the sample passed over the chip surface according to the sensorgram recordings. It was therefore expected to collect nine fractions, each containig 10 µl of the unbound prion rods that passed through the system. However, a very complex assembly of microchannels and microtubings in the integrated fluidic cartrigde (IFC), which is the core of the Biacore 1000 device, made such a precise collection not possible. Instead of nine, only five fraction could be collected, each containig slightly different volumes. These were then partially pooled and analyzed in the gel. Collection of the flow-through fractions during the dissociation phase was simpler. The build-in automatic method of the Biacore could be used. It directs the desired volume of the flow-through to a special recovery channel from which the sample can be recovered. Two fractions, each containing 50 µl of the dissociation flow-through, were recovered. In order to show the amount of prion rods used for a single injection a sample with 120 µl of the starting material was loaded onto the gel (lane 1, cf. Figure 3.19). This sample volume was used in every experiment, however, only 90 µl of it were truly injected over the chip surface. The remaining 30 µl were necessary for a proper preparation of the injection. Following three lanes correspond to the flow-through fractions collected during the measurement of PrP 27-30 over the raft-like layer (lanes 2, 3 and 4). As already mentioned a precise collection of the flow-through fractions was not possible, therefore fractions: 2 plus 4 and 7 plus 9 were pooled to two independent fractions, both with volumes of 65 and 50 µl, respectively. Fraction 1 was loaded separately. The analysis showed that in the first fraction

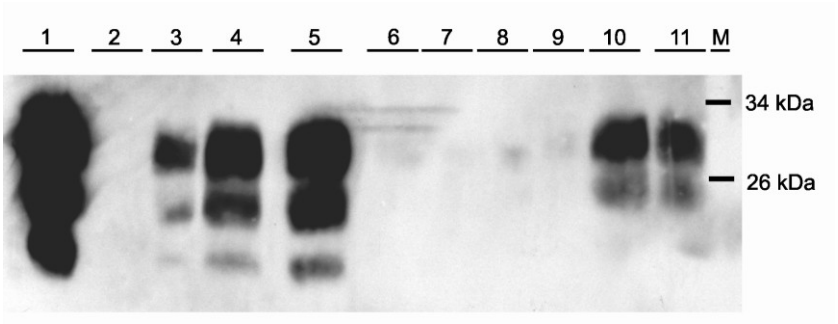

Figure 3.19 Gel analysis of the flow-through

Western blot analysis of staring material and flow-through fractions: **Lane 1**: analysis of the starting material. **Lane 2-4**: analysis of the flow-through fractions collected during the association phase measured on the raft-like lipid bilayer. **Lane 5**: pooled flow-through fractions collected during the association phase measured on the CHO-PrP^C saturated lipid bilayer. **Lane 6 -9**: flow-through fractions collected during dissociation phase measured on the raft-like lipid bilayer and CHO-PrP^C saturated lipid bilayer, respectively. **Lane 10-11**: empty, original tubes analyzed after the injection of aliquots over raft-like lipid bilayer and CHO-PrP^C saturated lipid bilayer, respectively. **M**: molecular size marker.

(lane 2) no prion rods specific signal was detected. This correlates with the observed steep binding occurring at the beginning of the association phase, when all incoming prion rods interact with the lipid bilayer. Lanes 3 and 4 both showed signals, corresponding to the unbound prion rods that passed over the raft-like lipid bilayer in the course of the association phase. Increase of the signal observed in the pooled fractions 7 and 9 could be explained by the fact, that the binding was nearly saturated ant most prion in the flow passed the surface without addition binding. Lane 5 shows all five fractions: 1 plus 4 plus 6 plus 7 plus 9 collected during the measurement over the CHO-PrP^C saturated lipid bilayer that were pooled to one fraction. However, the very inaccurate way of collecting flow-through fraction made a similar analysis as described above not possible. Therefore, in the case of PrP^C saturated bilayer only a general conclusion can be made demonstrating the difference between the amounts of the introduced and the unbound material that passed through the system. Following four lanes correspond to the fractions collected during the dissociation phases presenting the amount of released prion rods from both the raft-like and CHO-PrP^C saturated layer (lanes 6, 7, 8 and 9). The fact that these samples did not show any PrP 27-30-specific signal was in a good correlation with the SPR results. It could be demonstrated that the binding of prion rods to both types of layers was very strong and almost no loss of the bound material took place. The last two lanes represent the original tubes which were use for injection of each aliquot (lanes 10 and 11). After the 120 µl of

each sample were introduced to the Biacore device, the remaining tube was filled with sample buffer, heated and its content was loaded onto the gel in order to test it for the presence of prion rods that remained in the tube. As demonstrated in the gel a particular amount of PrP 27-30 stayed in the tubes, probably by "sticking" to its walls and bottom. However, in comparison to the starting material (lane 1) the remaining amounts were relatively small.

3.5 Control studies for the specificity

In order to confirm the specificity of the interaction observed between PrP 27-30 fibrillar structures and the anchored PrP^C other than prion protein interacting components have been tested. In the first control experiment a different type of fibrils was used and in the second the coating protein has been varied.

Insulin fibrils were prepared as described in chapter 2.9. After dilution with CBS buffer to a final concentration of 12.5 ng/µl and a sonication cycle at the same settings as for the prion rods, the SPR measurements over the raft-like lipid bilayer and CHO-PrP^C saturated bilayer were carried out. In the Figure 3.20 the recorded insulin binding curves have been presented as an overlay

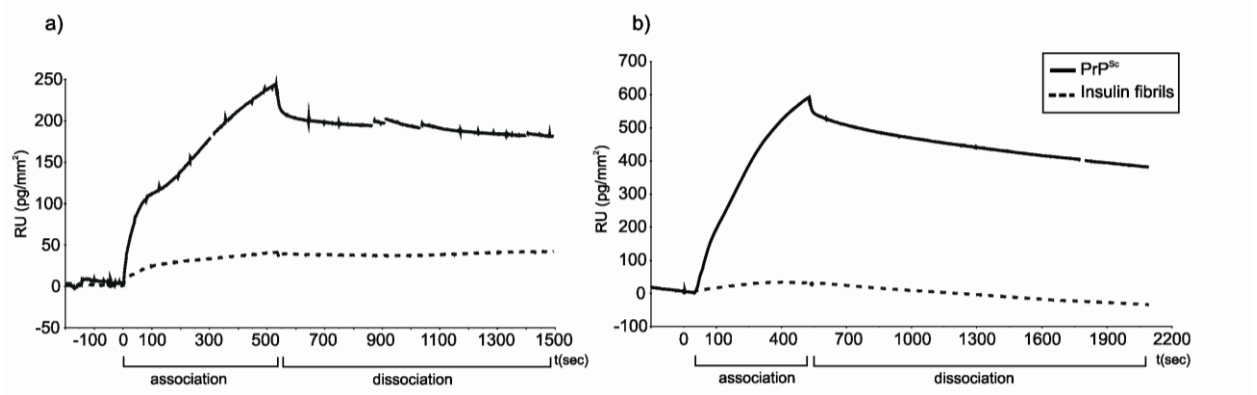

Figure 3.20 Interaction of insulin fibrils with raft-like lipid membrane and PrP^C

SPR measurement on raft-like lipid bilayer (**a**): 90 µl sample of highly purified PrP 27-30 injected at concentration of 12.5ng/µl (solid line) was compared with an injection of 90 µl insulin fibrils at concentration of 12.5ng/µl (dashed line). Both measurements were performed at a flow rate of 10 µl/min. The association phase lasted 540 sec and was followed by a dissociation observed for additional 960 sec.

SPR measurement on CHO-PrP^C saturated lipid bilayer (**b**): 90 µl sample of highly purified PrP 27-30 injected at concentration of 12.5ng/µl (solid line) was compared with an injection of 90 µl insulin fibrils at concentration of 12.5ng/µl (dashed line). Both measurements were performed at a flow rate of 10 µl/min. The association phase lasted 540 s and was followed by a dissociation observed for additional 1560 s.

with the corresponding PrP 27-30 curves. It could be demonstrated that this type of fibrils did not show the effects observed for prion rods fibrils: the very weak binding was not only significantly lower when compared to prion rods but also layer-unspecific.

The experiment described above confirmed that indeed only fibrils in form of prion rods could bind to the anchored PrP^C. However, it did not answer the question whether prion rods could also bind to a different kind of protein. In order to test this type of specificity the coating PrP^C has been replaced by an ovalbumin. As mentioned before, ovalbumin in the mixture with PrP^C did not show any binding to rafts-like lipid bilayer unless it was introduced in salt-lacking buffer like NaAc (cf. chapter 3.3). Therefore multiple injections of ovalbumin diluted in 1 mM NaAc to a final concentration of 100 ng/µl were performed in order to create an unspecific protein layer covering the lipids (data not shown). Once the signal increase reached a level of app. 800 RU a sample with prion rods has been passed over it. At this point one has to mention that the process of saturation with ovalbumin proceeded very slowly. This could be explained by the fact that ovalbumin lacks the GPI-anchor. As demonstrated in the Figure 3.21 prion rods showed very weak binding ability to the ovalbumin layer. In order to demonstrate this in more detail the original sensorgram was presented with the bulk effect of the running buffer shown at the beginning and at the end of the association phase. As long as PrP 27-30 was present in the

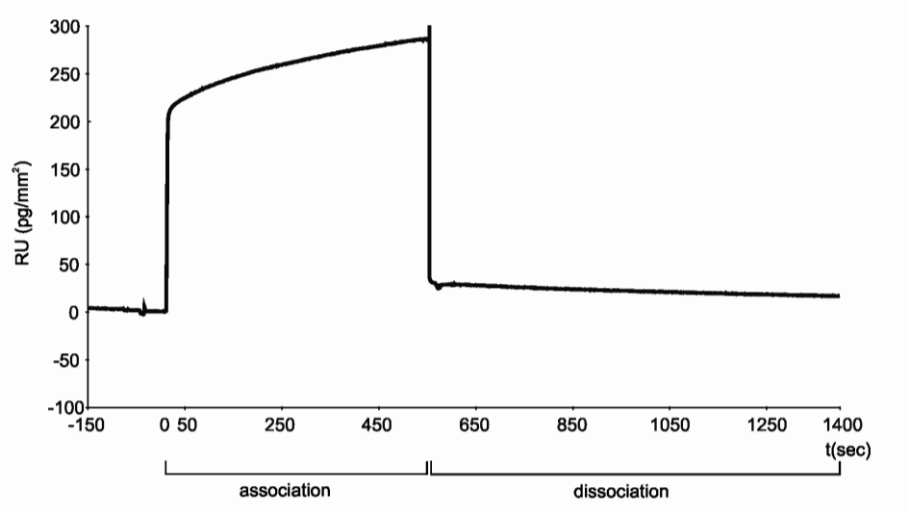

Figure 3.21 Prion rods do not bind to ovalbumin

SPR measurement: 90 µl sample of PrP 27-30 was injected over ovalbumin-coated lipid bilayer at a flow rate of 10 µl/min. The dramatic signal increase at the beginning of the association phase and decrease at the end of it corresponds to the bulk effect caused by the running buffer. The 540 sec long association phase was followed by a dissociation observed for additional 870 sec.

system a signal increase of app. 70 RU seemed to take place. However, the start of the dissociation phase, when only the running buffer passes the flow cell, revealed the true binding extent that prion rods achieved on this type of the layer, showed by a signal increase of only 25 RU (pg/mm^2). The apparent binding observed during the association phase, could be explained simply by the mass change that took place when prion rods entered the flow cell. Another explanation could be some sort of unspecific interaction that, however, was too weak to resist the buffer change and was ceased directly. Therefore this experiment also confirmed that interaction demonstrated for anchored PrP^C and fibrillar infectious PrP 27-30 is specific and depends on the presence of both partners.

3.6 Influence of the prion rods preparations

As already mentioned, all experiments described above utilized a single fraction from a sucrose gradient ultracentrifugation, from which the final samples of prion rods were obtained. In order to confirm the observed effects, two additional sucrose gradient fractions were sent from the laboratory of Dr. Prusiner. Compared to the previous fraction these new ones not only differed in their protein concentrations or infectivity of the prion rods but were also collected from the zonal rotor at later time points. These were the fractions eight and nine. The large scale purification method of PrP 27-30 starts with the hamster brain homogenates and utilizes several washing steps under different conditions, PK digestion of the material and finally a centrifugation step in a sucrose gradient with the help of a zonal rotor (Prusiner *et al.* 1983). This leads to a size dependent distribution of prion rods along the sucrose gradient. According to it the larger and more dense particles migrate faster to the bottom of the tube while the smaller, and less dense prion rods remain in the upper fractions. The collection of the fractions is performed in the direction: bottom to the top by piercing a hole in the bottom of the centrifugation tube.

Having this in mind, at first the fraction nine was prepared. According to the information sent along with it, it contained 192 µg of prion rods at a concentration of 4.8 µg/ml, which was one order of magnitude higher when compared to the previously used fraction. The fraction was prepared in the same way as the first one (cf. chapter 2.8) and, according to the information of the total amount of prion protein, a final concentration of 0.27 µg/µl of prion rods was estimated in the final samples. This correlated to a 8 µM concentration of monomeric PrP. Since the concentration of the starting material was significantly higher than before samples at different dilutions were measured with the membrane-PrP^C system in the Biacore device. Surprisingly, the

binding curves observed before could not be recorded for the newly prepared prion rods. Different dilutions that were tested (1:120, 1:36, 1:21, 1:16, 1:12, 1:6 or 1:1) showed either no binding effects at all, minor binding or even signal decreasing effects that occurred during the association phases (data not shown). Also the specificity of prion rods for the anchored PrP^C was lost. It is shown in the next figure, where a 90 µl sample of prion rods at a dilution of 1:16 that corresponded to an estimated concentration of 17 ng/µl, was injected over the raft-like lipid bilayer and CHO-PrP^C saturated lipids (cf. Figure 3.22). For the first time an opposite effect could be observed, namely that PrP 27-30 bound stronger to raft-like lipid bilayer (dashed line) than to the PrP^C saturated lipids (solid line). However, it has to be mentioned at this point that not only the swap of the specificity effect was alarming, but also the extent of binding altogether were much weaker when compared to the previous results.

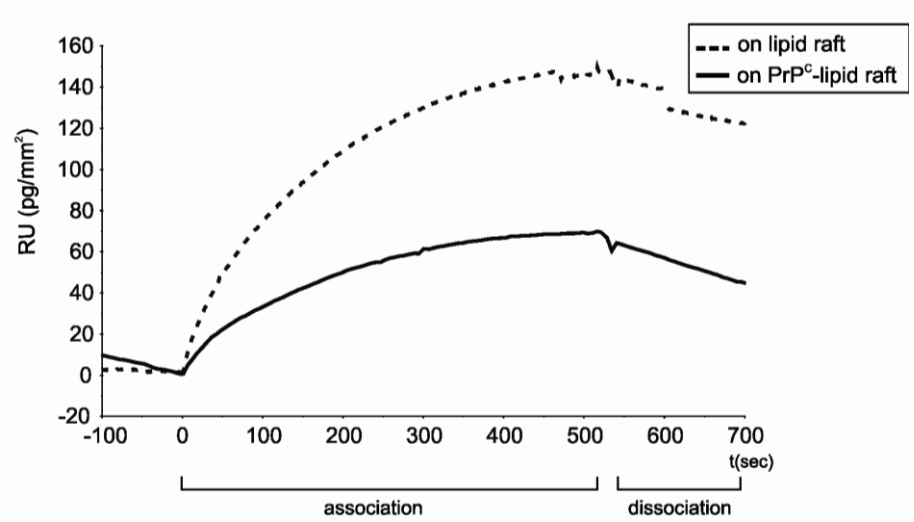

Figure 3.22 Loss of the prion rods specificity

SPR measurement: 90 µl samples of highly purified PrP 27-30 from new sucrose fraction were injected at concentration of 17 ng/µl over raft-like lipid bilayer (dashed line) and a CHO-PrP^C saturated bilayer (solid line) at the flow rate of 10 µl/min The 540 sec long association phase was followed by a very short dissociation observed for additional 200 sec.

One of the possible explanations for these new effects was that these fractions contained a somehow different kind of prion rods and that this difference could correlate with their size. According to the purification protocol smaller and less dense particles migrated slower in the sucrose fraction. It was also known that smaller prion rods often contain lipids impurities that influence their migration velocity (Riesner *et al.* 1996). Therefore, the preparation of the next

sucrose fraction, containing 300 µg of prion rods at a concentration of 7.7 µg/ml, was slightly altered. The precipitated pellet was divided into two portions: the first half was prepared according to the standard protocol, while the second half underwent an additional lipid extraction (cf. chapter 2.8.1). The final concentration of the prion rods in both, the lipid extracted and the not altered samples, was estimated at 0.2 µg/µl, according to the total amount of prion rods contained in that fraction. This correlated to a 6 µM concentration of the monomeric PrP. As shown in the next figure the prion rods after lipid extraction retrieved both their binding ability and the specificity for PrP^C (cf. Figure 3.23). A single injection of a sample containing PrP 27-30 at an estimated concentration of 33 ng/µl led to a signal increase of 37 and 90 RU (pg/mm^2) at the raft-like bilayer and CHO-PrP^C saturated lipids, respectively.

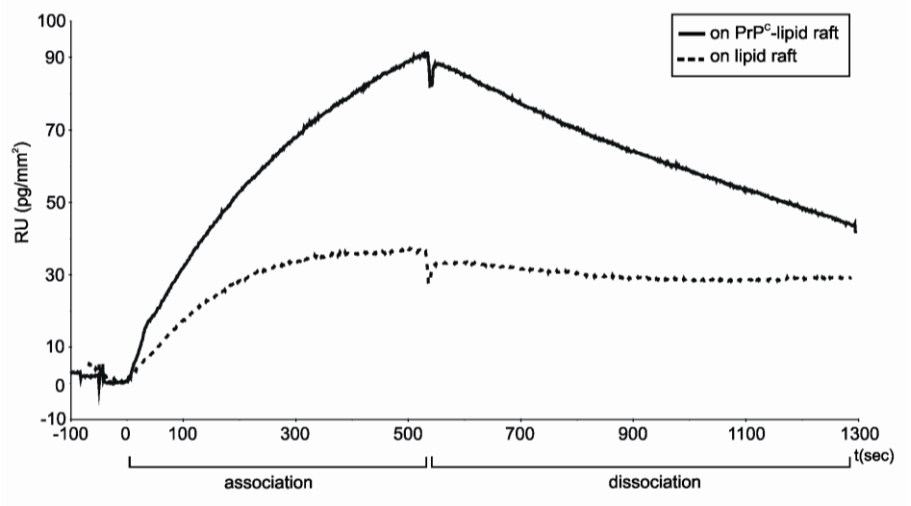

Figure 3.23 Lipid extraction restores the prion rods specificity

SPR measurement: 90 µl samples of PrP 27-30 after lipids extraction were injected at concentration of 33 ng/µl over rafts-like lipid bilayer (dashed line) and a CHO-PrP^C saturated bilayer (solid line) at the flow rate of 10 µl/min The 540 sec long association phase was followed by a dissociation observed for additional 200 sec.

The much weaker binding ability of this prion rods preparation could be explained by the results presented in the Figure 3.24. It shows a Western blot after an SDS-PAGE analysis of the starting material, flow-through fractions collected during the association phase and the original tube used for the Biacore measurement. The results presented in this Western blot are exemplary and correspond to the binding curve of prion rods after lipid extraction recorded at the raft-like bilayer. It has been demonstrated that there was only a slight difference between the amount of

PrP 27-30 contained in the starting material (lane 1) and the amount of PrP 27-30 remained in the tube after the SPR measurement (lane 2).

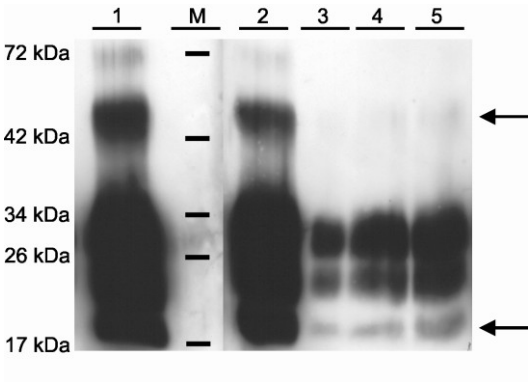

Figure 3.24 Gel analysis of the flow-through after lipid extraction

Western blot analysis of staring material and flow-through fractions: **Lane 1**: analysis of the starting material after lipid extraction. **M**: molecular size marker. **Lane 2**: empty, original tube analyzed after the injection of aliquot over raft-like lipid bilayer. **Lane 3 - 5**: analysis of the flow-through fractions collected during the association phase measured on the raft-like lipid bilayer.

Due to overexposure of this particular film one can see the differences most accurately when bands with the size of app. 55 kDa (marked by arrow) are compared. This means that unfortunately almost 90 % of prion rods stayed in the tube, probably "sticking" to its walls and bottom. Such an extremely high affinity of prion rods to the plastic surface was not observed for the first fraction (cf. Figure 3.19) and could not be eliminated even after increasing the sonication time from 15 sec to 5 min, as it was done in this experiment. Although this analysis revealed difficulties in handling the samples of these prion rods it also showed a positive result demonstrated in the flow-through fractions. The collection was carried out as described before, but this time only three fractions each containing app. 30 µl of the association flow-through were collected. As shown in the lanes 3, 4 and 5 the signal corresponding to prion rods increased gradually, meaning that with the time course of the association more and more prion rods passed the surface without showing any interaction with the more and more saturated lipids. This was demonstrated the best on the example of the app. 20 kDa size band (marked by arrow). This effect correlated well with the course of the recorded curve (dashed line) that first showed a fast signal increase, which eventually approached the saturation level. When one regards the amount of PrP 27-30 found in the fraction 3 (lane 5) as the amount of prion rods that passed through the flow cell without showing any binding, which correlates with the course of the curve, then the

signal found in the fraction 1 (lane 3) shows that app. 80 % - 90 % of these prion rods bound to the rafts-like lipid bilayer in the first phase of the association curve. This good correlation between the quantity and the quality of the observed effects proves that results obtained with a sophisticated method like the SPR measurement can be easily confirmed with a simple method like protein gel analysis.

4 Discussion

For the last years one of the main topics of prion protein research concentrated on solving the ongoing problem of the mechanisms underlying the onset of prion diseases. Although much effort was put in this subject, both the molecular mechanism and the subcellular site of the conversion process are still unknown. By unraveling *in vitro* the fundamentals underlying the conversion mechanism, the ultimate proof for the "protein-only" hypothesis could finally be found. Nowadays, the prion research provides a variety of *in vitro* systems as tools for solving problems of the primary site of the disease onset and the mechanism of conversion process. The primary site for the onset of prion diseases is hypothesized to be the cellular membrane, i.e. its special microdomains, called rafts. However, not many *in vitro* systems, developed till now, demonstrate high biological relevance in this particular aspect. The problems concern mostly the complex composition of natural PrP^{C} with its GPI-anchor, serious difficulties with its purification, presence of lipid membrane and its possible influence on the conversion process, the attachment of PrP^{C} to the membrane and finally use of purified prions. All this made a development of an *in vitro* system, which would be in a good accordance with the events occurring in nature, very challenging. There are, however, studies trying to approach the membrane aspect of the conversion process. It could be demonstrated that the recombinant mouse PrP-lipid interaction induced the conversion of prion protein to a PrP^{Sc}-like proteinase K (PK) resistant conformation in solution (Wang *et al.* 2007). It was also observed that full-length α-helix rich recombinant PrP was converted into different forms, one of them displaying a conformation similar to PrP^{Sc} with a PK-resistant core and increased β-sheet content. A different study demonstrated the use of planar surfaces. Work of Leclerc and colleagues showed that recombinant hamster PrP, both in its full-length and truncated form, could undergo the transition to PK-resistant PrP^{Sc}-like aggregates that occurred on a surface of a sensor chip (Leclerc *et al.* 2008). This transition was monitored with the help of epitope-specific antibody Fab fragments. As mentioned before, these experiments approached the aspect of membrane influence on prion conversion; however, they had one common weakness, namely the use of recombinant prion protein. It lacks, due to the expression in *E.coli* system, all posttranslational modifications that are present in the eukaryotic form and therefore cannot mimic properly the *in vivo* situation. This determined the main disadvantage of such system, namely that the fundamental interaction,

which takes place in nature, could not be granted. The electrostatic type of binding that occurs when GPI-anchor is absent, cannot reliably simulate the hydrophobic binding of PrP to the membrane. Therefore, it was of great importance to develop an *in vitro* system that would not only utilize the eukaryotic form of PrP, but also display the ability to relevantly mimic the natural onset of the prion disease, which is postulated to take place at the cellular membrane. This could successfully be done in this project and the results obtained with this novel *in vitro* system are discussed in the following chapters.

4.1 Complexity of the multi-component *in vitro* system

As already described in chapter 1.2.4, PrP^{C} in its natural state is anchored at the outer cell membrane. It was quite obvious to assume that this particular localization could act as the site of first contact with invading PrP^{Sc}. Therefore, in order to create a system that accurately simulates onset of the prion diseases one has to consider all three components: the membrane, the bound PrP^{C} and the invading PrP^{Sc}. In this chapter I am going to discuss the complexity and the main advantages of the *in vitro* system developed for the needs of my project.

To test the possibility of the outer membrane as a site for the prion conversion an earlier described system was used as basis for further studies. The results achieved by Elfrink showed that a GPI-anchor dependent reconstitution of PrP^{C} into model membranes was possible (Elfrink *et al.* 2007). Technique used in those experiments relied on a biophysical phenomenon known as the surface plasmon resonance (SPR; cf. chapter 2.17). In general, SPR was applied in the Biacore device creating a method that made study of direct molecular interactions possible. Interactions were measured as mass depositions occurring at a planar surface. One of the many advantages of this method was that it allowed analyzing molecular interactions in real time without addition of any secondary compounds. Another benefit of this method was that all measurements were performed on a planar surface. Reduction of the three-dimensional character of studies done in solutions to a two-dimensional one was, in the case of membrane-anchored protein, of extreme importance and the essential step towards the *in vivo* conditions. Furthermore, the basics settings, i.e. use of physiological buffer at pH 6 or temperature set to 37°C, were in good accordance with the conditions found *in vivo*.

Lipid bilayer as a cellular membrane

The first component of this *in vitro* system was the planar surface. It was provided in form of a chip with chemically altered surface allowing attachment of lipid vesicles. The lipophilic character of the chip surface led to formation of a lipid bilayer (cf. chapter 2.17.4). One of the characteristics of PrP^C is that its attachment to the outer cellular membrane occurs only at special domains, called rafts. This feature PrP^C shares with other GPI-anchored proteins. It has been therefore hypothesized that the distribution of PrP^C restricted to these specific microdomains may have an influence on the cellular function and/or on the conversion process of prion protein. The role of rafts in the latter process has been studied for years now, and although no definite results could be presented yet, it is clear that they play a crucial role in PrP^{Sc} formation (cf. chapter 1.2.5). Therefore, it was important to create system with the same lipid composition as observed in nature. The biochemical composition of rafts is already known and well described in the literature (Schroeder *et al.* 1994), and so it was possible to develop the first component of the *in vitro* system in form of raft-like lipid bilayer.

Attachment of PrP^C

Next step in imitation of nature was to reconstitute the PrP^C into model membranes. This could only be done with the help of prion protein that would possess all posttranslational modifications. As mentioned before PrP^C, belonging to the group of membrane-anchored proteins, acquires in its posttranslational processing pathway the GPI-anchor. However, this is not the only modification this protein has to undergo. Another one is the addition of two N-linked oligosaccharide chains. Figure 4.1 presents a structural model of membrane-anchored PrP^C with all these modifications (Bennion *et al.* 2004). It is more than likely that next to the influence on the solubility of the prion protein and its distribution in raft domains, these modifications could also take part in the interactions of PrP with other cellular components and/or in the conversion process of prion protein.

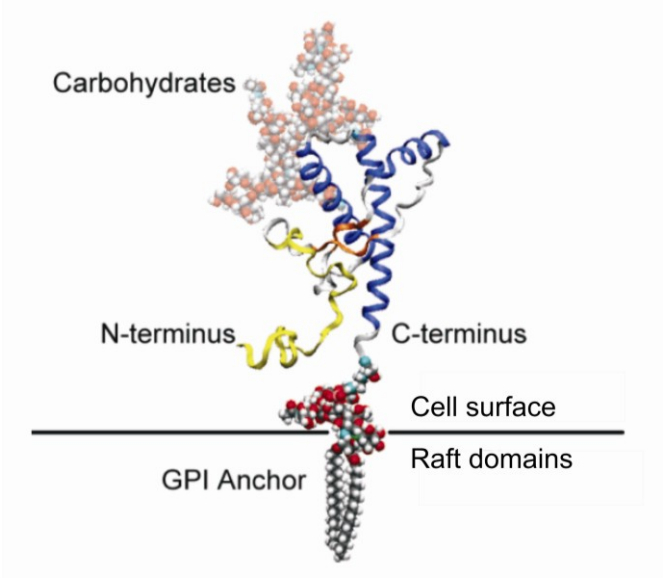

Figure 4.1 Structural model of membrane-anchored PrP^C

Model of the soluble hamster prion protein: residues 125-228 are from NMR structure modeled with carbohydrates (space-filling representation, background), the unstructured N-terminal region (yellow), and the GPI-anchor (space-filling representation, foreground). (Figure taken from Bennion *et al*., 2004).

Still, in most of the studies the recombinant prion protein, produced in *E.coli* cell lines, is being used. The great advantage of this system is its simplicity and a large yield of the protein of interest. However, a prokaryotic system can merely produce an unmodified form of prion protein, for it lacks the eukaryotic-specific pathways. Therefore, all studies performed with the help of recPrP cannot take in account possible influences of the natural modifications. The analysis of the PrP^C *in vivo* revealed that its total amount was very low, reaching barely a level of 0.1 % of all proteins found in the central nervous system. This made the attempts to purify it from brain homogenates extremely difficult. The finally developed protocols were forced to use either detergents or denaturing agents in order to solubilize the protein and to prevent it from aggregation (Turk *et al.* 1988; Pan *et al.* 1992). Therefore, they could only be seen as denaturing purification methods yielding an altered form of PrP^C. This was changed after introducing an eukaryotic cell lines that had the ability to overproduce PrP^C (Blochberger *et al.* 1997). It was demonstrated that a Chinese hamster ovary cell line could yield an amount of posttranslationally modified PrP^C that was fourteen times higher when compared to the amounts purified from hamster brain homogenates. The optimization of the protocol developed for this cell line, led to a stable production of natural PrP^C that has been purified in mild conditions, without addition of any detergents (Elfrink *et al.* 2004). The same protocol was used in this work, however, a slight

change had to be introduced. The purification method was based on two affinity chromatography steps, namely metal chelate and antibody affinity. Due to the deficiency of the antibody used in the original protocol, i.e. 3F4 antibody, an alternative had to be found. In this work I managed, with the help of Dr. Korth's laboratory, to replace the monoclonal 3F4 antibody with a recombinant one in form of a single chain fragment W226. This optimization step rescued indeed the PrP^C production, however, it also changed the character of the obtained product. The ongoing problem of PrP^C solubility that was almost entirely eliminated by the use of low amounts of Zwittergent 3-12 (0.15 %) in the old protocol, returned fully after the new antibody has been applied. It could be explained by the fact that the single chain antibody with its extremely high affinity to prion protein - a K_D of only 2 nM against recombinant mouse PrP (Muller-Schiffmann *et al.* 2009) was simply working too good and purifying indeed only PrP^C. This in case of a membrane protein and a protocol with only little amounts of stabilizing detergents led inevitably to an aggregation. This was strengthened by the observation that the PrP^C produced with the changed protocol yielded constantly protein with a much higher purity grade when compared to the results obtained with the original method. A possible explanation for this effect could be an often observed presence of lipids that co-purify with the membrane-attached proteins of interest influencing so their solubility. In order to solve the insolubility problem a protein stabilizer in form of ovalbumin was added to the final eluate. It showed positive effects preventing most of the PrP^C from aggregation. The mechanism underlying this effect relies probably on the small amounts of purified PrP^C. It is known that one of the factors that have an influence on the protein aggregation is their low concentration in solution. In order to change that, secondary components in form of other proteins are often added. They increase the saturation level in the solution preventing the protein of interest from interaction with its counterpart molecules and inhibiting so the aggregation.

The eventually obtained prion protein with all its modifications could finally be reconstituted into model membranes. Literature describes many different studies aiming at the interaction between PrP and membranes However, most of them either used shorter or longer PrP fragments (Dupiereux *et al.* 2005; Shin *et al.* 2008) or recPrP with chemically attached GPI-anchor-like structures (Eberl *et al.* 2004; Olschewski *et al.* 2007; Becker *et al.* 2008). As mentioned before the disadvantage of these systems was the artificial character of their main players. Therefore, first the successful reconstitution of natural PrP *via* its own GPI-anchor into model membranes gave a new, exciting opportunity for further studies (Elfrink *et al.* 2007). In this work the already

existing protocol for reconstitution has been adapted and act therefore as the second step in the formation of a multi-component *in vitro* system (cf. chapter 3.3).

Imitating the disease-onset

In iatrogenic and variant CJD the invading infectious prion protein is the causative agent that launches the disease. However, as already mentioned, the exact site where PrP^{Sc} meets the host PrP^{C} and starts to amplify the PrP^{Sc} conformation is still unknown. The set up of membrane-anchored PrP^{C} in the Biacore device allowed introducing the third and final component *via* continuous flow. This not only mimicked very well the *in vivo* state, where invading PrP^{Sc} possibly migrates free in the extracellular fluid but also allowed analysis of the outcome performed after the interaction phase. Another advantage of this particular *in vitro* system is that it shows no restrictions as to the character of the third component. Therefore, different kinds of particles were used in the search for the specific interaction with the anchored PrP^{C}.

The final set up of this complex multi-component *in vitro* system, established in the course of this project, is presented in the Figure 4.2. To summarize it: the first two components, namely the lipid bilayer and the PrP^{C} have not been changed throughout all experiments, while the third component was systematically varied. In this chapter, however, only the results achieved with prion rods will be discussed.

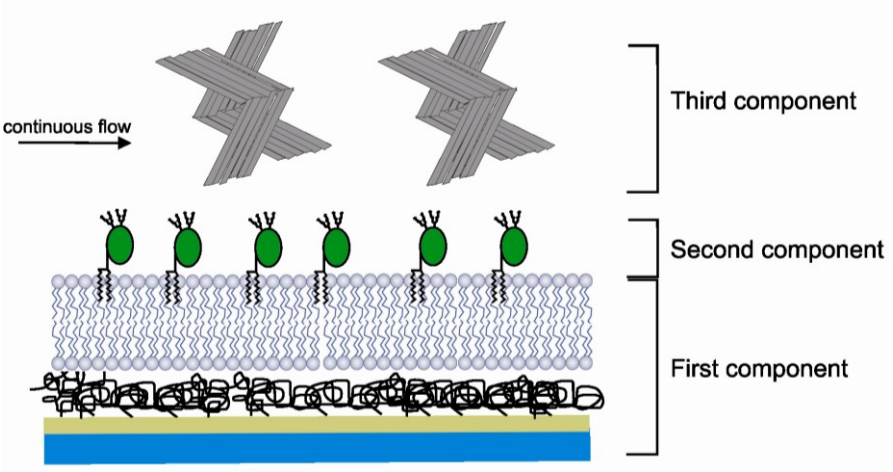

Figure 4.2 Multi-component *in vitro* system

Model of the *in vitro* system developed for the use in Biacore device. The chip surface with a modified dextran layer served as basis for attachment of lipid vesicles that spread in form of a bilayer (first component). Natural PrP^{C} with all posttranslational modifications was reconstituted stably into the model membranes (second component). Addition of third component in form of different molecules completed the system and allowed studies on the intermolecular interactions in the presence of the lipid membrane.

The main advantage of this material, in comparison with non-infectious aggregates and partially purified PrP^{Sc} (cf. chapter 3.4.1 and chapter 3.4.2), was its purity and a very well defined structure. This was demonstrated in the study, where PrP 27-30 polymerized into rod-shaped structures that showed the ultrastructural characteristics of an amyloid fibrils (Leffers *et al.* 2005). Use of natural prion rods made two different experiments possible: measurement of prion rods at empty membranes in comparison with PrP^{C}-saturated lipids (cf. chapter 3.4.3).

First, it has been demonstrated that the binding of PrP 27-30 to empty rafts-like lipid bilayer displayed a two phase character: a fast association was followed by a slower and steadily growing interaction (cf. Figure 4.3 a). These effects most probably corresponded to the GPI-dependent manner of binding. The assumption of a hydrophobic type of interaction was plausible

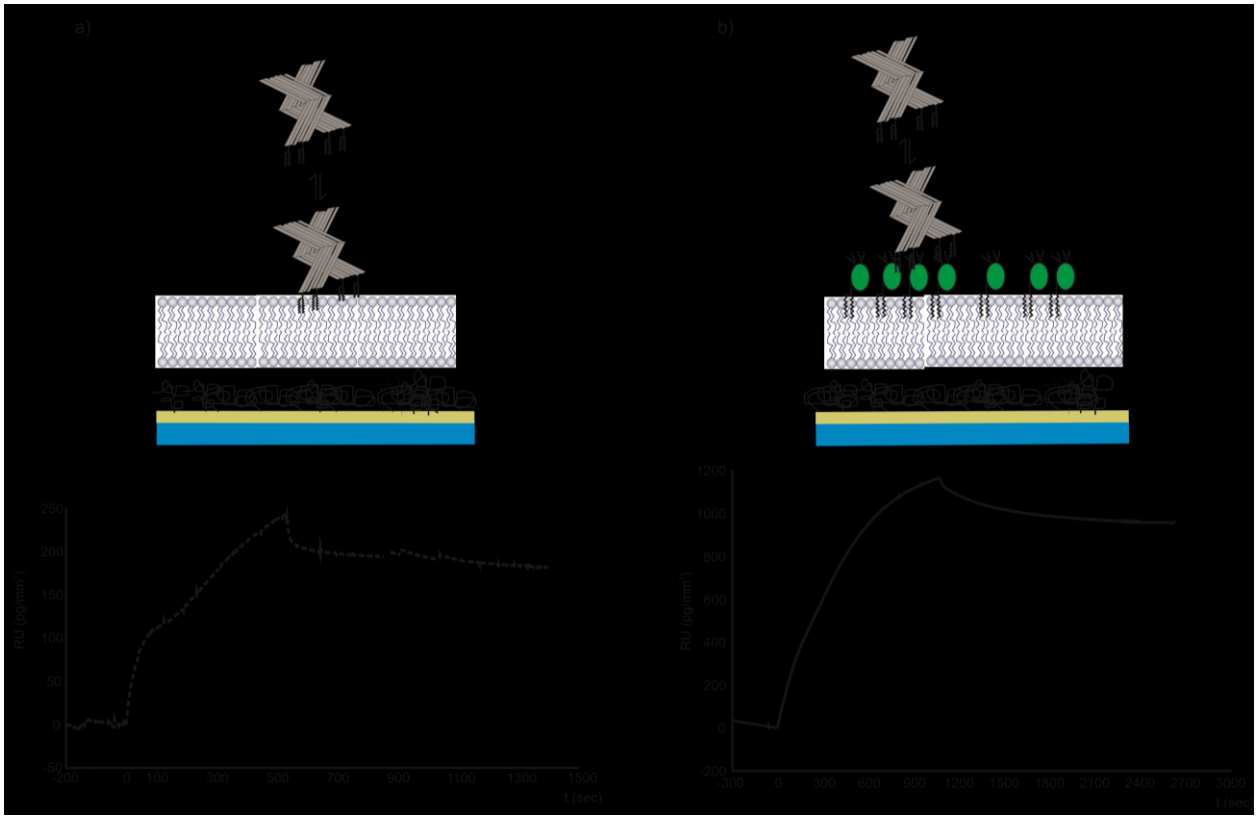

Figure 4.3 PrP 27-30 displays different types of interaction

Two experimental approaches and corresponding SPR measurements: PrP 27-30 displayed different types of interaction dependent on the absence (**a**) or presence of PrP^{C} (**b**) at the surface of model membranes.

because salt present in the buffer successfully weakened all electrostatic, unspecific binding sites but not the specific sites of PrP 27-30 possessing all posttranslational modification, including the

GPI-anchor. Therefore, the observed binding most probably represented in its first step an unspecific type of interaction that was followed by a specific rearrangement. One can imagine that at the beginning of the association phase a cluster of randomly bound molecules was formed. Out of it only the GPI-anchored molecules stayed stably anchored at the membrane. All molecules attached in a different way, i.e. randomly bound, dissociated briefly making new specific binding sites accessible again. This could lead to a rearrangement of the already bound molecules and to a further binding. However, due to partially occupied surface another random distribution was not possible and therefore the following, slower type of binding had to base on the interaction with the GPI-anchor only.

Another type of PrP^{Sc} binding was observed for the interaction between exogenously added PrP^{Sc} and membrane-anchored PrP^{C} (cf. Figure 4.3 b). Prion rods showed not only high affinity to the anchored PrP^{C}, but also high specificity for this particular partner. The high affinity was demonstrated by the mass of PrP 27-30 bound to the membrane-attached PrP^{C}. The recorded signal was significantly higher when PrP^{C} was present in the system. The specificity of this interaction was demonstrated by the fact that neither prion rods bound to another type of protein (cf. Figure 3.21) nor a different kind of fibrils was able to bind to anchored PrP^{C} (cf. Figure 3.20). These results also eliminated one of the postulated types of interaction between PrP^{C} and PrP^{Sc}, namely that invading PrP^{Sc} forces PrP^{C} to leave the membrane and converts it then in the extracellular fluid (cf. Figure 1.10). Since no “pull out” effects in form of dissociation of the PrP^{C} from the layer were observed when prion rods were used, the interaction mechanism must have been based on a direct binding of PrP 27-30 to the attached PrP^{C}. A direct comparison of association phases observed at both types of layers allowed assuming that invading PrP^{Sc} bound PrP^{C} in a specific manner, most probably through some unknown PrP^{C}-PrP^{Sc} interface. However, the exact molecular mechanism of this binding could not be revealed with the Biacore method.

Let’s assume that the observed, stable interaction would indeed have an influence on the conversion process and could lead to pathological effects. Then it would be plausible to postulate a fibril formation mechanism based on a recruitment of membrane-bound PrP^{C}. This idea is strengthened by the observation that prion rods as such acquire PrP^{C} molecules and transfer them into mature fibrils. Moreover, literature already describes studies performed on different types of fibrils showing similar effects. It was demonstrated that membrane disruption by human islet amyloid polypeptide (hIAPP) could be involved in the death of insulin-producing islet β cells involved in the type 2 diabetes mellitus (Engel *et al.* 2008). It was shown that the kinetic profile

of membrane damage was characterized by a lag phase and a sigmoidal transition, which matched the kinetic profile of hIAPP fibril growth. Similar growth kinetics were also observed for prion protein fibrils (Stohr *et al.* 2008). Furthermore, electron microscopy analysis showed that hIAPP fibrils lined the surface of distorted phospholipid vesicles, in agreement with the notion that hIAPP fibril growth at the membrane and membrane damage were physically connected. A fibril formation induced death of neuronal cells could also be seen as one of the potential mechanisms underlying prion diseases. However, to study the possible growth of prion rods on model membranes and its pathological consequence, much longer observation and adequate amounts of PrP 27-30 would be needed.

Prion rods preparation difficulty

As described in detail in the results (cf. chapter 3.4.2 and chapter 3.6) the main problem this project had to face, was the impurity of the PrP^{Sc} preparations. It not only precluded a proper evaluation of the data, as it was shown in the case of partially purified PrP^{Sc}, it also made the trials to reproduce the observed effects quite difficult. The main advantage of the developed *in vitro* system and at the same time its main complexity was the guaranteed high biological relevance. To assure the accordance with the physiological conditions animal brain homogenates were chosen as the source for infectious PrP^{Sc}. Although specific methods, i.e. sodium phosphotungstate (NaPTA) precipitation and large-scale purification were used, they could not guarantee a 100 % purity of the obtained material. At this point it has to be emphasized that the system applied is complex by itself and it could not be tolerated to make it even more complex by many other proteins and substances, like brain homogenate. Therefore, different approaches were undertaken in order to increase both the purity of the samples and consequentially the reproducibility rate. In this section only the set of problems connected with prion rods will be discussed. As a source for infectious PrP 27-30 fractions from a sucrose gradient ultracentrifugation performed after large-scale purification of prion rods were used. The first experiments, which utilized one such a fraction, demonstrated indeed very satisfying results that could easily be reproduced (cf. chapter 3.4.3). However, the use of a different fraction brought unexpected problems. Not only the binding extend decreased significantly, but also a sudden change of the affinities was observed, i.e. prion rods bound better to raft-like lipid membranes than to PrP^{C}-saturated membranes. Therefore, there must have been some difference between the prion rods from the first and the second fraction. And indeed, these fractions varied from each other in two main aspects: the amount of prion rods was different – one order of magnitude

higher in the second fraction, and they have been collected at different time points. The second aspect seemed to be the crucial one. The final step of the large-scale purification method is a centrifugation in the sucrose gradient with the help of a zonal rotor. It allows a size- and density-dependent distribution of prion rods along the gradient. The heavier particles migrate faster than the lighter ones and therefore, after fractionation that takes place from to bottom to the top the first collected fractions contain most probably heavier and bigger prion rods than the fraction collected later. However, the size of prion rods could not really have such a serious influence on their binding capacity, since all samples underwent a sonication before use. It had to be another factor, somehow connected with the size of prion rods that induced those differences. As mentioned before, the prion rods purification could not really yield a completely pure product. Evidence for that was found in our laboratory earlier, where lipid-rich fractions composed of small prion rods and heterogeneous particles containing high level of prion infectivity were found (Riesner *et al.* 1996). This demonstrated a connection between the size of prion rods and their purity grade, allowing an assumption that the fraction with smaller prion rods particles was at the same time contaminated with other substances. Similar observation and potential solution to this problem was demonstrated in another study: detailed analysis of the composition of PrP 27-30 showed a presence of polysaccharide scaffold and lipids in the natural prion preparations (Dumpitak *et al.* 2005). The suggested lipid extraction was performed and it demonstrated positive effects, by restoring the higher affinity of prion rods to membrane-bound PrP^{C}. Therefore, the purity of PrP^{Sc} preparations has to be considered as one of the most important factors influencing the results obtained with this *in vitro* system.

In summary, although the conversion process could not be shown in this work, because of material and method restrictions, collected data strengthened the importance of the lipid membrane in the interaction process between anchored PrP^{C} and invading, infectious PrP^{Sc} and suggest a possible function of PrP^{C} as a receptor for PrP^{Sc}.

4.2 PrP^{C} as a potential receptor for PrP^{Sc}

As already mentioned in the introduction, the definite role of PrP^{C} remains still not completely solved (cf. chapter 1.3). The fact, that PrP^{C} is expressed not only in neurons, but also on various other cell types suggests that its role extends beyond the neuronal functions. Till now, diverse activities and ligands have been described for PrP^{C}. Functions like adhesion, cell signaling, copper homeostasis, pro-apoptotic and anti-apoptotic effects have been described. This leads to a

quite chaotic and puzzling overall picture of PrP^C cellular function. One of the aspects in search of the function of PrP^C is its possible contribution to disease-associated prion formation. Although the mechanism of PrP^C to PrP^{Sc} conversion remains still to be explained, it seems clear that specific binding between these two molecules is necessary for a conformational change to take place. This is only strengthened by the observation that both prion protein isoforms can be found in the same membrane fraction (Vey *et al.* 1996; Naslavsky *et al.* 1997). Newest co-localization studies also confirm this: with the help of light and electron microscopic immunolocalization technique the distribution of PrP^C and PrP^{Sc} in scrapie-infected N2a mouse neuroblastoma cells was studied. It could be shown that PrP^{Sc} was present at the same sites where PrP^C is normally found, namely at the cell surface, in early and in late endosomes (Veith *et al.* 2009). Another study that utilized cryo-immunogold electron microscopy method found out that in the hippocampal sections of mouse brain both PrP^C and PrP^{Sc} were detected principally on the plasma membranes and on vesicles resembling the endocytic pathway and that the high proportion of detected PrP^{Sc} was of a oligomeric, protease-sensitive character (Godsave *et al.* 2008). Present study demonstrated directly that PrP^{Sc} displayed ability to specifically bind membrane-anchored PrP^C. This specific interaction can be seen as an evidence for PrP^C involvement in the first steps of the membrane-dependent conversion process and/or as a hint for possible PrP^C function as a receptor for PrP^{Sc}. The most plausible explanation presents PrP^C as a template for conversion and a key mediator in the neurotoxicity of PrP^{Sc}. The study of Rambold and colleagues presented evidence for the PrP^C-mediated neurotoxicity of PrP^{Sc} (Rambold *et al.* 2008). It was shown that the toxic effect of PrP^{Sc} and the postulated protective activity of PrP^C are interconnected. Novel co-cultivation assay showed that PrP^{Sc} induced apoptotic signaling in PrP^C-expressing cells. It was also demonstrated that PrP^C formed dimers and that this dimerization was linked to stress-protective activity of PrP^C. These data led to assumption presented in the Figure 4.4. This model suggest following scenario: PrP^C dimerizes and can induce protective signaling through a putative transmembrane receptor. The interaction of PrP^C with PrP^{Sc} leads to a pathogenic PrP complex, which is still able to interact with the putative PrP^C receptor, however, this interaction leads to an aberrant, toxic signaling. These data were confirmed by another study, which showed that membrane-anchored PrP^C formed dimers (Elfrink *et al.* 2008). With the help of time-resolved FTIR technique prion protein secondary structure changes, occurring upon binding to a raft-like lipid membrane *via* the GPI-anchor, were observed. It was demonstrated that membrane anchoring above a threshold concentration of PrP^C

induced refolding of the prion protein to intermolecular β-sheets. Such transition was membrane-specific and led to formation of dimers and oligomers of PrP^C.

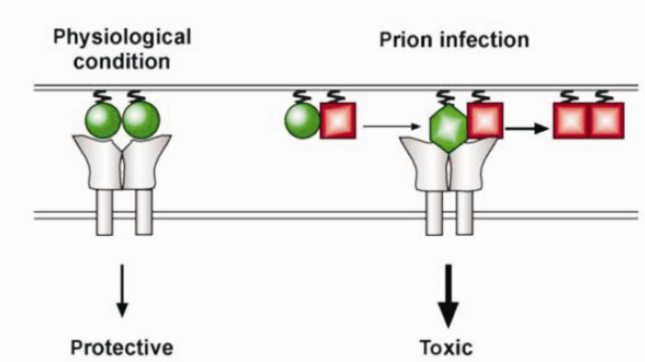

Figure 4.4 A model for stress protective and pro-apoptotic signaling of PrP^C

Under physiological conditions dimmers of PrP^C (green circle) display a stress protective role induced through interaction with a putative receptor (grey). In the case of prion infection (red square) PrP^C could form a toxic conformer with PrP^{Sc} (green diamond) that induces toxic signaling. (Figure taken from Rambold *et al*. 2008).

The fact that this project did not demonstrate a conversion process might have also reasons other than methodological restrictions. It is namely hypothesized that the interaction between PrP^C and PrP^{Sc} has to be supported by the presence of some sort of cofactor. The list of PrP^C-binding molecules is long and therefore, it is of great interest to determine how these molecules interact with PrP^C, whether they also interact with PrP^{Sc}, what are their interaction sites on both PrP^C and PrP^{Sc} and if they have a possible effect on formation of new PrP^{Sc} particles. Indeed, it is known that accessory molecules as chaperones, metal ions, lipids or polyanions can influence the aggregation of neurotoxin polypeptides. It has been demonstrated that with the help of protein misfolding cyclic amplification (PMCA) method a successful propagation of PrP^{Sc} took place after addition of polyanion molecules (Deleault *et al.* 2007). Another molecule identified as a possible receptor/cofactor was the 37-kDa/67-kDa laminin receptor and its precursor (LRP/LR) protein. It has been shown that LRP/LR may participate in the formation of new PrP^{Sc} particle (Vana *et al.* 2006). Different study reported that evidence for direct interaction between LRP/LR and PrP^{Sc} in mediating binding of exogenous PrP^{Sc} to enterocytes implying that it could have a role in the initial infection process (Morel *et al.* 2005). It is hypothesized that LRP/LP could serve as transporter or mediator during conversion process, bringing together the two substrates for the reaction: membrane-bound PrP^C and invading PrP^{Sc}. The *in vitro* system, developed in

this project, gives therefore a new opportunity to fully study the interactions between PrP^{C}, PrP^{Sc} and LRP/LR.

A different role of PrP^{C} has been discovered recently. Newest results in the field of Alzheimer's disease research showed a possible link to prion diseases. The key players in the Alzheimer's disease have been characterized to be small, soluble aggregates of abnormal amyloid-β (Aβ) peptide, known as Aβ oligomers. They impair memory by disrupting memory-related functions of synaptic junctions between neurons. A recent study has been published that showed cellular prion protein to be a mediator of the pathogenic effects of Aβ oligomers (Lauren *et al.* 2009). It has been known that Aβ binds and influences the function of many cellular proteins. Therefore in this study the search for a specific partner has been narrowed to proteins that show affinity only to Aβ oligomers. As result PrP was identified as a potential partner for the interaction with these oligomeric particles. This work, however, did not explore whether PrP^{C} would misfold upon binding to Aβ oligomers. Studies on the so called long-term potentiation (LTP), which provides information about synaptic plasticity related to learning and memory ability, showed that Aβ oligomers inhibited LTP only in the hippocampal region of normal mice and not in mice lacking PrP^{C}. Moreover, the LTP was not affected in the hippocampus of the normal mice, after the interaction between Aβ and PrP^{C} has been blocked. Therefore, PrP^{C} seems to be also the main receptor for Aβ oligomers, mediating their neuron damaging effect.

4.3 Outlook

Development of different *in vitro* systems gives us the opportunity to unravel and better understand mechanisms underlying many biological events. Use of various methods and techniques permits simulation of often complicated processes that happen in nature. In order to simulate the *in vivo* state, a biologically relevant *in vitro* system should take into account all aspects of the natural event, it is going to mimic. In this work, a development of a new *in vitro* system, displaying a good accordance with the processes happening in nature, was presented. It showed not only that the primary effect of prion disease is the interaction of PrP^{Sc} with membrane-anchored PrP^{C}, but also gave a new opportunity to apply it for other studies.

Determination of the binding domain involved in the interaction between PrP^{C} and PrP^{Sc}

In this work, a direct interaction between exogenously added PrP^{Sc} and membrane-anchored PrP^{C} has been demonstrated. However, the exact binding domain responsible for this interaction

could not be identified. This aspect of the specific binding might be investigated in future with the help of epitope-specific antibodies or short antibody Fab fragments directed against membrane-bound PrP^C. Determination of the epitopes that are involved in inhibition of the interaction would provide information about the binding domain or domains that are present on PrP^C.

Determination of cofactors mediating the binding between PrP^C and PrP^{Sc}

The same approach, as described above, might be applied in search of specific cofactors or ligands mediating the binding between anchored PrP^C and invading PrP^{Sc} and/or the conversion process. At least one molecule has been already identified as a possible mediator. The 37-kDa/67-kDa laminin receptor and its precursor (LRP/LR) protein demonstrated a role in mediating the binding of exogenous PrP^{Sc} to cells (Morel *et al.* 2005). Therefore, it would be interesting to study in detail the mode of interaction that mediates the binding of membrane-anchored PrP^C and the laminin receptor. Furthermore, the postulated influence of the membrane-bound complex between PrP^C and LRP/LR on the binding ability to invading PrP^{Sc} could be determined.

Alzheimer's disease connection

The newest discovery that natural PrP^C might have an influence on the pathogenesis of Alzheimer's disease opened a completely new field in the research on the function of prion protein. It has been demonstrated that in cell culture PrP^C interacted with soluble oligomers of Aβ, which have been identified as the main cause of Alzheimer's disease. The *in vitro* system, developed in this work, gives an opportunity to study in detail the interaction between Aβ oligomers and membrane-bound PrP^C. Following aspects could be analyzed: the mode of the interaction, determination of the binding domain with the help of epitope-specific antibodies directed against natural PrP^C, inhibition of the pathogenic character of Aβ oligomers and the ability of the complex to bind PrP^{Sc} leading to a possible link between the prion and Alzheimer's disease. Answers to these questions could accelerate the development of therapy approaches, which in the case of a disease that afflicts more than 20 million people worldwide, is of great importance.

Development of therapeutics

The Alzheimer's disease and the prion diseases have not only their neurological etiology in common: for both diseases there is also no therapy available yet. The development of

therapeutics against prions is characterized by two main approaches applied in the past: the disruption of infectious PrP^{Sc} and the stabilization of non-infectious PrP^{C}. The first approach applies the so called β-sheet-breakers, which could have the ability to bind to the aggregated form of PrP^{Sc} and to induce a change in its secondary structure. This would eventually lead to a disruption of prions and elimination of their infectivity. The second approach is focused on stabilization of the non-infectious, membrane-bound conformation of PrP^{C}. Such stabilization could preclude the conversion into new, infectious PrP^{Sc} particles. The tested substances have to show a high affinity to the PrP^{C}. Application of the *in vitro* system, presented in this work, could help in search of such compounds that had to be specific for a natural membrane-bound PrP^{C}. This work opens up a new and third alternative of intervention. Substances might be tested for their ability to interfere with the primary contact of PrP^{C} and PrP^{Sc} on the membrane.

5 Summary

Prion diseases are a group of neurological disorders that have been named after their extraordinary causative agent – the prion. Prions are remarkably different from other known disease-related agents and this difference lies in their composition. They are composed of a single protein, called therefore the prion protein. Although coding nucleic acid was excluded in the composition of the agent, the prions are able to replicate themselves and to cause a transmissible disease. Prion protein has been identified as a host-encoded protein that can exist in two different isoforms: non-infectious, cellular isoform – PrP^{C} and infectious, disease-related isoform – PrP^{Sc}. They have the same amino acid sequence and their posttranslational modifications do not differ from each other. One way to differentiate between PrP^{C} and PrP^{Sc} is analysis of their biophysical and chemical properties. PrP^{C} shows mostly α-helical secondary structure, is soluble in mild detergents and sensitive against proteolytic digestion with a proteinase K (PK). PrP^{Sc}, on the other hand, contains an increased level of β-sheets, is present in form of insoluble aggregates and demonstrates a partial resistance to digestion with PK. One assumes that the mechanism underlying progression of prion diseases is the conversion of natural PrP^{C} into infectious PrP^{Sc}. This process involves a change in the secondary conformation of PrP^{C} and most probably takes place at the outer cell membrane or in its close proximity.

In order to study in detail the character of interaction between natural PrP^{C} and invading PrP^{Sc} a new *in vitro* system has been developed. In comparison with other *in vitro* systems, it successfully mimicked the *in vivo* situation by using following components: lipid membrane, membrane-anchored PrP^{C} and infectious PrP^{Sc}. The application of a lipid membrane in form of a bilayer that composition was in good accordance with the natural microdomains, where PrP^{C} is found, was the first step in the development of this system. In the second step a natural PrP^{C} with all its posttranslational modifications was used. One of these modifications is a glycosyl-phosphatidylinositol (GPI) anchor. It was possible to attach PrP^{C} *via* its anchor to the lipid membrane, mimicking the cellular positioning. This GPI-dependent anchoring opened a new possibility for further studies, namely the introduction of a third component. This step completed the simulation of the onset of prion diseases by adding infectious, highly purified PrP^{Sc}. All these components, brought together, created an unique and complex system with a high biological relevance. It could be demonstrated that invading PrP^{Sc} displayed a high specificity for a

membrane-anchored PrP^{C}. The specificity of this interaction was demonstrated by the fact that neither fibrillar PrP^{Sc} bound to another type of protein, i.e. ovalbumin, nor a different kind of fibrils were able to bind to anchored PrP^{C}, i.e. insulin fibrils. This strong interaction that occurred at the surface of a lipid membrane could be seen as a first step in the membrane-dependent conversion process and/or as a hint for a possible function of PrP^{C} as a receptor for PrP^{Sc}.

6 Zusammenfassung

Prion-Krankheiten sind fatale neurodegenerative Erkrankungen, die nach ihrem außergewöhnlichen Erregertyp – den Prionen, benannt wurden. Prionen unterscheiden sich auf Grund ihrer Zusammensetzung stark von anderen Erregertypen. Sie bestehen zum größten Teil aus Protein, dem so genannten Prion Protein (PrP). Obwohl sie keine codierenden Nukleinsäuren besitzen, können sie sich replizieren und eine übertragbare Krankheit hervorrufen. Bei dem Prion Protein handelt es sich um ein wirtseigenes Protein, das in zwei verschiedenen Isoformen auftritt: der nicht infektiösen, zellulären Form – PrP^{C}, und der infektiösen, krankheitsassoziierten Form – PrP^{Sc}. Beide Isoformen besitzen identische Primärsequenzen und tragen die identischen posttranslationalen Modifikationen. Eine deutliche Unterscheidung von PrP^{C} und PrP^{Sc} ist erst nach der Analyse deren physikalisch-chemischen Eigenschaften möglich. PrP^{C} besitzt eine überwiegend α-helikale Sekundärstruktur, ist in milden Detergentien löslich und sensitiv gegenüber proteolytischer Verdauung mittels Proteinase K (PK). PrP^{Sc} weist einen deutlich erhöhten Anteil an β-Struktur auf, bildet unlösliche Aggregate und zeigt eine partielle Resistenz gegen PK-Verdauung. Es wird angenommen, dass der Mechanismus, der für die Ausbreitung von Prion-Krankheiten verantwortlich ist, auf einer Konversion von PrP^{C} zu der infektiösen Isoform PrP^{Sc} basiert. Die Konversion entspricht dabei einer Konformationsänderung des Prion Proteins, die höchst wahrscheinlich auf der Zellmembran oder in deren Umgebung stattfindet.

Um genauer den Charakter der Wechselwirkung zwischen natürlichen PrP^{C} und exogenen PrP^{Sc} zu untersuchen, wurde im Rahmen dieser Abreit ein neues *in vitro* System entwickelt. Dieses *in vitro* System zeigte eine hohe biologische Relevanz, in dem es sich aus folgenden Komponenten zusammensetzte: einer Lipidmembran, Membran-verankerten PrP^{C} und infektiösen PrP^{Sc}. Der erste Schritt in der Entwicklung dieses neuen Systems, war der Einsatz einer Lipidmembran in Form eines Bilayers. Die Lipidzusammensetzung entsprach der von raft Domänen, da PrP^{C} *in vivo* in raft Domänen lokalisiert ist. Als zweites wurde das natürliche PrP^{C} mit seinen posttranslationalen Modifikationen – dem Glykosyl-Phosphatidyl-Inositol-Anker (GPI-Anker) und den glykolisierungen – eingesetzt. Das PrP^{C} wurde mittels seines GPI-Ankers in der Membran verankert, was sehr gut den *in vivo* Zustand imitierte. Diese GPI-Anker-vermittelte Immobilisierung ermöglichte die Analyse einer dritten Komponente in Form von infektiösen, hoch reinen PrP^{Sc}. Die Kombination dieser drei Komponenten führte zur Entwicklung eines

neuen, hoch komplexen und biologisch relevanten *in vitro* System, mit dessen Hilfe es möglich war eine spezifische Wechselwirkung zwischen Membran-verankerten PrP^{C} und exogenem PrP^{Sc} zu zeigen. Die Spezifität dieser Wechselwirkung wurde durch Versuche bestätigt in deren weder eine Bindung von PrP^{Sc} zu anderen Proteinen gezeigt werden konnte, noch andere Proteinfibrillen mit Membran-verankerten PrP^{C} wechselwirkten. Die starke Wechselwirkung zwischen Membran-verankerten PrP^{C} und PrP^{Sc} kann als der erste Schritt der Membran-abhängigen Konversion von PrP^{C} zu PrP^{Sc} gesehen werden.

7 References

Alper, T., W. A. Cramp, et al. (1967). "Does the agent of scrapie replicate without nucleic acid?" Nature **214**(5090): 764-6.

Arnold, J. E., C. Tipler, et al. (1995). "The abnormal isoform of the prion protein accumulates in late-endosome-like organelles in scrapie-infected mouse brain." J Pathol **176**(4): 403-11.

Basler, K., B. Oesch, et al. (1986). "Scrapie and cellular PrP isoforms are encoded by the same chromosomal gene." Cell **46**(3): 417-28.

Becker, C. F., X. Liu, et al. (2008). "Semisynthesis of a glycosylphosphatidylinositol-anchored prion protein." Angew Chem Int Ed Engl **47**(43): 8215-9.

Bendheim, P. E., H. R. Brown, et al. (1992). "Nearly ubiquitous tissue distribution of the scrapie agent precursor protein." Neurology **42**(1): 149-56.

Benes, M., D. Billy, et al. (2004). "Surface-dependent transitions during self-assembly of phospholipid membranes on mica, silica, and glass." Langmuir **20**(23): 10129-37.

Bennion, B. J., M. L. DeMarco, et al. (2004). "Preventing misfolding of the prion protein by trimethylamine N-oxide." Biochemistry **43**(41): 12955-63.

Blochberger, T. C., C. Cooper, et al. (1997). "Prion protein expression in Chinese hamster ovary cells using a glutamine synthetase selection and amplification system." Protein Eng **10**(12): 1465-73.

Bolton, D. C., M. P. McKinley, et al. (1982). "Identification of a protein that purifies with the scrapie prion." Science **218**(4579): 1309-11.

Borchelt, D. R., A. Taraboulos, et al. (1992). "Evidence for synthesis of scrapie prion proteins in the endocytic pathway." J Biol Chem **267**(23): 16188-99.

Brange, J. and L. Langkjaer (1997). "Insulin formulation and delivery." Pharm Biotechnol **10**: 343-409.

Brown, D. A. and E. London (1997). "Structure of detergent-resistant membrane domains: does phase separation occur in biological membranes?" Biochem Biophys Res Commun **240**(1): 1-7.

Brown, D. R., F. Hafiz, et al. (2000). "Consequences of manganese replacement of copper for prion protein function and proteinase resistance." EMBO J **19**(6): 1180-6.

Brown, P., F. Cathala, et al. (1987). "The epidemiology of Creutzfeldt-Jakob disease: conclusion of a 15-year investigation in France and review of the world literature." Neurology **37**(6): 895-904.

Bueler, H., A. Aguzzi, et al. (1993). "Mice devoid of PrP are resistant to scrapie." Cell **73**(7): 1339-47.

Bueler, H., M. Fischer, et al. (1992). "Normal development and behaviour of mice lacking the neuronal cell-surface PrP protein." Nature **356**(6370): 577-82.

Cassirer, R. (1898). "Über die Traberkrankheit der Schafe: pathologisch-anatomische und bakterielle Untersuchung." Pathol. Anat. Rhysiol. **153**: 89-110.

Caughey, B., R. E. Race, et al. (1988). "Detection of prion protein mRNA in normal and scrapie-infected tissues and cell lines." J Gen Virol **69 (Pt 3)**: 711-6.

Caughey, B., R. E. Race, et al. (1989). "Prion protein biosynthesis in scrapie-infected and uninfected neuroblastoma cells." J Virol **63**(1): 175-81.

Caughey, B. and G. J. Raymond (1991). "The scrapie-associated form of PrP is made from a cell surface precursor that is both protease- and phospholipase-sensitive." J Biol Chem **266**(27): 18217-23.

Chandler, R. L. (1961). "Encephalopathy in mice produced by inoculation with scrapie brain material." Lancet **1**(7191): 1378-9.

Chesebro, B., R. Race, et al. (1985). "Identification of scrapie prion protein-specific mRNA in scrapie-infected and uninfected brain." Nature **315**(6017): 331-3.

Cohen, F. E., K. M. Pan, et al. (1994). "Structural clues to prion replication." Science **264**(5158): 530-1.

Cohen, F. E. and S. B. Prusiner (1998). "Pathologic conformations of prion proteins." Annu Rev Biochem **67**: 793-819.

Collinge, J. (1997). "Human prion diseases and bovine spongiform encephalopathy (BSE)." Hum Mol Genet **6**(10): 1699-705.

Collinge, J. (1999). "Variant Creutzfeldt-Jakob disease." Lancet **354**(9175): 317-23.

Collinge, J., M. S. Palmer, et al. (1991). "Genetic predisposition to iatrogenic Creutzfeldt-Jakob disease." Lancet **337**(8755): 1441-2.

Collinge, J., K. C. Sidle, et al. (1996). "Molecular analysis of prion strain variation and the aetiology of 'new variant' CJD." Nature **383**(6602): 685-90.

Cousens, S. N., M. Zeidler, et al. (1997). "Sporadic Creutzfeldt-Jakob disease in the United Kingdom: analysis of epidemiological surveillance data for 1970-96." BMJ **315**(7105): 389-95.

Cuille, J., Chelle, P. L. (1936). "La maladie dite tremblante du mouton est-elle inoculable?" C. R. Acad. Sci. Paris **203**: 1552-1554.

Deleault, N. R., B. T. Harris, et al. (2007). "Formation of native prions from minimal components in vitro." Proc Natl Acad Sci U S A **104**(23): 9741-6.

Dodelet, V. C. and N. R. Cashman (1998). "Prion protein expression in human leukocyte differentiation." Blood **91**(5): 1556-61.

Dumpitak, C., M. Beekes, et al. (2005). "The polysaccharide scaffold of PrP 27-30 is a common compound of natural prions and consists of alpha-linked polyglucose." Biol Chem **386**(11): 1149-55.

Dupiereux, I., W. Zorzi, et al. (2005). "Interaction of the 106-126 prion peptide with lipid membranes and potential implication for neurotoxicity." Biochem Biophys Res Commun **331**(4): 894-901.

Eberl, H., P. Tittmann, et al. (2004). "Characterization of recombinant, membrane-attached full-length prion protein." J Biol Chem **279**(24): 25058-65.

Eigen, M. (1996). "Prionics or the kinetic basis of prion diseases." Biophys Chem **63**(1): A1-18.

Elfrink, K., L. Nagel-Steger, et al. (2007). "Interaction of the cellular prion protein with raft-like lipid membranes." Biol Chem **388**(1): 79-89.

Elfrink, K., J. Ollesch, et al. (2008). "Structural changes of membrane-anchored native PrP(C)." Proc Natl Acad Sci U S A **105**(31): 10815-9.

Elfrink, K. and D. Riesner (2004). Purification of PrP^{C}. Methods and tools in Biosciences and Medicine: Techniques in Prion Research., S. Lehmann J. Grassi**:** 4-15.

Engel, M. F., L. Khemtemourian, et al. (2008). "Membrane damage by human islet amyloid polypeptide through fibril growth at the membrane." Proc Natl Acad Sci U S A **105**(16): 6033-8.

Godsave, S. F., H. Wille, et al. (2008). "Cryo-immunogold electron microscopy for prions: toward identification of a conversion site." J Neurosci **28**(47): 12489-99.

Gorodinsky, A. and D. A. Harris (1995). "Glycolipid-anchored proteins in neuroblastoma cells form detergent-resistant complexes without caveolin." J Cell Biol **129**(3): 619-27.

Govaerts, C., H. Wille, et al. (2004). "Evidence for assembly of prions with left-handed beta-helices into trimers." Proc Natl Acad Sci U S A **101**(22): 8342-7.

Heukeshoven, J., Dernick, R. (1985). "Simplified method for silver staining of proteins in polyacrylamid gels and the mechanism of silver staining." Electrophor. **6**: 103-112.

Hill, A. F., R. J. Butterworth, et al. (1999). "Investigation of variant Creutzfeldt-Jakob disease and other human prion diseases with tonsil biopsy samples." Lancet **353**(9148): 183-9.

Hill, A. F., M. Zeidler, et al. (1997). "Diagnosis of new variant Creutzfeldt-Jakob disease by tonsil biopsy." Lancet **349**(9045): 99-100.

Hjelmeland, L. M. and A. Chrambach (1984). "Solubilization of functional membrane proteins." Methods Enzymol **104**: 305-18.

Hosszu, L. L., N. J. Baxter, et al. (1999). "Structural mobility of the human prion protein probed by backbone hydrogen exchange." Nat Struct Biol **6**(8): 740-3.

Ironside, J. W. (1998). "Neuropathological findings in new variant CJD and experimental transmission of BSE." FEMS Immunol Med Microbiol **21**(2): 91-5.

Jackson, G. S., I. Murray, et al. (2001). "Location and properties of metal-binding sites on the human prion protein." Proc Natl Acad Sci U S A **98**(15): 8531-5.

Jansen, K., O. Schafer, et al. (2001). "Structural intermediates in the putative pathway from the cellular prion protein to the pathogenic form." Biol Chem **382**(4): 683-91.

Jeffrey, M., C. M. Goodsir, et al. (1992). "Infection specific prion protein (PrP) accumulates on neuronal plasmalemma in scrapie infected mice." Neurosci Lett **147**(1): 106-9.

Kaneko, K., M. Vey, et al. (1997). "COOH-terminal sequence of the cellular prion protein directs subcellular trafficking and controls conversion into the scrapie isoform." Proc Natl Acad Sci U S A **94**(6): 2333-8.

Kascsak, R. J., R. Rubenstein, et al. (1987). "Mouse polyclonal and monoclonal antibody to scrapie-associated fibril proteins." J Virol **61**(12): 3688-93.

Kimberlin, R. H. and R. F. Marsh (1975). "Comparison of scrapie and transmissible mink encephalopathy in hamsters. I. Biochemical studies of brain during development of disease." J Infect Dis **131**(2): 97-103.

Klein, T. R., D. Kirsch, et al. (1998). "Prion rods contain small amounts of two host sphingolipids as revealed by thin-layer chromatography and mass spectrometry." Biol Chem **379**(6): 655-66.

Kretzschmar, H. A., S. B. Prusiner, et al. (1986). "Scrapie prion proteins are synthesized in neurons." Am J Pathol **122**(1): 1-5.

Laemmli, U. K. (1970). "Cleavage of structural proteins during the assembly of the head of bacteriophage T4." Nature **227**(5259): 680-5.

Lauren, J., D. A. Gimbel, et al. (2009). "Cellular prion protein mediates impairment of synaptic plasticity by amyloid-beta oligomers." Nature **457**(7233): 1128-32.

Leclerc, E. and S. Vetter (2008). "Conformational changes and development of proteinase K resistance in surface-immobilized PrP." Arch Virol **153**(4): 683-91.

Leffers, K. W., H. Wille, et al. (2005). "Assembly of natural and recombinant prion protein into fibrils." Biol Chem **386**(6): 569-80.

Legname, G., I. V. Baskakov, et al. (2004). "Synthetic mammalian prions." Science **305**(5684): 673-6.

Liu, H., S. Farr-Jones, et al. (1999). "Solution structure of Syrian hamster prion protein rPrP(90-231)." Biochemistry **38**(17): 5362-77.

Masters, C. L. and E. P. Richardson, Jr. (1978). "Subacute spongiform encephalopathy (Creutzfeldt-Jakob disease). The nature and progression of spongiform change." Brain **101**(2): 333-44.

Mehlhorn, I., D. Groth, et al. (1996). "High-level expression and characterization of a purified 142-residue polypeptide of the prion protein." Biochemistry **35**(17): 5528-37.

Morel, E., T. Andrieu, et al. (2005). "Bovine prion is endocytosed by human enterocytes via the 37 kDa/67 kDa laminin receptor." Am J Pathol **167**(4): 1033-42.

Muller-Schiffmann, A., B. Petsch, et al. (2009). "Complementarity determining regions of an anti-prion protein scFv fragment orchestrate conformation specificity and antiprion activity." Mol Immunol **46**(4): 532-40.

Naslavsky, N., R. Stein, et al. (1997). "Characterization of detergent-insoluble complexes containing the cellular prion protein and its scrapie isoform." J Biol Chem **272**(10): 6324-31.

Oesch, B., D. Westaway, et al. (1985). "A cellular gene encodes scrapie PrP 27-30 protein." Cell **40**(4): 735-46.

Olschewski, D., R. Seidel, et al. (2007). "Semisynthetic murine prion protein equipped with a GPI anchor mimic incorporates into cellular membranes." Chem Biol **14**(9): 994-1006.

Palmer, M. S., A. J. Dryden, et al. (1991). "Homozygous prion protein genotype predisposes to sporadic Creutzfeldt-Jakob disease." Nature **352**(6333): 340-2.

Pan, K. M., M. Baldwin, et al. (1993). "Conversion of alpha-helices into beta-sheets features in the formation of the scrapie prion proteins." Proc Natl Acad Sci U S A **90**(23): 10962-6.

Pan, K. M., N. Stahl, et al. (1992). "Purification and properties of the cellular prion protein from Syrian hamster brain." Protein Sci **1**(10): 1343-52.

Pauly, P. C. and D. A. Harris (1998). "Copper stimulates endocytosis of the prion protein." J Biol Chem **273**(50): 33107-10.

Pergami, P., H. Jaffe, et al. (1996). "Semipreparative chromatographic method to purify the normal cellular isoform of the prion protein in nondenatured form." Anal Biochem **236**(1): 63-73.

Post, K., M. Pitschke, et al. (1998). "Rapid acquisition of beta-sheet structure in the prion protein prior to multimer formation." Biol Chem **379**(11): 1307-17.

Prusiner, S. B. (1982). "Novel proteinaceous infectious particles cause scrapie." Science **216**(4542): 136-44.

Prusiner, S. B. (1998). "Prions." Proc Natl Acad Sci U S A **95**(23): 13363-83.

Prusiner, S. B., D. C. Bolton, et al. (1982). "Further purification and characterization of scrapie prions." Biochemistry **21**(26): 6942-50.

Prusiner, S. B., D. F. Groth, et al. (1981). "Thiocyanate and hydroxyl ions inactivate the scrapie agent." Proc Natl Acad Sci U S A **78**(7): 4606-10.

Prusiner, S. B., M. P. McKinley, et al. (1983). "Scrapie prions aggregate to form amyloid-like birefringent rods." Cell **35**(2 Pt 1): 349-58.

Prusiner, S. B., M. Scott, et al. (1990). "Transgenetic studies implicate interactions between homologous PrP isoforms in scrapie prion replication." Cell **63**(4): 673-86.

Raether, H. (1977). Physics of thin films **9**(145).

Rambold, A. S., V. Muller, et al. (2008). "Stress-protective signalling of prion protein is corrupted by scrapie prions." EMBO J **27**(14): 1974-84.

Riek, R., S. Hornemann, et al. (1996). "NMR structure of the mouse prion protein domain PrP(121-321)." Nature **382**(6587): 180-2.

Riesner, D. (2002). "Molecular basis of prion diseases." J Neurovirol **8 Suppl 2**: 8-20.

Riesner, D. (2003). "Biochemistry and structure of PrP(C) and PrP(Sc)." Br Med Bull **66**: 21-33.

Riesner, D., K. Kellings, et al. (1996). "Disruption of prion rods generates 10-nm spherical particles having high alpha-helical content and lacking scrapie infectivity." J Virol **70**(3): 1714-22.

Rochet, J. C. and P. T. Lansbury, Jr. (2000). "Amyloid fibrillogenesis: themes and variations." Curr Opin Struct Biol **10**(1): 60-8.

Safar, J., H. Wille, et al. (1998). "Eight prion strains have PrP(Sc) molecules with different conformations." Nat Med **4**(10): 1157-65.

Salwierz, A. (2004). Influence of pH on the secondary structure of recombinant prion protein rec PrP(90-231) and its possible hysteresis.

Sanders, P. G. and R. H. Wilson (1984). "Amplification and cloning of the Chinese hamster glutamine synthetase gene." EMBO J **3**(1): 65-71.

Schroeder, R., E. London, et al. (1994). "Interactions between saturated acyl chains confer detergent resistance on lipids and glycosylphosphatidylinositol (GPI)-anchored proteins: GPI-anchored proteins in liposomes and cells show similar behavior." Proc Natl Acad Sci U S A **91**(25): 12130-4.

Shin, J. I., J. Y. Shin, et al. (2008). "Deep membrane insertion of prion protein upon reduction of disulfide bond." Biochem Biophys Res Commun **377**(3): 995-1000.

Sigurdsson, B. (1954). "A chronic encephalitis of sheep." Brit. Vet. J. **110**: 341-354.

Stahl, N., M. A. Baldwin, et al. (1990). "Identification of glycoinositol phospholipid linked and truncated forms of the scrapie prion protein." Biochemistry **29**(38): 8879-84.

Stahl, N., M. A. Baldwin, et al. (1992). "Glycosylinositol phospholipid anchors of the scrapie and cellular prion proteins contain sialic acid." Biochemistry **31**(21): 5043-53.

Stohr, J., N. Weinmann, et al. (2008). "Mechanisms of prion protein assembly into amyloid." Proc Natl Acad Sci U S A **105**(7): 2409-14.

Taraboulos, A., A. J. Raeber, et al. (1992). "Synthesis and trafficking of prion proteins in cultured cells." Mol Biol Cell **3**(8): 851-63.

Taraboulos, A., M. Scott, et al. (1995). "Cholesterol depletion and modification of COOH-terminal targeting sequence of the prion protein inhibit formation of the scrapie isoform." J Cell Biol **129**(1): 121-32.

Tobler, I., S. E. Gaus, et al. (1996). "Altered circadian activity rhythms and sleep in mice devoid of prion protein." Nature **380**(6575): 639-42.

Turk, E., D. B. Teplow, et al. (1988). "Purification and properties of the cellular and scrapie hamster prion proteins." Eur J Biochem **176**(1): 21-30.

Vana, K. and S. Weiss (2006). "A trans-dominant negative 37kDa/67kDa laminin receptor mutant impairs PrP(Sc) propagation in scrapie-infected neuronal cells." J Mol Biol **358**(1): 57-66.

Veith, N. M., H. Plattner, et al. (2009). "Immunolocalisation of PrPSc in scrapie-infected N2a mouse neuroblastoma cells by light and electron microscopy." Eur J Cell Biol **88**(1): 45-63.

Vey, M., S. Pilkuhn, et al. (1996). "Subcellular colocalization of the cellular and scrapie prion proteins in caveolae-like membranous domains." Proc Natl Acad Sci U S A **93**(25): 14945-9.

Wang, F., F. Yang, et al. (2007). "Lipid interaction converts prion protein to a PrPSc-like proteinase K-resistant conformation under physiological conditions." Biochemistry **46**(23): 7045-53.

Wang, T. Y., R. Leventis, et al. (2000). "Fluorescence-based evaluation of the partitioning of lipids and lipidated peptides into liquid-ordered lipid microdomains: a model for molecular partitioning into "lipid rafts"." Biophys J **79**(2): 919-33.

Weissmann, C., H. Bueler, et al. (1993). "Molecular biology of prion diseases." Dev Biol Stand **80**: 53-4.

Welford, K. (1991). Opt. Quant. Elect. **23**(1).

Wells, G. A., J. W. Wilesmith, et al. (1991). "Bovine spongiform encephalopathy: a neuropathological perspective." Brain Pathol **1**(2): 69-78.

Wilesmith, J. W. (1988). "Bovine spongiform encephalopathy." Vet Rec **122**(25): 614.

Wille, H., M. D. Michelitsch, et al. (2002). "Structural studies of the scrapie prion protein by electron crystallography." Proc Natl Acad Sci U S A **99**(6): 3563-8.

Windl, O., M. Dempster, et al. (1996). "Genetic basis of Creutzfeldt-Jakob disease in the United Kingdom: a systematic analysis of predisposing mutations and allelic variation in the PRNP gene." Hum Genet **98**(3): 259-64.